Structural and Functional Characterization of the ATP-Driven Glycolipid-Efflux Pump DevBCA-TolC and its Homologues in the Filamentous Cyanobacterium *Anabaena* sp. PCC 7120

Dissertation

der Mathematisch-Naturwissenschaftlichen Fakultät

der Eberhard Karls Universität Tübingen

zur Erlangung des Grades eines

Doktors der Naturwissenschaften

(Dr. rer. nat.)

vorgelegt von

Peter Staron

aus Liegnitz

Tübingen

2012

Tag der mündlichen Qualifikation:	30.03.2012
Dekan:	Prof. Dr. Wolfgang Rosenstiel
1. Berichterstatter:	PD Dr. Iris Maldener
2. Berichterstatter:	Prof. Dr. Karl Forchhammer

Table of contents

Abstract

On depletion of combined nitrogen, the filamentous cyanobacterium *Anabaena* sp. PCC 7120 forms N_2-fixing heterocysts from vegetative cells. To protect the oxygen-sensitive nitrogenase, a heterocyst-specific layer composed of heterocyst glycolipids (HGLs) that functions as an O_2-diffusion barrier is deposited on top of the heterocyst cell wall. In this work, the exporter of the HGLs was identified. DevBCA and TolC were shown to form an ATP-driven *trans*-envelope efflux pump (or type 1 secretion system) required for the translocation of HGLs across the Gram-negative cell wall. DevA and DevC form a cytoplasmic membrane-integral ABC exporter, TolC is an outer membrane-integral pore, and DevB is a periplasmic connector between both membrane proteins.

DevAC was responsive toward HGLs by increasing its ATP-hydrolyzing activity. This feature was absolutely depending on the presence of DevB, but not TolC. Surface plasmon resonance and isothermal titration calorimetry predicted a DevB hexamer interacting with both DevAC and TolC. Mutations in DevB that impaired hexamer formation led to a remarkable decrease in binding affinities to DevAC and TolC. Advanced structure-function investigations using modified variants of the participants confirmed a central DevB hexamer interacting with TolC, and further predicted a cogwheel-like tip-to-tip interaction interface between them.

In addition, only a DevB hexamer was able to promote substrate recognition of DevAC. All DevB variants impaired in hexamerization were not able to do so. The physiological relevance of this observation was demonstrated in complementation studies using a single site mutation variant of DevB impaired in hexamerization. This variant was not able to rescue the phenotype of a mutant in *devB* (heterocysts were not able to export HGLs). DevBCA-TolC -or type 1 secretion systems in general- reflect a novel pathway of glycolipid export.

Furthermore, six close homologues of DevBCA predicted from the genome of *Anabaena* sp. PCC 7120 were analyzed in this work. Two of them, All0809/8/7 and All5347/6, were shown to be crucial for diazotrophic growth by inactivating the respective DevB homologue. All0809/8/7-TolC could also be shown to form a typical ATP-driven efflux pump like DevBCA-TolC. However, a distinct substrate could not be identified.

In this comprehensive study, the first TolC-dependent ATP-driven *trans*-envelope efflux pumps of cyanobacteria were described.

Zusammenfassung

Bei Stickstoffmangel differenziert das filamentöse Cyanobakterium *Anabaena* sp. PCC 7120 N_2-fixierende Heterozysten aus vegetativen Zellen. Um die sauerstoffempfindliche Nitrogenase zu schützen, lagern Heterozysten eine spezifische Schicht aus Heterozysten-Glykolipiden (HGLs) auf der Heterozystenzellwand ab, welche als O_2-Diffusionsbarriere dient. In dieser Arbeit wurde der Exporter der HGLs identifiziert. Es konnte gezeigt werden, dass DevBCA und TolC eine ATP-getriebene Effluxpumpe (oder ein Typ-1-Sekretionssystem) bilden, welche die gesamte Zellhülle durchspannt und für die Translokation von HGLs über die Gram-negative Zellwand erforderlich ist. DevA und DevC stellen einen integralen ABC-Exporter in der Cytoplasmamembran dar, TolC bildet eine Pore in der äußeren Membran, und das periplasmatische Protein DevB verbindet beide Membranproteine.

DevAC reagierte auf die Anwesenheit von angereicherten HGLs durch eine Erhöhung der ATP-Hydrolyse-Aktivität. Diese Reaktion war strikt abhängig von DevB, jedoch nicht von TolC. Durch Oberflächenplasmonresonanz und Isothermale Titrationskalorimetrie konnte ein DevB-Hexamer vorhergesagt werden, welches sowohl mit DevAC als auch mit TolC interagierte. Mutationen in DevB, die die Bildung eines Hexamers beeinträchtigten, führten zu einem starken Rückgang der Bindungsaffinitäten zu DevAC und TolC. Erweiterte Struktur-Funktions-Analysen mit modifizierten Varianten der Teilnehmer bestätigten eine zentrale Rolle des DevB-Hexamers bei der Interaktion mit TolC. Weiterhin konnte eine Zahnrad-ähnliche Interaktionsschnittstelle zwischen den Spitzen der α-helicalen Domänen von DevB und TolC festgestellt werden.

Darüber hinaus konnte nur ein DevB-Hexamer die Substraterkennung von DevAC vermitteln. Alle Varianten von DevB, bei denen die Hexamerisierung beeinträchtigt war, waren dazu nicht in der Lage. Die physiologische Relevanz dieser Beobachtung wurde in Komplementationsstudien mit einer DevB-Variante demonstriert, die durch die Mutation einer einzigen Aminosäure in der Hexamerisierung beeinträchtigt war. Diese Variante konnte den Phänotyp einer *devB*-Mutante nicht komplementieren (Heterocysten waren nicht in der Lage, HGLs zu exportieren). DevBCA-TolC -oder Typ-1-Sekretion-Systeme im Allgemeinen- stellen einen neuartigen Weg des Glykolipidexports dar.

Zudem wurden in dieser Arbeit sechs zu *devBCA* homologe Gencluster im Genom von *Anabaena* sp. PCC 7120 analysiert. Durch Inaktivierung des jeweiligen zu *devB* homologen Gens konnte gezeigt werden, dass *all0809-7* und *all5347-6* unabdingbar für das diazotrophe Wachstum sind. Weiterhin wurde gezeigt, dass auch All0809/8/7-TolC eine typische ATP-getriebene Effluxpumpe wie DevBCA-TolC bilden. Jedoch konnten im Gegensatz zu DevBCA-TolC keinerlei Substrate identifiziert werden.

In dieser umfassenden Studie wurden die ersten TolC-abhängigen, ATP-getriebenen, und die Zellhülle-durchspannenden Effluxpumpen von Cyanobakterien beschrieben.

1. Introduction

1.1 The Gram-negative cell envelope

All biological membranes are composed of lipid bilayers. Depending on phylogenetic affiliation, the cell function and environmental influences, each type of cell envelope has additional lipid, protein or sugar components. Those compositions make cell envelopes unique, but they also allow categorization of different types of cell envelopes (Silhavy *et al*. 2010). So, nearly all bacteria can be categorized into two groups by using a simple staining procedure (Gram 1884). One group retains this so called Gram-stain (Gram-positive), and the other group does not (Gram-negative). This is due to structural differences in the cell envelope of these two groups of bacteria. In contrast to Gram-positive bacteria, the cell envelope of Gram-negative ones shows three layers instead of two: the inner or cytoplasmic membrane (CM), peptidoglycan (PG), and the outer membrane (OM). Both the CM and the OM comprise the PG inside an additional cell compartment, the periplasm (Fig. 1).

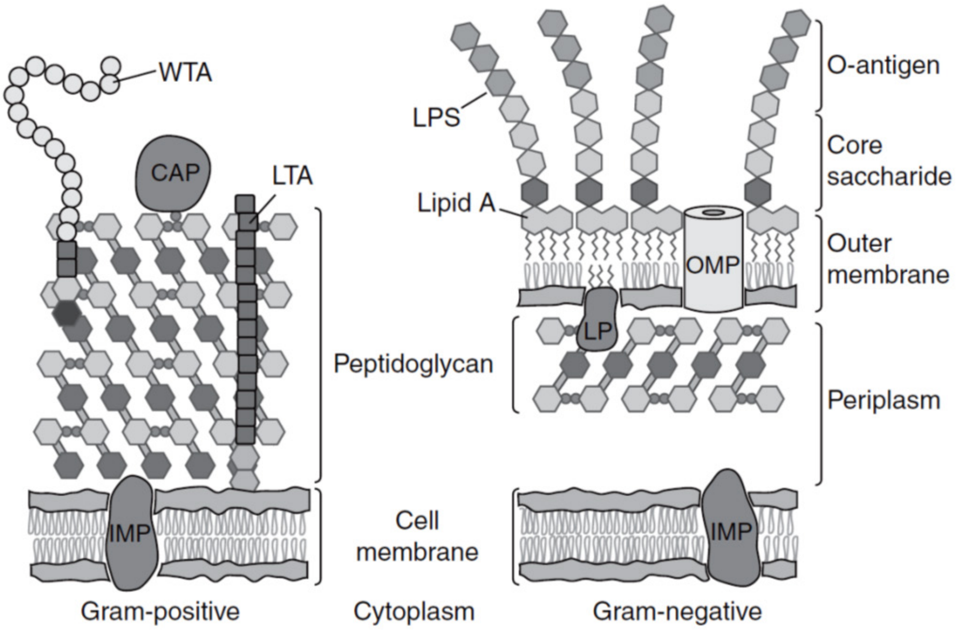

Figure 1. Schematic representation of Gram-positive and Gram-negative cell envelopes.

CAP = covalently attached protein; IMP = integral membrane protein; LP = lipoprotein; LPS = lipopolysaccharide; LTA = lipoteichoic acid; OMP = outer membrane protein; WTA = wall teichoic acid (taken from Silhavy *et al*. 2010).

Both the periplasm and the OM are distinguishing features of Gram-negative bacteria. The periplasm is described as an aqueous compartment densely packed with proteins, and therefore, it is more viscous than the cytoplasm (Mullineaux *et al.* 2006). The additional OM is distinct to "ordinary" cytoplasmic membranes: although it is a lipid bilayer, the leaflets show an asymmetric lipid composition. The inner leaflet is composed of phospholipids (like both leaflets of the CM), but the outer leaflet is made up of glycolipids (Kamio and Nikaido 1976). In addition, the protein composition of the OM also differs to the one present in the CM (Silhavy *et al.* 2010). While the CM mostly contains enzymes involved in synthesis, energy production, and (active) transport, the OM contains only a few enzymes. Almost all proteins of the OM can be classified into integral β-barrel proteins or lipoproteins attached to the OM (Silhavy *et al.* 2010). Some β-barrel proteins seem to fulfill a structural role, while most known β-barrel proteins are involved in passive or specific diffusion, or they participate in large complexes with proteins in the CM to provide dedicated transport or motility functions. Some lipoproteins attached to the OM are involved in various functions like the biogenesis of the outer membrane, the transport of a variety of molecules, and signal transduction. The function of most lipoproteins is not known (Narita 2011).

1.2 Traversing the Gram-negative envelope

Bacteria are often faced with unpredictable environmental conditions. Therefore, they have evolved a protective cell envelope. The envelope must allow the selective import of nutrients or signaling molecules from the outside, and the export of waste products or functional molecules from the inside.

The transport mechanisms of Gram-negative and Gram-positive bacteria (and eukaryotes) are similar with respect to traversing the cytoplasmic membrane only. To export molecules beyond the whole cell envelope, and not just across the primary membrane, Gram-negative bacteria evolved adaptations regarding the additional OM. At least seven secretion systems have been described in Gram-negative bacteria (Fig. 2, next page).

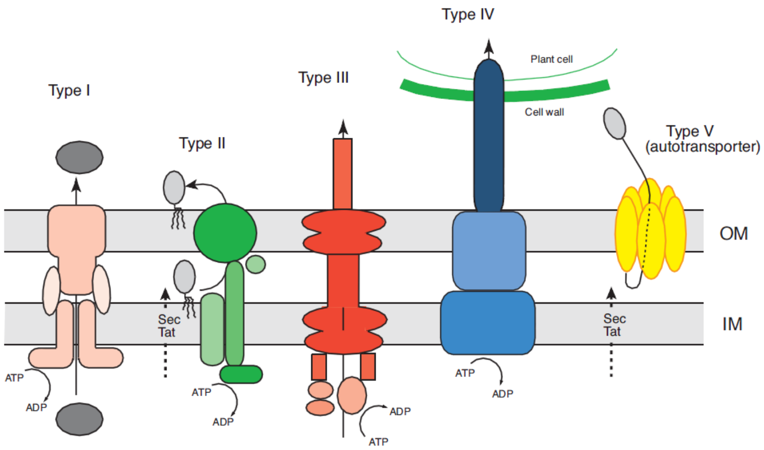

Figure 2. Gram-negative secretion systems

Type I to V refer to T1SS to T5SS (taken from Tokuda 2009).

Type I secretion systems (T1SS) or efflux pumps (EP) are tripartite export machineries. They export various proteins and non-proteinaceous substrates in a single step by forming a contiguous channel traversing the whole Gram-negative cell envelope. This *trans*-envelope channel is formed by a cytoplasmic membrane-integral exporter, a β-barrel protein in the OM, and a periplasmic adaptor protein connecting both the IM protein and the OM protein (Zgurskaya 2009).

Like T1SSs, T3SSs and T4SSs allow a single-step transfer of substrates. Both secretion systems are not similar to T1SSs. T3SSs are homologous to the flagellar body (Izoré *et al*. 2011), while T4SSs are homologous to the conjugation machinery of Gram-negative bacteria (Yeo and Waksman 2004).

Different to single-step secretion systems, T2SSs and T5SSs depend on the initial export of substrate proteins into the periplasm via the Sec or Tat systems. In the pathway of a T2SS, substrates are secreted by a multimeric assembly of pore-forming secretion proteins in addition to further proteins of the CM and the OM (Cianciotto 2005). Substrate proteins of the T5SSs form a β-barrel that inserts into the OM allowing the remaining peptide to pass the additional membrane (Henderson *et al*. 2004).

The mechanisms of T6SSs and the release of outer membrane vesicles (“T7SS”) are not well understood yet. T6SSs seem to share a common evolutionary origin with phage tail-associated proteins (Veesler and Cambillau 2011). In contrast to the other mentioned secretion systems, outer membrane vesicles provide substrate secretion without involving multiprotein complexes across the cell envelope (Kulp and Kuehn 2010).

1.3 Tripartite Gram-negative efflux pumps

As mentioned above, Gram-negative bacteria use tripartite exporters that span the CM, the periplasm, and the OM, to export a wide variety of substrates. These EPs or T1SSs are composed of (cytoplasmic/) inner membrane factors (IMFs) and outer membrane factors (OMFs), and both are connected by central periplasmic membrane fusion proteins (MFPs) (Zgurskaya 2009).

IMFs can be classified in any of three structurally diverse superfamilies (Fig. 3): (**i**) ATP hydrolysis-driven ATP-binding cassette superfamily (ABC; Holland *et al.* 2005). Tripartite EPs utilizing ABC exporters are also termed T1SS. (**ii**) H^+-driven resistance-nodulation-division superfamily (RND; Tseng *et al.* 1999). (**iii**) H^+-driven major facilitator (MF; Saier *et al.* 1999).

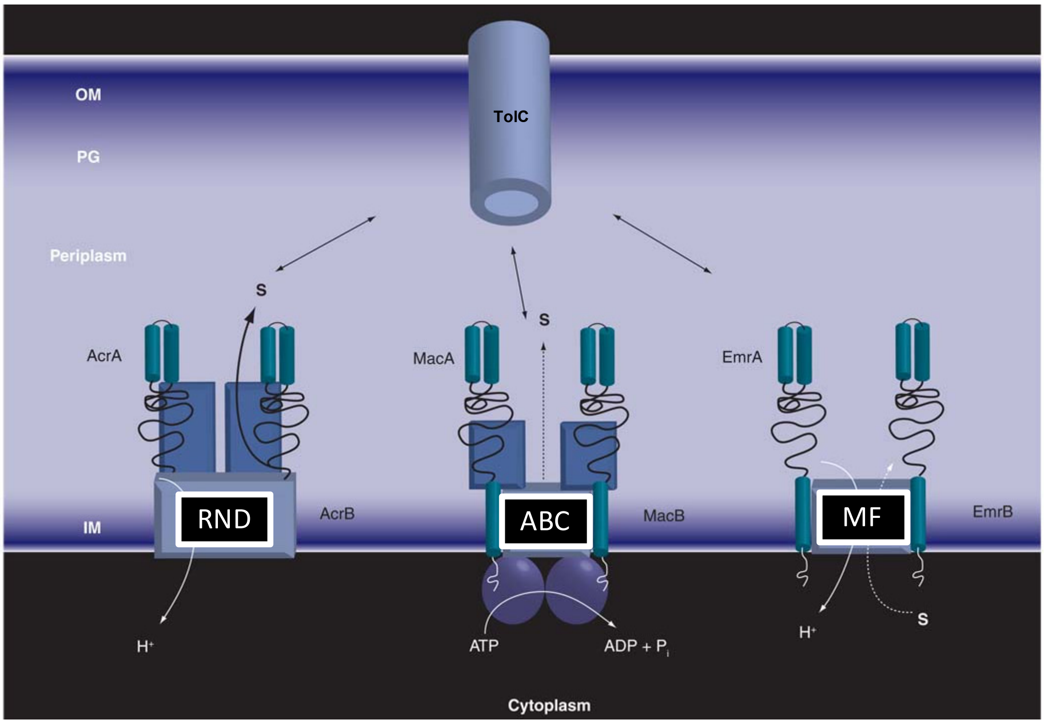

Figure 3. General models of tripartite Gram-negative efflux pumps

This scheme reflects basic structural and mechanical characteristics of all 3 known types of Gram-negative *trans*-envelope EPs (taken from Zgurskaya 2009 and modified). OM = outer membrane; PG = peptidoglycane; IM = cytoplasmic membrane; S = substrate; TolC = OMF of the TolC familiy, AcrA/AcrB = MFP/IMF of the RND-type EP AcrAB-TolC; MacA/MacB = MFP/IMF of the ABC-type EP/T1SS MacAB-TolC; EmrA/EmrB = MFP/IMF of the MF-type EP EmrAB-TolC.

1.3.1 Inner membrane factors

ATP hydrolysis-driven ABC-type IMFs are supposed to form functional dimers (Lin *et al.* 2009). Each monomer consists of a CM-integral substrate binding domain (SBD) and a cytoplasmic nucleotide binding domain (NBD) for ATP hydrolysis. In contrast to most other known ABC exporters not participating in tripartite *trans*-envelope EPs, ABC-type IMFs locate their NBD on the N-terminus of the SBD. Furthermore, they have less transmembrane helices in their SBD (4 per monomer; Zgurskaya 2009). Each ABC-type IMF is predicted to have a remarkable periplasmic region between transmembrane helices 1 and 2 that is yet unknown in function (Xu *et al.* 2009).

H^+ gradient-driven RND-type IMFs are proposed to form trimers (Murakami *et al.* 2002). Each monomer consists of a CM-integral domain and a large periplasmic domain protruding approximately 7 nm into the periplasm. In contrast to other IMFs, RND exporters were demonstrated to bind to the OMF (Tamura *et al.* 2005).

The oligomeric state of the H^+ gradient-driven MF-type IMFs is controversially discussed (Borges-Walmsley *et al*. 2003; Yin *et al*. 2006; Sigal *et al*. 2007; Tanabe *et al*. 2009). MF-type IMFs are not predicted to have RND- or ABC-like periplasmic domains (Zgurskaya 2009).

1.3.2 Membrane fusion proteins

MFPs are located in the periplasm and act on both membranes to enable drug efflux across the whole cell envelope. They are thought to enable the functional fit between conserved OMFs and diverse IMFs (Zgurskaya *et al.* 2009). They differ from each other in sequence, molecular mass and biochemical attributes, but they are similar with respect to their overall structure (Tikhonova *et al*. 2009).

A typical ABC-type MFP consists of the following structural elements: an N-terminal cytoplasmic tail, a transmembrane anchor in the CM, a CM proximal β-roll, a β-barrel domain, a lipoyl domain and an α-helical domain protruding towards the OMF (Zgurskaya 2009). ABC-type MFPs are assumed to stimulate the ATPase activity of the respective ABC-type IMF, and to actively recruit the OMF to the tripartite complex (Modali and Zgurskaya 2011).

In contrast to ABC-type MFPs, a typical RND-type MFP lacks a cytoplasmic tail and a CM anchor. Instead, the N-terminus is anchored to the CM by a lipid modification. In addition, their α-helical domain is shorter than the ones from ABC-type MFPs (Zgurskaya 2009). RND-type MFPs are assumed to form stable complexes with the OMF, and not to recruit the OMF in an ABC-type MFP-like manner (Tamura *et al*. 2005; Touzé *et al.* 2004; Tikhonova *et al.* 2004)
Like their ABC-type counterparts, MF-type MFPs are predicted to have a cytoplasmic tail and a membrane anchor in the CM (Zgurskaya 2009). MF-type MFPs were shown to bind the substrate of the EP (Borges-Walmsley *et al.* 2003).

1.3.3 Outer membrane factors

OMFs are structurally conserved trimers belonging to the TolC superfamily. They form a β-barrel pore through the OM and extend approximately 10 nm into the periplasm with an α-helical tunnel-like domain (Koronakis *et al.* 2000). Since the same OMF can be used in very different types of efflux pumps, this "channel-tunnels" provide a promiscuous exit duct for various substrates (Koronakis *et al.* 2004; Zgurskaya *et al.* 2011).

1.3.4 Topology of tripartite efflux pumps

The RND-type EP AcrAB-TolC was assumed to assemble in a molar ratio of 3:3:3 of the IMF AcrB to the MFP AcrA to the OMF TolC (Lobedanz *et al*. 2007; Bavro *et al.* 2008; Symmons *et al.* 2009). AcrAB-TolC is involved in providing general chemical stress and antibiotic resistance by exporting a large variety of substrates (Zgurskaya 2009). *In vivo* cross-linking revealed distinct contact sites in the distal α-helical domain of the MFP AcrA and the distal α-helical barrel of the OMF TolC. It was proposed that AcrA\`s α-helical domain docks into pockets provided by the surface of TolC\`s helices 7/8 and 3(/4). Thus, three molecules of AcrA would wrap around TolC (Lobedanz *et al*. 2007; Fig. 4A, next page). Furthermore, the IMF AcrB was shown to be in direct contact with TolC (Tamura *et al*. 2005; Touzé *et al.* 2004; Tikhonova *et al.* 2004; Fig. 4B, next page).

Crystals of MacA, the MFP of the ABC-type efflux pump MacAB-TolC, suggest a completely different pump topology (Yum *et al.* 2009). MacAB-TolC is involved in the export of macrolides (Kobayashi *et al.* 2001) and heat stable enterotoxin II (Yamanaka *et al.* 2008). In the bridging model proposed by Yum *et al*. (2009), a hexameric MFP MacA is assumed to connect the IMF MacB and the OMF TolC. Here, MacA and TolC interact in a cogwheel-like assembly between the tip-regions of the α-helical domain of MacA and of the α-helical barrel of TolC (Fig. 4C). Despite sharing common structural motifs with the TolC-docking domain of AcrB (Fig. 4D), the periplasmic domain of the IMF MacB is not assumed to be in stable contact with TolC (Xu *et al*. 2009).

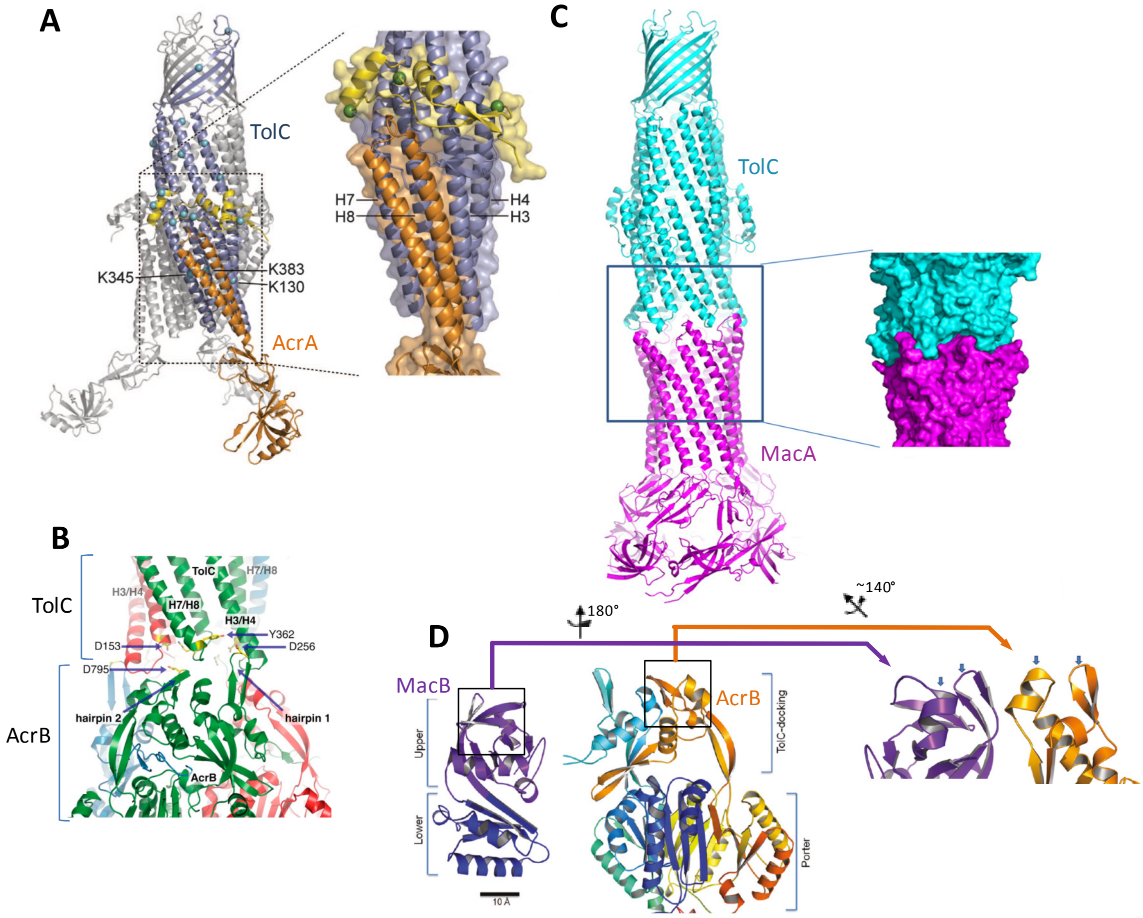

Figure 4. Efflux pump topology of RND-type pump and of ABC-type pumps

(A) Wrapping model of the interaction of the MFP AcrA with the OMF TolC (taken from Lobedanz *et al*. 2007 and modified). **(B)** Docking of TolC to AcrB (taken from Bavro *et al*. 2008 and modified). **(C) Bridging model** of the interaction of the MFP MacA with the OMF TolC (taken from Xu *et al.* 2010 and modified). **(D)** Common structural motifs of the periplasmic domains of MacB (purple) and AcrB (orange and blue). Arrows indicate (putative) characteristic structural motifs (taken from Xu *et al*. 2009 and modified).

Recent studies confirmed a bridging model assuming a hexameric MFP MacA tip-to-tip interacting with the OMF TolC: a native MacA hexamer interacted with a MacA hexamer carrying the tip regions of TolC`s α-helical barrel instead of the native ones. The stable association of this complex was captured by (cryo) electron microscopy (Xu *et al.* 2010; Fig. 5).

Interestingly, a similar tip-to-tip interaction of the RND-type MFP AcrA and the OMF TolC was observed by using the same technique. Here, a MacA hexamer carrying the α-helical domain of AcrA interacted with the MacA-αTolC-hybrid mentioned above (Xu *et al.* 2011; Fig. 5). In addition, the RND-type efflux pump MtrCDE from *N. gonorrhoeae* was shown to adopt a 3:6:3 ratio of the IMF to the MFP to the MtrE (Janganan *et al.* 2011; MtrCDE is involved in providing general chemical stress and antibiotic resistance).

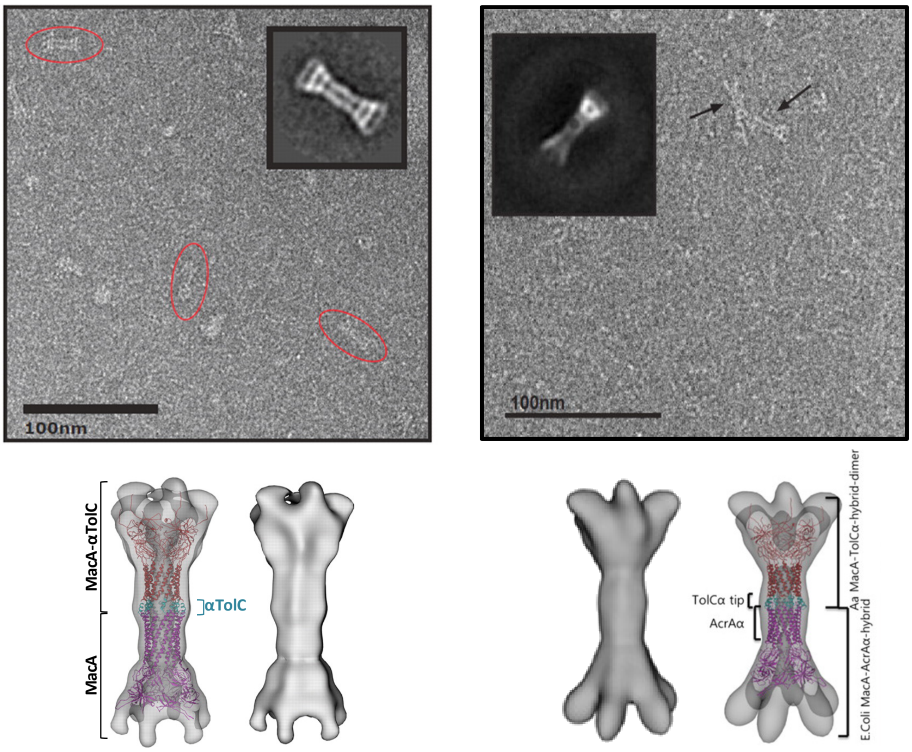

Figure 5. Tip-to-tip interfaces between MacA and TolC, and between AcrA and TolC

Cryo electron micrographs of MacA hexamers interacting with MacA-TolC-hybrid (on the left; taken from Xu *et al.* 2010) and of Mac-TolC-hydrids interacting with MacA-AcrA-hybrids (on the right; taken from Xu *et al.* 2011). MacA-TolC-hybrids are MacA proteins carrying the tip-regions of TolC instead of the native ones. MacA-AcrA hybrids are MacA proteins carrying the α-helical domain of AcrA instead of the native one.

1.4 *Anabaena* sp. strain PCC 7120

The filamentous bacterium *Anabaena* sp. PCC 7120 (referred to as *Anabaena* in the following) is a model organism for studying prokaryotic multicellularity, cell differentiation and nitrogen fixation. It is a representative of the diverse phylogenetic group of cyanobacteria. *Anabaena* is an obligate photoautotroph: it produces reduction equivalents and ATP by converting solar energy into membrane potential. It uses CO_2 as carbon source, which is fixed in the Calvin cycle. *Anabaena* forms filaments of >100 photosynthetic active vegetative cells in presence of combined nitrogen (Wolk *et al*. 1994; Fig. 6).

Like the cell envelope of any other Gram-negative bacterium, the one of *Anabaena* is composed of a CM and an OM comprising the periplasm and the peptidoglycan in between. The diameter of the periplasm was reported to be unusually large (~46 nm; Wilk *et al.* 2011), and therefore it is larger than the periplasm of most Gram-negative bacteria. Also, the peptidoglycan was reported to be much thicker (Hoiczyk and Hansel 2000) Due to *Anabaena*`s filamentous shape, only the CM is exclusive to each single cell, while the OM surrounds the entire filament. So, the OM and the periplasm are continuous for the whole filament (Flores *et al*. 2006, Mariscal *et al.* 2007). In addition, *Anabaena* has a third type of membrane: the intracellular thylakoid membrane (TM). Thylakoid membranes encompass the thylakoid lumen, an additional compartment inside the cytoplasm. In general, thylakoids are the site of photosynthesis and of subsequent light-dependent reactions like ATP synthesis and providing reducing equivalents (Gantt 1994).

Figure 6. *Anabaena* sp. PCC 7120

Vegetative filament of *Anabaena* (courtesy of Iris Maldener). Bar = 1 µm.

1.5 Heterocyst maturation in *Anabaena* sp. strain PCC 7120

Anabaena is able to reduce atmospheric N_2, and to assimilate reduced nitrogen via the GS-GOGAT cycle (Wolk *et al.* 1994). The key enzymes for N_2 fixation are termed nitrogenase system, an O_2-sensitive enzyme complex. Due to this sensitivity, nitrogen fixation and oxygenic photosynthesis are incompatible *a priori*.

To challenge this problem, *Anabaena* evolved a strategy of spatially separating both processes (Wolk *et al.* 1994): upon depletion of the combined nitrogen source, some vegetative cells develop into nitrogen-fixing heterocysts (Fig. 7) in a semi-regular pattern. This differentiation is completed within one generation time (~ 20-24 h), and it is not reversible. Heterocysts inactivate and degrade the oxygen-evolving photosystem II, increase the O_2 consumption, and develop additional layers on the top of their Gram-negative cell envelope to decrease the amount of O_2 that enters the heterocyst. The outermost additional layer is composed of polysaccharides (heterocyst envelope polysaccharides (HEPs)) and protects a so-called laminated layer below (Fig. 7). The laminated layer represents the actual barrier for O_2 diffusion. It is composed of heterocyst-specific glycolipids (HGLs).

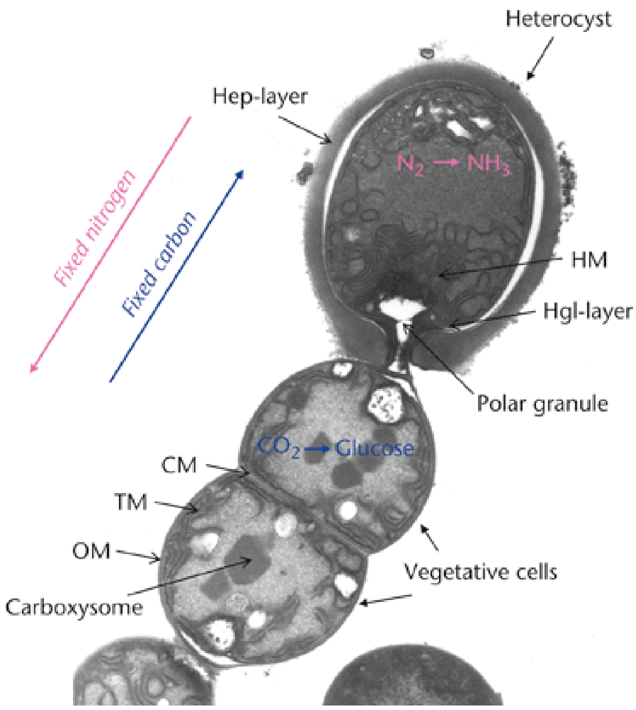

Figure 7. Mutual metabolite exchange between vegetative cells and heterocysts

Electron micrograph of a terminal heterocyst and vegetative cells of *Anabaena* (taken from Maldener and Muro-Pastor 2010).

Taken these adaptations together, *Anabaena* filaments are able to provide a microoxic environment for the fixation of N_2 despite simultaneously performing oxygenic photosynthesis. So, during nitrogen starvation both cell types of the filament rely on mutual metabolite exchange: while heterocysts provide vegetative cells with fixed nitrogen compounds, they in return obtain fixed carbon and reductants necessary for the assimilation of atmospheric N_2.

1.6 Tripartite efflux pumps involved in heterocyst maturation

Knock-out mutations in the *Anabaena* genes *alr3710*, *alr3711* or *alr3712* result in immature heterocysts which are unable to grow on N_2 as sole nitrogen source. Mutants in these genes did not form the laminated layer (Fig. 8B, Fig. 8A = wild type), although the synthesis of the HGLs was not impaired (Maldener *et al.* 1994; Fiedler *et al.* 1998). It has been shown that *devBCA* are induced in the course of heterocyst maturation, and that their transcription rates depend on NtcA and HetR (Fiedler *et al.* 2001; Olmedo-Verd *et al.* 2005). In general, NtcA and HetR were shown to regulate the transcription of genes responsible for heterocyst differentiation and nitrogen metabolism (Zhang *et al.* 2006). The genes *alr3710*, *alr3711*, and *alr3712* were shown to be arranged in an operon encoding subunits of an ATP-driven EP. *Alr3710* was predicted to encode an MFP, *alr3711* the SBD of an ABC-type IMF, and *alr3712* the associated NBD (Fiedler *et al.* 1998). Due to their contribution to heterocyst <u>dev</u>elopment, the genes were termed *devBCA*.

Alr2887 was predicted to encode a TolC-like OMF (Maldener *et al*. 2003, Moslavac *et al.* 2007). As a knock-out mutation of *alr2887* led to the same laminated layer-lacking phenotype as mutations in *devBCA* (Fig. 8C), DevBCA-TolC were assumed to form an tripartite ATP-driven *trans*-envelope efflux pump involved in the export and deposition of heterocyst glycolipids (Fig. 8D). Therefore, Alr2887 was designated HgdD (<u>h</u>eterocyst <u>g</u>lycolipid <u>d</u>eposition protein <u>D</u>). HgdD is the only one TolC-like OMF predicted from the genome of *Anabaena* (Moslavac *et al.* 2007). Alr2887/HgdD will be referred to as TolC in the following work.

Nevertheless, it remained unclear which substrate the postulated DevBCA-TolC machinery would gate the periplasm for. Three possibilities were suggested:

(**i**) transport of HGLs (1-(O-α-D-glucopyranosyl)-3,25-hexacosanediol and the 3-keto-tautomer) or their moieties, (**ii**) transport of assembly factors like proteins or unknown compounds required for the formation of the laminated layer, or (**iii**) both (Moslavac *et al.* 2007).

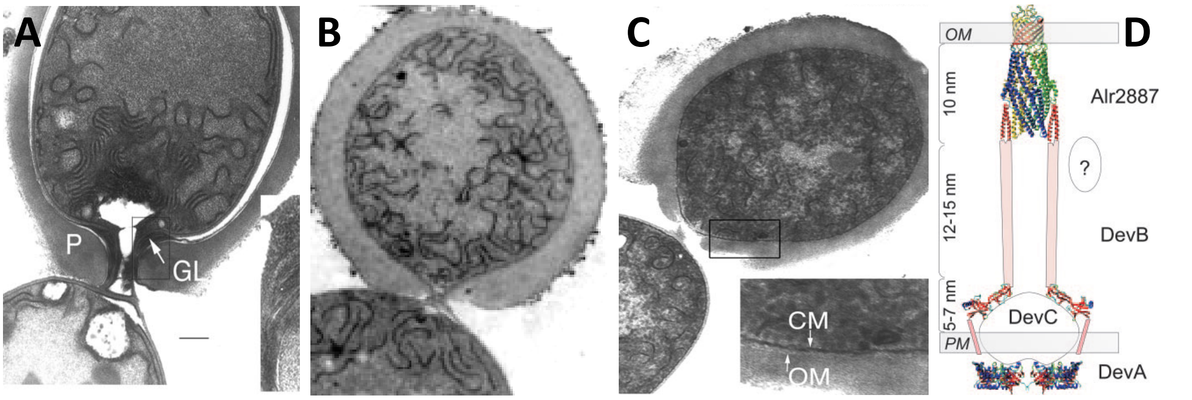

Figure 8. DevBCA-TolC is involved in the formation of the laminated layer

(A) Electron micrograph (EM) of wild type heterocysts of *Anabaena* sp. PCC 7120 (taken from Moslavac *et al.* 2007). P = HEP-layer, GL = laminated layer **(B)** EM of a heterocyst of a *devA* (*alr3712*) transposon mutant (taken from Fiedler *et al*. 1998). **(C)** EM of a heterocyst of a *tolC* (*alr2887*) knock-out mutant (taken from Moslavac *et al.* 2007). **(D)** Model of the DevBCA-TolC export machinery (taken from Moslavac *et al.* 2007).

Mutations in *all5346* or *all5347* lead to heterocysts showing aberrant laminated layers (Fig. 9). Both genes seem to be involved into the correct spatial and temporal assembly of the O_2-diffusion barrier (Fan *et al.* 2005). While a mutant in *all5346* shows an unusually thick HGL layer at the heterocyst pole, a mutant in *all5347* shows two laminated layers. Latter mutant seems to deposit HGLs twice, *i.e.* before and after the HEP has been formed (and *vice versa*; not shown). Due to their function in encoding proteins necessary for the correct deposition of heterocyst glycolipids, *all5346* and *all5347* were designated *hgdC* and *hgdB* (heterocyst glycolipid deposition proteins C and B). *HgdC* is predicted to encode the SBD of an ABC-type IMF homologous to DevC, while *hgdB* encodes an MFP homologous to DevB. The associated NBD has not been determined yet. Nevertheless, HgdC and HgdB are candidates to form an EP together with TolC.

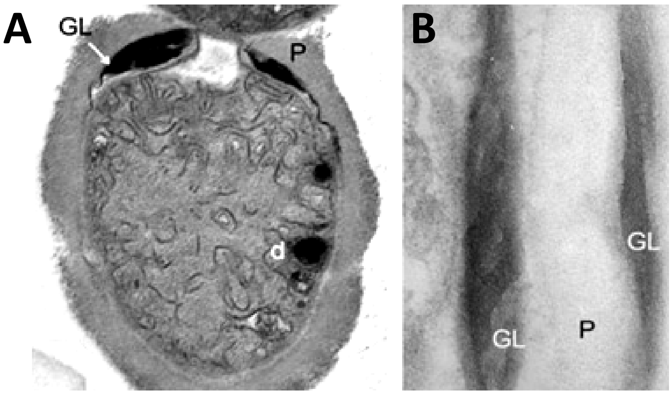

Figure 9. All5346 and All5347 are involved in the formation of the HGL layer

The electron micrographs showing a mutant in *all5436* **(A)** and in *all5347* **(B)** were taken from Fan *et al.* (2005). GL = laminated layer, P = HEP-layer.

1.7 Objectives

Since mutations in *devBCA* and *tolC* led to the same laminated layer-lacking phenotype (1.6), it was suggested that DevBCA-TolC form a tripartite *trans*-envelope efflux pump system required for the deposition of the laminated layer.

One major goal of this work was to prove this assumption. Therefore, the formation of a putative DevBCA-TolC complex should be demonstrated *in vitro* and *in vivo*. For studies *in vitro*, the participants should be heterologously expressed and purified from *E. coli*, and their interaction was intended to be analyzed in surface plasmon resonance and isothermal titration calorimetry. If the purified proteins and the measured interaction turned out to be stable, the investigation of further protein variants should provide a deeper insight into the complex formation of ATP-driven efflux pumps/type 1 secretion systems in general. These protein variants were modified in their structural characteristics, and they should reveal contact sites and stoichiometric relations between the cytoplasmic membrane-integral protein DevAC, the outer membrane-integral protein TolC, and the periplasmic connector DevB. For studies *in vivo*, tagged baits of the innermost participant DevA or the outermost participant TolC should be introduced into *Anabaena* sp. PCC 7120. The tags would allow purification of either DevA or TolC together with its interacting proteins, maybe including DevC and DevB. In both cases, the assumed remaining participants of DevBCA-TolC should be immunodetected.

Another important aspect of this work was to identify substrates of DevBCA-TolC. Since DevA is predicted to contain an ATPase domain, the substrate binding domain DevC and DevA could possibly react toward the presence of substrates. So, a fusion protein of DevA and DevC should be exposed to different fractions of *Anabaena* sp. PCC 7120, and the ATPase activity should be monitored. In another approach, DevBCA and TolC should be to incorporated into two different proteoliposomes, and the translocation of substrate mixes from one liposome to the other should be analyzed.

With *all5347* and *all5346*, two further genes have been identified that are predicted to encode very close homologues to DevB and DevC. Both are involved in heterocyst maturation. Another goal of this work was to analyze further homologues of DevB involved in heterocyst maturation. They should be determined *in silico*, and knock-out mutants should be constructed to investigate their contribution toward diazotrophic growth.

2. *In silico* analysis of DevBCA and TolC

2.1 Background

Between the first detailed description of *devBCA*`s gene function (Fiedler *et al.* 1998), the first prediction of DevBCA-TolC (Moslavac *et al.* 2007), and this work, a plenty of data was risen on Gram-negative EPs. Many at that time unknown EPs in various organisms have been detected -and some known have been extensively described (*e.g.* MtrCDE (Janganan *et al.* 2011))- but also some milestones have been achieved (*e.g.* the crystallization of the ABC-type MFP MacA as first of its kind (Yum *et al.* 2009)). This work will have a strong focus on structural details of ATP-driven EPs. Previous works on DevBCA-TolC did not have such a strong structural intention, and they did not have a large amount of mechanistical and structural data available today. In the following chapter, DevBCA and TolC will be more extensively investigated regarding their structural (and functional) properties *in silico*.

2.2 Methods

Protein sequences

All protein sequences were obtained from the NCBI protein database. The accession numbers were NP_487750.1 for DevB, NP_487751.1 for DevC, NP_487752.1 for DevA, and BAB74586.1 for TolC. The accession numbers of proteins compared to DevBCA and TolC are given in the respective figure legends.

Prediction of protein function

Function predictions were performed by using NCBI CDD (Conserved Domain Database; Marchler-Bauer *et al.* 2011). Further informations were obtained by using NCBI`s protein BLAST (Altschul *et al.* 1997), and by using ClustalOmega 1.0.3 (Sievers *et al.* 2011).

Prediction of secondary structures and transmembrane helices

Secondary structures were predicted by using MINNOU (Membrane protein identification without explicit use of hydropathy profiles and alignments, Cao *et al.* 2006). Predictions were verified by using Jpred3 (Cole *et al.* 2008). Predictions of transmembrane helices were also performed by using MINNOU, and the results were verified by TMHMM 2.0c (Krogh et al. 2001). The shown illustrations are based on this data (the most important predictions of MINNOU are shown in appendix 11.1, pages 117-123), and they were created in Power Point 2010 (Microsoft).

Prediction of DevB`s tertiary structure

The tertiary structure model of DevB was created by using PyMol 1.5 (The PyMOL Molecular Graphics System, Version 1.2r3pre, Schrödinger, LLC). DevB was modeled on the basis of the crystal structure of MacA from *E. coli* available at the RCDS protein databank (DOI: 10.2210/pdb3fpp/pdb). The sequence of the DevB was introduced via the "mutagenesis" command of PyMOL, the secondary structures were corrected by the "alter" command. The basis for assigning secondary structures was the prediction by using MINNOU (described above). Additionally, identical and homologous positions were assigned by using ClustalOmega 1.0.3.
It should be noted that the created model does not claim validity. It was created to illustrate DevB and to support the design of further experiments described later in this work.

Illustration of DevA`s, DevC`s and TolC`s tertiary structure

The tertiary structures of DevA and TolC were not modeled as it has been done for DevB. The illustrated proteins are homologues of DevA and of TolC respectively. Their structures are available at the RCDS protein databank. To roughly picture DevA, the homologous nucleotide binding domain MJ0796 from *Methanocaldococcus jannaschii* is shown (DOI: 10.2210/pdb1f3o). To illustrate *Anabaena*`s TolC, the OMF TolC from *E. coli* is shown (DOI: 10.2210/pdb1ek9). DevC could only be partially illustrated, since only one homologue of DevC (MacB from *Aggregatibacter actinomycetemcomitans*) could only be partially crystallized to date (DOI: 10.1021/bi900415t).

2.3 Results

2.3.1 DevB

As already mentioned by Fiedler *et al.* (1998), *in silico* analysis predicts *devB* to encode an MFP. DevB is classified as a heterocyst_DevB-like MFP (Fig. 10). This family is mostly found in (filamentous and unicellular) cyanobacteria and planctomycetes. In contrast to former studies comparing DevB with HlyD, an MFP of the HlyBD-TolC T1SS involved in exporting hemolysin (Holland *et al.* 2005), this classification is much more accurate (CDD`s E-value 9.39e-66 to 8.27e-11). DevB is also distantly related to RND-type MFPs (E-value 1.09e-06), and to MF-type MFPs (1.66e-08). Like any MFP (Zgurskaya 2009), DevB contains biotinyl-lipoyl domains of unknown function (Fig. 10).

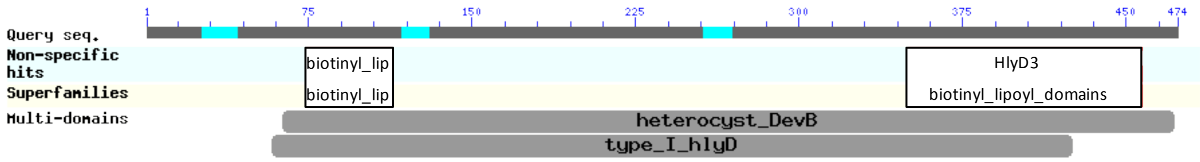

Figure 10. CDD analysis of DevB

DevB was analyzed by using NCBI CDD (2.2). This figure shows a part of the full results. The picture was modified for better readability. The numbers refer to numerical aa positions.

DevB shows following structural elements: an N-terminal cytoplasmic tail, a transmembrane helix, a β-barrel domain, a lipoyl domain, and an unusually large α-helical coiled-coil domain of up to 17 nm in lenght (Fig. 11 and 12, next page). To date crystallized MFPs from *E. coli* show α-helical domains ranging from ~4.5 nm (RND-type MFP MexA) to ~6.7 nm (ABC-type MFP MacA) in length. In *E. coli*, the longest MFP is considered to be HlyD with a predicted α-helical domain of ~10.8 nm. Like all members of the heterocyst_DevB family in *Anabaena*, DevB is lacking a β-roll domain present in most other described MFPs (Zgurskaya 2009; Fig. 11, next page).

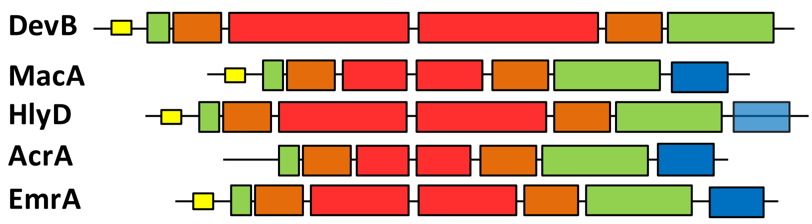

Figure 11. Structural elements of DevB in comparison to prominent MFPs

Secondary structures and transmembrane helices were predicted by using MINNOU (2.2; Fig. 32-35 in appendix 11.1, page 117 and 118). Yellow = transmembrane helix; green = β-barrel domain; brown = lipoyl domain; red = α-helical domain; blue = β-roll. MacA (accession no. BAA35597.1) = ABC-type MFP from MacAB-TolC; HlyD (CAA74193.1) = ABC-type MFP from HlyBD-TolC; AcrA (AEK27039.1) = RND-type MFP from AcrAB-TolC. EmrA (BAA16547.1) = MF-type MFP from EmrAB-TolC.

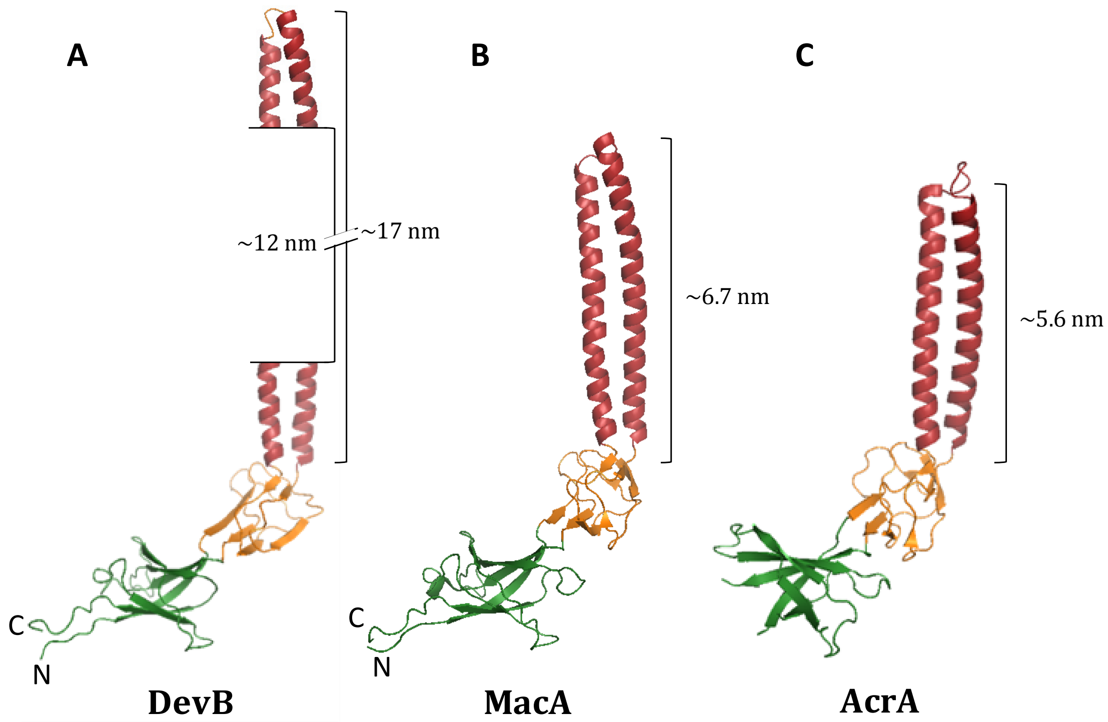

Figure 12. Tertiary structure of DevB, MacA, and AcrA

Red = α-helical domain; brown = lipoyl domain; green = β-barrel domain; N = N-terminus; C = C-terminus. **(A)** Theoretical model of DevB based on the crystal structure of MacA from *E. coli* (DOI: 10.2210/pdb3fpp/pdb). In PyMOL (2.2), MacA was refined by introducing secondary structures of DevB predicted by MINNOU (2.2). The N-terminal transmembrane helix was not modeled. **(B)** Crystal structure of the ABC-type MFP MacA from *E. coli*. The N-terminal transmembrane helix was not solved. **(C)** Crystal structure of the RND-type MFP AcrA from *E. coli* (DOI: 10.2210/pdb2f1m/pdb). The β-barrel domain was not completely solved.
There are no crystal structures of MF-type MFPs yet.

2.3.2 DevC

The gene *devC* is predicted to encode the SBD of an ABC-type IMF. DevC is classified as DevC-type protein family frequently found in cyanobacteria. It shows similarities to the periplasmic core domain (PCD) of MacB (Fig. 13), the IMF of the MacAB-TolC EP involved in exporting macrolides (Kobayashi *et al.* 2001). Both C-termini of DevC and of MacB show homologies to FtsX, the SBD of FtsEX (Fig. 13). This ABC exporter is crucial for cell division, but the transport function is not clearly known yet (Yang *et al.* 2011). Further prominent representatives of the MacB_PCD superfamily are LolC and LolE, two slightly different SBDs of the ABC exporter LolCDE that was shown to be involved in lipid trafficking to the OM (Tokuda 2009).

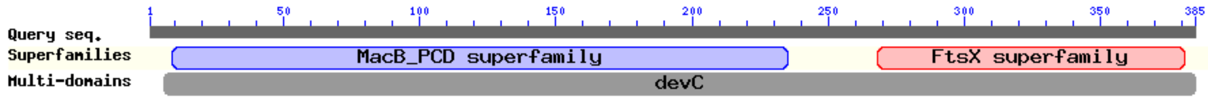

Figure 13. CDD analysis of DevC

DevC was analyzed by using NCBI CDD (2.2). This figure shows the concise results. The numbers refer to numerical aa positions.

Like any typical ABC-type IMF (e.g. Fig, 42-45 in appendix 11.1, pages 120 and 121), DevC has 4 transmembrane helices, and a MacB-like periplasmic core domain (MacB_PCD in Fig. 13) between helices 1 and 2. A partial model of MacB`s (and therefore DevC`s) tertiary structure is given in Fig. 14 (next page).

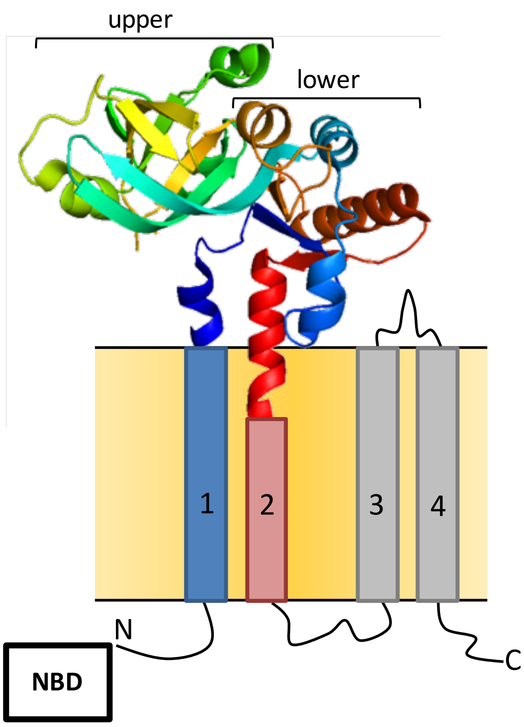

Figure 14. Model of the DevC homologue MacB

Draft of the transmembrane helices in the cytoplasmic membrane (orange) combined with the crystal structure of the periplasmic core domain of MacB from *A. actinomycetemcomitans* (DOI: 10.2210/pdb3ftj/pdb; compare Fig. 4D, page 10 and Fig, 42-45 in appendix 11.1, pages 120 and 121). Numerics indicate the helix number. N = N-terminus; C = C-terminus; the relative position of the NBD is indicated.

2.3.3 DevA

The gene *devA* is predicted to encode a highly conserved NBD of an ABC-type IMF. DevA is classified as member of the ABC_MJ0796_Lol1CDE_FtsE family (Fig. 15). LolD, FtsE, and the NBD of MacB are the NBDs of the ABC exporters LolCDE and FtsEX, and of the T1SS MacAB-TolC mentioned above (2.3.2).

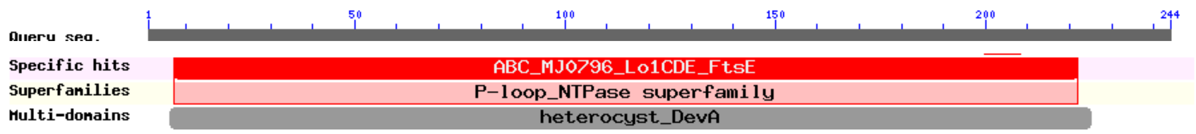

Figure 15. CDD analysis of DevA

DevA was analyzed by using NCBI CDD (2.2). This figure shows the concise results. The numbers refer to numerical aa positions.

The nucleotide binding domain DevA is not translationally fused to the substrate binding domain DevC like in e.g. MacB (Zgurskaya 2009). However, it shows a typical ABC fold (Fig. 16).

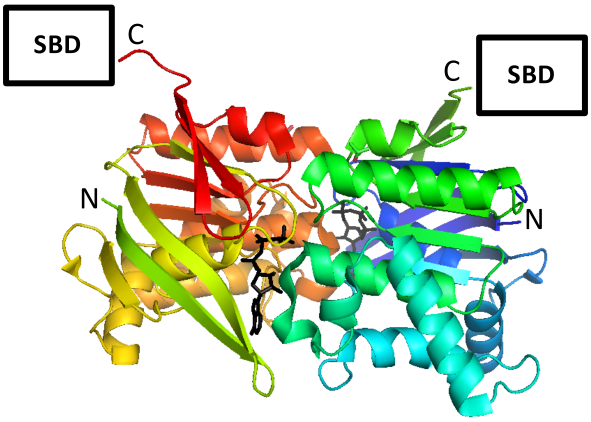

Figure 16. Quaternary structure of a homologue of DevA

Crystal structure of a MJ0796 dimer from *Methanocaldococcus janaschii* (DOI: 10.2210/pdb1l2t/pdb). In black = ATP; N = N-terminus; C = C-terminus; the relative position of the SBD is indicated.

2.3.4 TolC

The gene *tolC* (*hgdD*) is predicted to encode an outer membrane protein belonging to the TolC family (Fig. 17; and see Moslavac *et al.* 2007). It is the only TolC-like protein encoded in the genome of *Anabaena* sp. PCC 7120. The first 287 aa`s of TolC do not encode parts of any known OMF. They are not clearly related to a known OM-function (PRK14971 would refer to DNA polymerase III subunits gamma and tau; Fig. 17). Starting from aa 288, TolC represents a typical OMF as known from other Gram-negative bacteria.

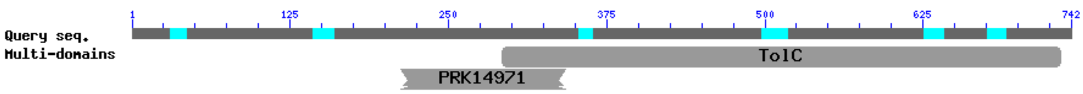

Figure 17. CDD analysis of TolC

TolC was analyzed by using NCBI CDD. This figure shows the concise results. The numbers refer to numerical aa positions.

TolC does not seem to have remarkable differences in domain substructure or domain size as compared to other crystallized homologues (Fig. 18; Fig. 48/49, appendix 11.1, pages 122 and 123).

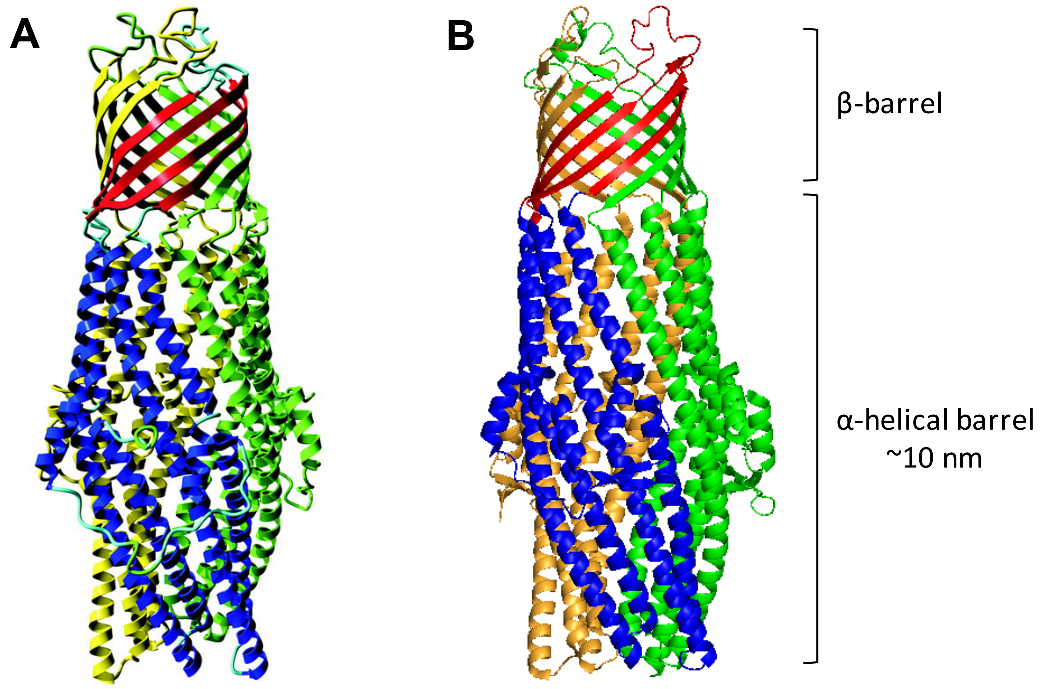

Figure 18. Quaternary structure of a TolC trimer from *Anabaena* and from *E. coli*

(A) Theoretical quaternary structure of TolC from *Anabaena* (taken from Moslavac *et al*. 2007).
(B) Crystal structure of TolC from *E. coli* (DOI:10.2210/pdb1ek9/pdb).
Compare Fig. 48 and 49 in appendix 11.1, pages 122 and 123.

2.4 Summary

The genes *devBCA* and *tolC* encode subunits of an ABC-type EP. DevB differs from known ABC-type MFPs in the larger size of its α-helical domain, and it lacks a β-roll domain. DevA and DevC represent a typical ABC-type IMF. DevAC show high structural similarities to ABC exporters not utilizing MFPs, but also to the EP-type ABC exporter MacB. Besides the unstructured N-terminus, *Anabaena*`s TolC seems to represent a typical TolC-like OMF. MacAB-TolC seems to be the most comparable system to DevBCA-TolC described so far.

3. Publication: Novel ATP-driven pathway of glycolipid export involving TolC protein

THE JOURNAL OF BIOLOGICAL CHEMISTRY VOL. 286, NO. 44, pp. 38202–38210, November 4, 2011

Novel ATP-driven Pathway of Glycolipid Export Involving TolC Protein*[S]

Received for publication, June 19, 2011, and in revised form, September 13, 2011 Published, JBC Papers in Press, September 14, 2011, DOI 10.1074/jbc.M111.269332

Peter Staron, Karl Forchhammer, and Iris Maldener[1]

From the Department of Microbiology/Organismic Interactions, Interfaculty Institute of Microbiology and Infection Medicine Tübingen, University of Tübingen, 72076 Tübingen, Germany

Background: The ABC exporter DevBCA and the outer membrane protein TolC are necessary for maturation of heterocysts in filamentous cyanobacteria.
Results: DevBCA-TolC form an ATP-driven efflux pump and export heterocyst-specific glycolipids.
Conclusion: DevBCA-TolC provide a novel pathway for glycolipid export.
Significance: Mechanistic details of efflux pumps/ABC exporters are important for understanding various bacterial processes such as cell differentiation, acclimatization processes, or drug resistance.

Upon depletion of combined nitrogen, N_2-fixing heterocysts are formed from vegetative cells in the case of the filamentous cyanobacterium *Anabaena* sp. strain PCC 7120. A heterocyst-specific layer composed of glycolipids (heterocyst envelope glycolipids (HGLs)) that functions as an O_2 diffusion barrier is deposited over the heterocyst outer membrane and is surrounded by an outermost heterocyst polysaccharide envelope. Mutations in any gene of the *devBCA* operon or *tolC* result in the absence of the HGL layer, preventing growth on N_2 used as the sole nitrogen source. However, those mutants do not have impaired HGL synthesis. In this study, we show that DevBCA and TolC form an ATP-driven efflux pump required for the export of HGLs across the Gram-negative cell wall. By performing protein-protein interaction studies (*in vivo* formaldehyde cross-linking, surface plasmon resonance, and isothermal titration calorimetry), we determined the kinetics and stoichiometric relations for the transport process. For sufficient glycolipid export, the membrane fusion protein DevB had to be in a hexameric form to connect the inner membrane factor DevC and the outer membrane factor TolC. A mutation that impaired the ability of DevB to form a hexameric arrangement abolished the ability of DevC to recognize its substrate. The physiological relevance of a hexameric DevB is shown in complementation studies. We provide insights into a novel pathway of glycolipid export across the Gram-negative cell wall.

Efflux pumps are widespread among Gram-negative bacteria and mediate the secretion of various proteins and a wide variety of other molecules (1–5). They bridge the periplasm, allowing a one-step transfer of substrates beyond the outer membrane. Typical efflux pumps consist of three components: (i) an inner membrane factor (IMF),[2] (ii) a periplasmic membrane fusion protein (MFP), and (iii) an outer membrane factor (OMF; supplemental Fig. S1). The OMFs are usually structurally conserved trimers belonging to the TolC superfamily. They form a pore through the outer membrane and extend into the periplasm with an α-helical tunnel-like domain (6–8). MFPs vary in sequence, molecular mass, and biochemical attributes but are similar with respect to the overall structure that includes an α-helical domain, a lipoyl domain, and a β-barrel domain (6, 9–14). IMFs belong to the following three superfamilies that differ with respect to topology, oligomerization state, and energy source: resistance-nodulation-division, major facilitator, and ATP-binding cassette (ABC) (15–17).

Although several proteobacterial efflux pumps have been largely investigated, very little is known about cyanobacterial systems. For the filamentous cyanobacterium *Anabaena* strain PCC 7120, only one potential TolC-involving ABC-type exporter has been proposed on the basis of mutational analysis and *in silico* predictions: DevBCA (also referred to as Alr3710/3711/3712) could possibly be a part of an efflux pump together with the only TolC member predicted in the sequence of *Anabaena* sp. PCC 7120 genome (also referred to as HgdD or Alr2887) (18–22). The *devB* gene is predicted to encode a MFP-like protein; *devC*, the substrate-binding domain of an IMF; and *devA*, the nucleotide-binding domain of an IMF. Mutations in any gene of the *devBCA* operon or *tolC* lead to the loss of one of the key characteristics of *Anabaena* sp.: diazotrophic growth.

Upon depletion of the combined nitrogen source, some of the vegetative cells of the *Anabaena* sp. PCC 7120 filament develop into nitrogen-fixing heterocysts (23). These specialized cells provide the photosynthetic active filament with fixed nitrogen and conversely obtain reductants and carbohydrates for N_2 fixation. Heterocysts inactivate and degrade the oxygen-evolving photosystem II, increase O_2 consumption, and develop a specific envelope outside their Gram-negative cell

* This work was supported by the Deutsche Forschungsgemeinschaft (DFG-Ma1359/5-1).

[S] The on-line version of this article (available at http://www.jbc.org) contains supplemental Tables S1 and S2 and Figs. S1–S4.

[1] To whom correspondence should be addressed: Dept. of Microbiology/Organismic Interactions, Auf der Morgenstelle 28, 72076 Tübingen, Germany. Tel.: 49-7071-29-78847; Fax: 49-7071-29-5843; E-mail: iris.maldener@uni-tuebingen.de.

[2] The abbreviations used are: IMF, inner membrane factor; HGL, heterocyst glycolipid; OMF, outer membrane factor; MFP, membrane fusion protein; ABC, ATP-binding cassette; SPR, surface plasmon resonance; ITC, isothermal titration calorimetry; 8H, octahistidine; 6H, hexahistidine tag; RU, resonance units.

wall to decrease the amount of O_2 that enters into the cell (23, 24). The envelope consists of two distinct layers: the outer layer is composed of polysaccharides (heterocyst envelope polysaccharides) and protects a so-called laminated layer below. The laminated layer represents the actual barrier for O_2 diffusion. It is composed of specific glycolipids (heterocyst envelope glycolipids (HGLs)) (23, 25–27). Several genes encoding proteins putatively involved in synthesis of the HGLs (1-(*O*-α-D-glucopyranosyl)-3,25-hexacosanediol and the 3-ketotautomer) have been identified (28–30); however, the transport of HGLs and assembly of the laminated layer remained unclear. Mutations in *devBCA* or *tolC* result in the absence of the HGL layer, but the synthesis of HGLs is not impaired; therefore, it was assumed that TolC-DevBCA form an efflux pump involved in the transport and/or assembly of the HGL layer (19–21). Nevertheless, it remained unclear which substrate is transported by the postulated TolC-DevBCA machinery across the cell wall. Three possibilities were suggested: (i) transport of HGLs or their moieties, (ii) transport of assembly factors like proteins or unknown compounds required for the formation of the laminated layer, or (iii) both.

In this work, we show that TolC-DevBCA form an ATP-driven efflux pump mediating the export of entire HGLs from the location of their synthesis, the cytoplasmic membrane, to beyond the outer membrane. The exporter requires a distinct stoichiometry that includes a hexameric MFP DevB to recognize and export its substrate.

EXPERIMENTAL PROCEDURES

Anabaena Strains and Growth Conditions—The *Anabaena* strains used in this study are listed in Table 1. Wild-type *Anabaena* sp. PCC 7120 was grown photoautotrophically at 28 °C in liquid $BG11_0$ medium (31). Mutants that could not fix N_2 were grown in $BG11_0$ medium supplemented with 5 mM NH_4Cl and 5 mM TES-NaOH buffer, pH 7.8. The different *Anabaena* mutant strains were grown in the presence of the appropriate antibiotics listed in Table 1 (for applied concentrations, see (18–21)). Media were solidified with 1.5% agar (Difco, Heidelberg, Germany). Induction of heterocyst formation, isolation, and fractioning of cell compartments were performed as described previously (20).

Generation of Mutant Anabaena Strains—All of the *Anabaena* mutants were generated by triparental mating as described previously (32), aiming for single recombination. The mutants $DR181^{TolC\_c6H}$ and $M7^{DevA\_c6H}$ (pIM318/322 constructs listed in supplemental Table S1) were generated by the conjugation of pRL271 ligated to XhoI fragments containing amplified *tolC* or *devA* fused to a 3′-hexahistidine tag (supplemental Table S2: oligonucleotides 271_TolC_c6H/271_DevA_c6H). To generate the templates for those fusion inserts, both genes were cloned into pQE60 (Qiagen, Hilden, Germany) by ligating total DNA amplified products via NcoI and BamHI (oligonucleotides 60_TolC_c6H/60_DevA_c6H).

The mutants $DR74^{DevB}$ (pIM442 construct, supplemental Table S1) and $DR74^{DevB\_N333A}$ (pIM444) were complemented by the conjugation of pCSEL24 (33) ligated to EcoRI and PstI fragments containing total DNA-amplified *devBCA* or $devB^{N333A}CA$ (supplemental Table S2: oligonucleotides 24_BCA). The $devB^{N333A}CA$ mutation was introduced by using primers directly flanking and overlapping the region to be mutated (oligonucleotides DevB_N333A).

Expression Analysis—Total RNA was extracted from 50-ml samples of *Anabaena* cultures in different states of combined nitrogen deprivation (before and at 3, 6, 9, 12, and 24 h after nitrogen step-down; as described in Ref. 20) by using the High Pure RNA Isolation Kit (Roche Applied Science, Mannheim, Germany), according to the manufacturer's instructions. RNA samples were reverse transcribed and amplified using the One Step RT-PCR Kit (Qiagen), according to the manufacturer's instructions. For *rnpB* amplification, the RNA samples were boiled at 95 °C for 5 min before amplification. The primers used for RT-PCR are listed in supplemental Table S2. The products were analyzed on a 2% agarose gel stained with 0.05% ethidium bromide.

Construction, Overexpression, and Purification of Recombinant Proteins—TolC, DevB, and DevAC were overexpressed as GST-tagged fusion proteins in *Escherichia coli* strain Rosetta-Gami^{TM}(DE3) (Merck, Darmstadt, Germany) by using the multitag expression vector pET42a (Merck; supplemental Table S2, oligonucleotides 42_TolC, 42_DevB, and 42_DevAC). Recombinant proteins were purified using GST SpinTrap or GSTrap FF columns (GE Healthcare). The N-terminal GST tag was cleaved off using Factor Xa, and the protease was removed using Xa Removal Resin (Qiagen). According to the role of the respective construct in interaction studies, the protein designed to be immobilized carried a C-terminal octahistidine tag (8H; from pET42a) if a tag had not already been introduced inside the protein (Table 2).

To ensure that a high amount of soluble protein was available for *in vitro* experiments, a membrane barrel-free version of TolC was constructed. OM-barrel-forming amino acids located between positions 365 and 417 and between positions 587 and 624 were replaced with four repeats of G and S (4GS; pIM378 construct, supplemental Table S1) or an octahistidine tag (pIM380). Both constructs were amplified as PCR fusion products by using primers directly flanking the predicted barrel elements and carrying respective self-priming sequences as a 3′ clamp (oligonucleotides TolC_iGS and TolC_i8H). The first 287 N-terminal amino acids of the predicted TolC protein were not taken into account for the constructs used in this work. BLAST analysis showed that they were not clearly related to any known function and are not present in other known TolC systems. The full-length TolC was highly unstable *in vitro* (data not shown).

All of the *in vitro* DevB constructs were amplified after replacing the membrane anchor region (amino acids 23–40) with GS repeats (oligonucleotides DevB_MA). The α-hairpin 8H tag DevB variant (pIM384) was constructed by fusing PCR products as described for the TolC constructs above (oligonucleotides DevB_i8H). The mutation V469C (pIM397; oligonucleotides DevB_V469C) was introduced as described for mutant $DR74^{DevB\_N333A}$. The amino acids to be replaced and/or omitted in TolC and DevB were predicted using models and methods as described previously (20).

DevC and DevA were fused by omitting the stop codon of *devA* and placing *devA* in the 5′ region of *devC*, linked via a 4GS

TABLE 1
***Anabaena* strains used in this work**
alr2887 = *tolC* (referred as *hgdD* in Ref. 20), *alr3710* = *devB*, *alr3711* = *devC*, *alr3712* = *devA*. $Fox^{+/-}$, is able/is not able to fix N_2 under aerobic conditions; Hgl^+, produces HGLs.

Anabaena strain	Genotype	Resistance	Properties	Source
PCC 7120	Wild-type		Fox^+Hgl^+	C. P. Wolk
DR181	*alr2887::C.K3*	Nm^r	Fox^-Hgl^+	Ref. 20
$DR181^{TolC\_c6H}$	*alr2887::C.K3, alr2887′::alr2887*^{c6H,a}	Nm^r, Cm^r, Em^r	Fox^+Hgl^+	This work
M7	*alr3712::Tn5*	Nm^r, Sm^r,	Fox^-Hgl^+	Ref. 18
$M7^{DevA\_c6H}$	*alr3712::Tn5 + alr3712′::alr3712*^{c6H,a}	Nm^r, Sm^r, Cm^r, Em^r	Fox^+Hgl^+	This work
DR74	*alr3710::C.K3*	Nm^r	Fox^-Hgl^+	Ref. 18
$DR74^{DevB}$	*alr3710::C.K3 + nucA::alr3710-12*^{b}	Nm^r, Sm^r, Sp^r	Fox^+Hgl^+	This work
$DR74^{DevB\_N333A}$	*alr3710::C.K3 + nucA::alr3710*^{N333A}*-12*^{b}	Nm^r, Sm^r, Sp^r	Fox^-Hgl^+	This work

[a] Single recombination of pRL271, including *tolC* or *devA* into the 5′ region of the respective gene.
[b] Recombination of pCSEL24, including *devBCA* or *devB*^{N333A}*CA* into *nucA* of the α-plasmid of *Anabaena* sp. PCC 7120.

or 8H sequence (pIM409/410 constructs; oligonucleotides 42_DevAC, DevAC_iGS, and DevAC_i8H).

In Vivo Cross-linking—Anabaena strains $DR181^{TolC\_c6H}$ or $M7^{DevA\_c6H}$ (Table 1) were deprived of combined nitrogen for 9 h in 50 ml of $BG11_0$ medium. To obtain a final concentration of 0.5% formaldehyde in the culture, 7.15 ml of a prewarmed (overnight at 70 °C) paraformaldehyde solution (4% in PBS, pH 7.4, 10 mM Na_2HPO_4, 1.8 mM KH_2PO_4, 137 mM NaCl, and 2.7 mM KCl) was added. The cross-linking reaction was quenched after 5–20 min by washing the culture three times with 100 mM Tris-NaOH buffer, pH 8.0. The cells were broken by 10 passes through a French pressure cell (24,000 psi) and separated into a soluble cytoplasmic/periplasmic and an insoluble membrane fraction by centrifugation (30,000 × *g*, 30 min, 4 °C). The debris was solubilized with a final concentration of 0.1% Triton X-100 for 30 min at 25 °C. After consecutive centrifugation (30,000 × *g*, 30 min, 4 °C), the supernatant was purified with nickel-nitrilotriacetic acid spin columns (Qiagen), according to the manufacturer's instructions. To remove cross-linking methylene bridges, the eluate was incubated for 30 min at 75 °C in a modified SDS sample buffer (final concentration, 10 mM Tris, pH 6.8; 0.5% SDS; 2% glycerol; and 150 mM mercaptoethanol). The proteins were separated on a 10% SDS-PAGE with subsequent colloidal Coomassie G staining (34) or transferred to a PVDF membrane for immunodetection.

Immunodetection—PVDF membranes were blocked for 10 min with TBS buffer (20 mM Tris-HCl, pH 7.5, 150 mM NaCl) containing 1% powdered milk and then incubated with primary antibody solution (in TBS containing 0.1% powdered milk) at 4 °C overnight. After three consecutive washes with TBS, the membrane was incubated with horseradish peroxidase-conjugated secondary α-rabbit antibody (1:100,000; Sigma-Aldrich, Munich, Germany) for 1 h at room temperature. The signals were captured using a Kodak Gel Logic 1500 imaging system. The primary antibodies used for Western blotting were αTolC (αD; 1:10,000), αDevB (αB; 1:2500), αDevC (αC; 1:10,000), and αDevA (αA; 1:25,000). The antibodies αDevC, αDevA, and αTolC were raised against the purified His-tagged full-length proteins by Pineda, Munich, Germany (data not shown). DevB antibodies were raised against the peptide sequences NRIRAEQRNAQVDAG and AISQQERDRRRLTATT by Pineda.

Surface Plasmon Resonance—Surface plasmon resonance (SPR) experiments were performed using a Biacore X biosensor system (Biacore AB, Uppsala, Sweden) as described previously (35). Purified recombinant His-tagged proteins were bound to flow cell 2 (FC2) of a Ni^{2+}-loaded nitrilotriacetic acid sensor chip prepared according to instructions from Biacore. Thiol coupling was performed as reported previously (10). Binding assays were performed in reaction buffer (25 mM MES-NaOH at pH 6.0–6.4 or HEPES-NaOH at pH 7.0, 150 mM NaCl, and 0.05% Triton X-100) at 25 °C. Samples were injected into the FC1 and FC2 of the sensor chip at a flow rate of 20 μl/min, and the response difference (FC2-FC1) was recorded. The reaction parameters were calculated from received data and fitted using the BiaEvaluation (Biacore AB) and Origin (version 6.0, OriginLab, Northampton) software.

Isothermal Titration Calorimetry—Isothermal titration calorimetry (ITC) experiments were performed in reaction buffer (25 mM MES-NaOH buffer, pH 6.2, 150 mM NaCl, and 0.05% Triton X-100) at 25 °C, using a VP-ITC microcalorimeter (MicroCal, GE Healthcare). In experiments with TolC and DevB, a 10 μM TolC solution ($TolC^{sol}$_iGS construct, Table 2) was titrated with 100 μM of DevB ($DevB^{sol}$). In experiments with DevAC and DevB, a 3 μM DevAC (DevAC_iGS, Table 2) solution was titrated with 30 μM of DevB ($DevB^{sol}$). Ten microliters of the ligand solution were injected each of 40 times into the 1.43-ml cell, with stirring at 350 rpm. The interaction parameters were calculated using MicroCal Origin software.

Chromatography—DevB oligomerization was analyzed via a gel filtration column (HiLoad 26/60-Superdex, GE Healthcare). The column was equilibrated with reaction buffer (25 mM MES-NaOH, pH 6.2, 150 mM NaCl, and 0.05% Triton X-100), and the proteins (0.1 mg/ml) were injected in the same reaction buffer, at a flow rate of 1 ml/min. The molecular mass standards used were β-amylase (200 kDa), β-galactosidase (116 kDa), BSA (66 kDa), and carbonic anhydrase (29 kDa).

Lipid Analysis—Total lipids were extracted from filaments, isolated heterocysts, or cell fractions by adding a methanol-chloroform mixture (1:2). The organic solvent was evaporated in a stream of air. The lipids were dissolved in 200 μl of chloroform and chromatographed on thin-layer plates of silica gel (Kieselgel 60, Merck) in 170 ml of chloroform, 30 ml of methanol, 20 ml of acetic acid, and 7.4 ml of distilled water. Lipids were visualized by sprinkling the plate with 25% sulfuric acid and exposing it to 200 °C for 90–120 s. Pure HGLs were prepared as described in Ref. 36, and cell fractions were prepared as described in Ref. 20.

ATP Hydrolysis Assay—The assay was performed with 0.1 μg/ml DevAC and 0.2 μg/ml DevB and indicated concentrations of substrate mixes in ATPase reaction buffer (50 mM

TABLE 2
Protein derivatives used in this work
Primers used for construction are listed in supplemental Table S2.

Construct	Modification	Purpose
TolC^{sol}_iGS	Membrane barrel replaced (2 × 4GS instead)	SPR, ITC
TolC^{sol}_i8H	Membrane barrel replaced (2 × 8H instead)	SPR
TolC_c6H	C-terminal 6H	Cross-link bait
DevB^{sol}	Membrane anchor replaced (GS instead)	SPR, ITC
DevB^{sol}_c8H	Membrane anchor replaced (GS instead), C-terminal 8H	SPR
DevB^{sol}_i8H	Membrane anchor replaced (GS instead), hairpin 8H	SPR
DevB^{sol}_V469C	Membrane anchor replaced (GS instead), V469C	SPR
DevB^{sol}_N333A	Membrane anchor replaced (GS instead), N333A	SPR
DevB_N333A	N333A	Complementation
DevAC_iGS	Stop codon of DevA removed, 4GS between DevA and DevC	SPR, ITC
DevAC_i8H	Stop codon of DevA removed, 8H between DevA and DevC	SPR
DevA_c6H	C-terminal 6H	Cross-link bait

MES-NaOH, pH 6.5, 1.5 mM DTT, and 0.05% Triton X-100) supplemented with a regeneration system (6 mM P-enolpyruvate, 3 μg/ml pyruvate kinase), 3 μg/ml lactate dehydrogenase, 0.5 mM NADH, and 2 mM ATP at 25 °C. Absorbance data were collected at 340 nm using a SPECORD 205 spectrophotometer (Analytik Jena AG) and evaluated using the WinASPECT software (version 2.2.1.0). The rate of hydrolysis in units was calculated as mol of ATP hydrolyzed per minute and per milligram of the ATPase DevAC.

Electron Microscopy—Samples for transmission electron microscopy were prepared as described previously (19). In brief, fixation and post-fixation were performed using glutaraldehyde and potassium permanganate; ultrathin sections were stained with uranyl acetate and lead citrate. The samples were examined with a Philips Tecnai electron microscope at 80 kV.

RESULTS

TolC Interacts with DevBCA in Vivo—Because of the similar phenotypes of mutants in *devBCA* and *tolC* and sequence similarities to proteobacterial secretion systems, previous studies proposed that TolC (also referred to as Alr2887 and HgdD) of *Anabaena* sp. PCC 7120 forms a secretion complex with DevBCA (20, 21). Cross-linking experiments were performed to clarify whether the subunits of this putative efflux pump interact *in vivo*. According to a typical model of this type of exporter, TolC in the outer membrane and DevA in the cytoplasm/cytoplasmic membrane should be the most distant participants (supplemental Fig. S1). Therefore, these proteins were fused to a His tag and used as baits for the rest of DevBCA-TolC. To obtain the best yield rate, the maximum protein expression of the proteins during heterocyst induction by nitrogen stepdown was investigated. In our immunoblots and RT-PCR analysis, we confirmed previous transcription studies of *tolC* and *devB* (19–21). TolC and DevB showed maximum expression at 9 h after depletion of combined nitrogen (Fig. 1*A*). The filaments that had been depleted of combined nitrogen for 9 h were chosen for cross-linking experiments.

Using cells expressing His-tagged TolC (TolC_c6H in Table 2), a dominant TolC band (Fig. 1*B*, *SDS+* at ~75 kDa and *αD*) and several weaker bands of lower mass (Fig. 1*B*, *SDS+*) were obtained after formaldehyde cross-linking and purification of the bait. Some of the lower bands could be identified using specific antibodies against DevB, DevC, and DevA in immunoblots. DevB and DevC were easily detectable (Fig. 1*B*, dominant bands in *lanes αB* and *αC*, respectively). A weak band corresponding to the molecular weight of DevA was obtained in longer exposed immunoblots (Fig. 1*B*, *αA*). Other proteins could not be detected in an eluate from non-cross-linked cell extracts (Fig. 1*B*, *SDS−*).

A similar cross-linking approach was used with cells expressing His-tagged DevA as bait (DevA_c6H in Table 2 and Fig. 1*C*). DevA_c6H was the only detectable band in eluants from non-cross-linked cell extracts (Fig. 1*C*, *SDS−* at ~28 kDa), whereas it eluted together with a couple of bands of higher mass in the presence of 0.5% formaldehyde (Fig. 1*C*, *SDS+*). All of the four assumed participants of the DevBCA-TolC complex could be detected readily by immunoblotting (Fig. 1*C*, *αA*, *αC*, *αB*, and *αD*). In contrast to using TolC_c6H as bait, less cross-reacting bands could be detected with antibodies against DevB and DevC (Fig. 1*C*; *αB* and *αC*).

In summary, the four components seem to be at least in very close proximity. The proposed *in vivo* interaction of DevBCA and TolC (20) seems likely.

DevB Hexamer Completes TolC-DevBCA Efflux Pump—To confirm the *in vivo* results, we investigated the interaction between distinct partners of the proposed complex by using SPR. First, the binding of DevB (DevB^{sol} construct in Table 2) to the chip surface-bound TolC (TolC^{sol}_i8H) was analyzed. Roughly in agreement with the results obtained for the homologue systems from *E. coli* (10), the highest response occurred at an acidic pH of 6.2, whereas interaction was remarkably impaired at higher pH values (Fig. 2*A*). To exclude an unwanted effect of the His tag due to the low pH used, thiol coupling of DevB onto the chip surface was used instead of His-tagged protein to verify the reaction optimum. The pH optimum obtained using this approach was the same as that obtained using His-tagged proteins (supplemental Fig. S2).

The best fit for TolC-DevB interaction at pH 6.2 was obtained by evaluating the SPR data in a two-stage binding model (heterogeneous ligand model in BiaEvaluation software). The affinities of surface-bound TolC (TolC^{sol}_i8H in Table 2) to DevB (DevB^{sol}) were K_{d1} = 37 nM and K_{d2} = 110 nM (Fig. 2*B*). Although higher surface densities of TolC did not affect the binding constants and/or fitting model, they were crucial in the case of surface-bound DevB (DevB^{sol}_c8H). Compared with the interaction of immobilized TolC (~440 RU) to ligand DevB (Fig. 2*B*), more mass of immobilized DevB (~2400 RU) was necessary to

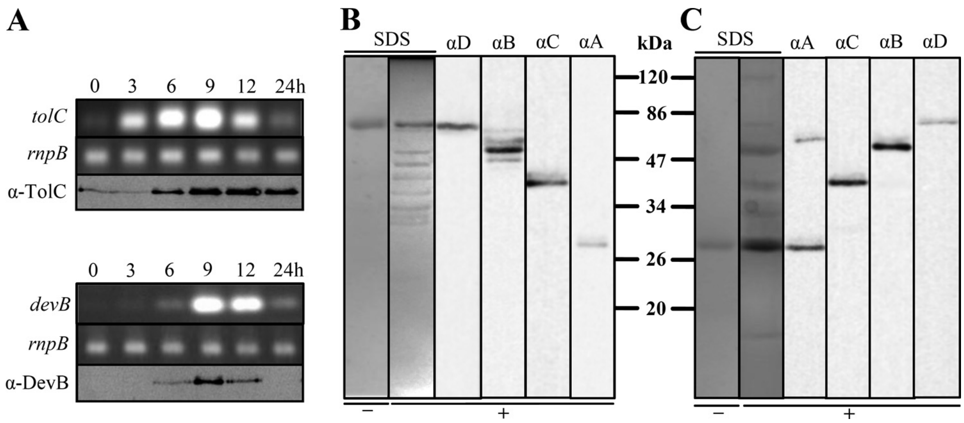

FIGURE 1. **Expression pattern of *devB* and *tolC* and interaction of TolC-DevBCA *in vivo*.** *A*, time-dependent expression pattern of *tolC* and *devB* analyzed by RT-PCR (*italic*) or immunoblots. *RnpB* refers to the loading control ribonuclease B. RNA or cell extracts were obtained from the same culture after indicated time points of nitrogen starvation. *B*, formaldehyde cross-link of His-tagged TolC *in vivo*. After 9 h of nitrogen starvation, filaments of mutant DR181^{TolC_c6H} were treated with 0.5% formaldehyde for 15 min (+). His-tagged TolC (TolC_c6H; Table 2) was purified and separated via SDS-PAGE. The proteins were stained with colloidal Coomassie G (SDS) or transferred to a PVDF membrane for immunodetection of TolC (α*D*), DevB (α*B*), DevC (α*C*), or DevA (α*A*). A purified sample of TolC-c6H from DR181^{TolC_c6H} without addition of formaldehyde was loaded on a SDS gel for control (−). *C*, formaldehyde cross-link of His-tagged DevA *in vivo*. DevA_c6H and the mutant M7^{DevA_c6H} were treated as described for TolC_c6H and mutant DR181^{TolC_c6H} in *B*.

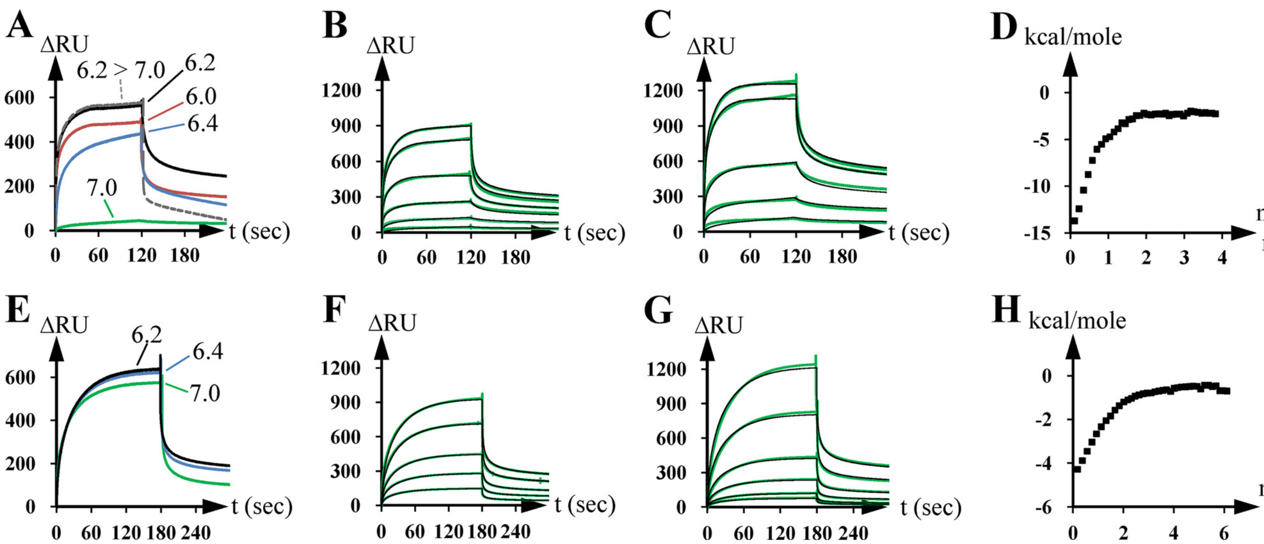

FIGURE 2. **Interaction of the OMF TolC with the MFP DevB and of the IMF DevAC with DevB *in vitro*.** *A*, SPR analysis of the interaction of immobilized TolC (TolC^{sol}_i8H in Table 2; ~400 RU) with DevB (DevB^{sol}; 0.8 μM) in dependence of indicated pH values. *B*, SPR analysis of the interaction of immobilized TolC (TolC^{sol}_i8H; ~440 RU) to DevB (DevB^{sol}). DevB was injected at concentrations doubling from 0.05 μM to 1.6 μM. The *green lines* show the experimental data, the *black lines* the fit by using a two-stage/heterogeneous ligand model. *C*, SPR analysis of the interaction of immobilized DevB (DevB^{sol}_c8H; ~2400 RU) to TolC (TolC^{sol}_iGS). TolC was injected at concentrations doubling from 0.1 to 1.6 μM. The *green lines* show the experimental data, and the *black lines* show the fit by using a two-stage/heterogeneous ligand model. *D*, ITC analysis of the interaction of TolC (TolC^{sol}_iGS) to DevB (DevB^{sol}). 10 μM TolC were titrated 40 times with 100 μM DevB at pH 6.2. The *squares* represent the measured and integrated energy release peaks. *E*, SPR analysis of the interaction of immobilized DevAC (DevAC_i8H; ~440 RU) to DevB (DevB^{sol}; 0.8 μM) in dependence of indicated pH values. *F*, SPR analysis of the interaction of immobilized DevAC (DevAC_i8H; ~470 RU) to DevB (DevB^{sol}). DevB was injected at concentrations doubling from 0.05 to 1.6 μM. The *green lines* show the experimental data, and the *black lines* show the fit by using a two-stage/heterogeneous ligand model. *G*, SPR analysis of the interaction of surface-bound DevB (DevB^{sol}_i8H; ~2400 RU) to DevAC (DevAC_iGS). DevAC was injected at concentrations doubling from 0.1 to 1.6 μM. The *green lines* show the experimental data, and the *black lines* show the fit by using a two-stage/heterogeneous ligand model. *H*, ITC analysis of the interaction of DevAC (DevAC_iGS) to DevB (DevB^{sol}). 3 μM DevAC were titrated 40 times with 30 μM DevB at pH 6.2. The *squares* represent the measured and integrated energy release peaks.

obtain similar binding constants to ligand TolC (TolC^{sol}_iGS, Fig. 2*C*). Binding constants of immobilized DevB to ligand TolC were K_{d1} = 55 nM and K_{d2} = 140 nM (Fig. 2*C*). Applying lower surface densities of DevB led to a different and highly complex evaluation. To clarify this issue, we repeated the interaction experiment using a surface- and orientation-independent ITC approach (Fig. 2*D*). Consistent with the results of the SPR experiments, the ITC data provided the best fit on using a two-stage model. The binding constants of TolC (TolC^{sol}_iGS) to injected DevB (DevB^{sol}) were K_{d1} = 88 nM and K_{d2} = 380 nM.

Interestingly, both approaches predicted saturation of DevB binding to TolC near to a molar ratio of 2:1 (ITC in Fig. 2*D*; SPR in Fig. 2, *B* and *C*). A saturation molar ratio of ~1.72:1 for the binding of DevB to TolC was obtained from ITC data, whereas the ratio found to be ~1.71:1 (~900 RU of 51.9-kDa DevB bound to ~440 RU of immobilized 43.5-kDa TolC, Fig. 2*B*) or ~1.54:1 (~1240 RU of 42.3-kDa TolC bound to ~2400 RU of immobilized 53.1-kDa DevB, Fig. 2*C*) upon using SPR. The use of higher ligand concentrations did not considerably increase the response (data not shown).

Next, the interaction between the MFP DevB and the IMF DevC was investigated. Studies on proteobacterial ABC exporter systems have reported that the nucleotide-binding domain (corresponding to DevA) and the substrate-binding domain (DevC) of the respective IMF can be located together on one polypeptide (15, 37–39). To avoid artifacts caused by missing protein parts, DevAC hybrids (42_DevAC and DevAC_iGS or DevAC_i8H in Table 2) were used instead of DevC alone. Similar to the results obtained for the binding of DevB to TolC (Fig. 2*A*), the pH optimum of the DevB response toward immobilized DevAC was 6.2 (Fig. 2*E*), but the response did not change considerably until pH 7.0.

The best fit for SPR data for the interaction of immobilized DevAC (DevAC_i8H in Table 2) to DevB ($DevB^{sol}$) was also obtained by using a two-stage binding model, resulting in the binding constants K_{d1} = 940 nM and K_{d2} = 3911 nM (Fig. 2*F*). The surface density of immobilized DevAC did not have a remarkable influence on the reaction, but low surface densities of immobilized DevB led to problems similar to those described for the interaction between TolC and immobilized DevB. The binding constants of immobilized DevB ($DevB^{sol}$_i8H) to DevAC (DevAC_i8GS) were K_{d1} = 531 nM and K_{d2} = 3708 nM (Fig. 2*G*).

The response saturation data predicted a DevB to DevAC ratio of nearly 3:1. In the case of immobilized DevAC, it was 2.84:1 (~970 RU of 51.9-kDa DevB bound to ~470 RU of immobilized 71.3-kDa DevAC, Fig. 2*F*), and in the case of surface-bound DevB, it was 2.64:1 (~1220 RU of 71.2-kDa DevAC bound to ~2400 RU of immobilized 53.1-kDa DevB, Fig. 2*G*). ITC data predicted a reaction saturation at a DevB:DevAC ratio of 2.90:1 (Fig. 2*H*).

In summary, the results of our *in vitro* studies show that TolC, DevB, and DevAC interact in a molar ratio of 3:6:2 (on assuming average DevB:TolC and DevB:DevAC ratios of 2:1 and 3:1, respectively). Such molar ratios have been postulated earlier for the ATP-driven efflux pump MacAB-TolC (40–42). Our data indicate that TolC and DevBCA also seem to form an ATP-driven efflux pump (because *devA* is predicted to encode an ATPase), as hypothesized in earlier studies (18–20).

HGLs Are a Substrate for TolC-DevBCA—HGLs, their moieties, or accessory factors necessary for the formation of the laminated layer could be substrates of DevBCA-TolC. Missing any of these components would result in the phenotype of the *devBCA/tolC* mutants (19, 20). To identify substrates of DevBCA-TolC, we exposed the IMF and ATPase DevAC and the MFP DevB (Fig. 3*A*, *ACB*) to complex substrate mixes such as whole-cell extracts of *Anabaena*, membranes, and soluble fractions (Fig. 3*B* reflects the lipid composition of the fractions). The ATP-hydrolyzing activity slightly increased in the presence of whole-cell extracts of cells depleted of nitrogen for 9 h (Fig. 3*A*, *HCE*). Heterocyst membranes (cell wall and cytoplasmic and thylakoid membranes) were slightly better enhancers (Fig. 3*A*, *HMF*), whereas heterocyst cell walls caused an even stronger enhancement (Fig. 3*A*, *HCW*). DevACB activity was not modified by pretreating the cell wall fractions with proteinase K, so the substrates should not be proteinaceous (data not shown). The only known differences between the cell walls of heterocysts and vegetative cells are protein (43) and the additional layers (polysaccharide and glycolipids) of the heterocyst. Finally, purified HGLs were used as substrates in the ATPase assay with DevBCA. This exposure caused a nearly 7-fold boost in the rate of ATP hydrolysis (Fig. 3, *A* and *B*, *HGL*).

The TolC knock-out mutant DR181 forms a heterocyst envelope polysaccharide layer and synthesizes HGLs but does not assemble an HGL layer (21). The cell walls of the heterocysts of this mutant did not remarkably affect the ATPase activity of DevACB (Fig. 3*A*, *MCW*). On using the cytoplasmic membrane fraction, where the glycolipids get stuck in DR181 (compare devB mutant in Fig. 3*B*, MT), an increase could be observed in the ATPase activity (Fig. 3*A*, *MCM*).

The response of DevACB was proportional to the amount of fractions containing HGLs (Fig. 3*A* and supplemental Fig. S4, *gray bars*), whereas no enhancement of ATP activity was detected using fractions not containing HGLs (Fig. 3*A* and supplemental Fig. S4, *white bars*). Therefore, the glycolipids are good candidates for DevBCA-TolC substrates. It has to be noted that substrate-dependent activation of the ATPase activity of DevAC toward the presence of HGLs was observed only in the presence of the DevB (Fig. 3*A*, *ACB* and *AC*).

A mutation at Asn-333 to Ala in DevB abolished the ability of $DevACB^{N333A}$ to respond to HGLs (Fig. 3*A*, *MT*). This mutation impaired DevB hexamer formation (supplemental Fig. S3). SPR data from DevB_N333A interaction with surface-bound TolC or DevAC showed altered binding and could not predict the TolC:DevB:DevAC molar ratio of 3:6:2 described above (Fig. 3*C*). This stoichiometry is crucial for *in vivo* function of the HGL exporter: complementation of the *devB* mutant DR74 with a wild-type copy of *devB* results in a functional HGL layer (Fig. 3*D*, $DR74^{DevB}$), whereas the mutant N333A could not rescue the DR74 phenotype. Heterocysts of mutant $DR74^{DevB\_N333A}$ lack the glycolipid layer (Fig. 3*E*), and the HGLs stay in the cytoplasmic membrane (Fig. 3*B*, *HCM/MT*).

The mutated version of the MFP DevB could not fulfill its function in exporting HGLs. The ability to form stable hexamers is a prerequisite for the transport process of HGLs.

DISCUSSION

In recent years, numerous genes of *Anabaena* sp. PCC 7120, which encode enzymes involved in the synthesis of special polysaccharides, heterocyst glycolipids, and components of the heterocyst envelope, have been identified in studies that mostly involved transposon mutagenesis (reviewed in Ref. 43). However, the mechanism by which the molecules traverse the Gram-negative cell wall of the developing heterocyst remained unknown. The data presented in this study show that DevB, DevC, DevA, and TolC form an ATP-driven efflux pump for the export of HGLs. This system is, to our knowledge, the first of its kind described for the synthesis of the unique Gram-negative cell envelope of heterocysts.

Promiscuous Role of TolC—Both *devB*, the first gene of the *devBCA* operon, and *tolC* are induced during heterocyst differentiation, showing maximum abundance at 9 h after nitrogen step-down. The signal strength of TolC remained constant but that of DevB/*devB* decreased rapidly. This could be due to the specific contribution of DevBCA to the developing cell wall of heterocysts (export of HGLs). TolC-like proteins have been

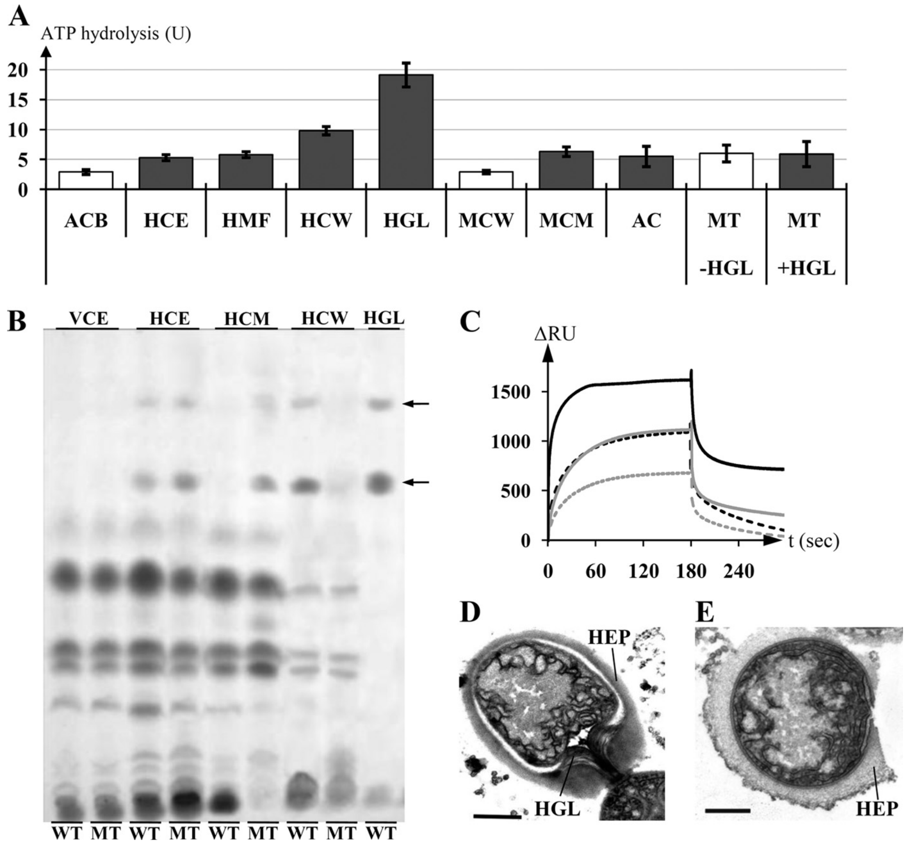

FIGURE 3. **The substrate of TolC-DevBCA.** *A*, ATP hydrolysis rates of DevAC in presence of indicated substrate mixes. *ACB* represents DevAC with DevB; *HCE* represents DevAC, DevB, and heterocyst cell extract; *HMF* represents DevAC, DevB, and heterocyst membranes; *HCW* represents DevAC, DevB, and heterocyst cell walls; *HGL* represents DevAC, DevB, and purified HGLs; *MCW* represents DevAC, DevB, and cell walls of mutant DR181; *MCM* represents DevAC, DevB, and cytoplasmic membranes of mutant DR181; *AC* represents DevAC without DevB; *MT* represents DevAC and $DevB^{N333A}$, +/−*HGL* represents with/without purified HGLs. All substrate concentrations were adjusted to 4 μg of the respective protein fraction or equal to 4 μg cell wall protein in the case of adding HGLs. *Gray bars* indicate the presence of HGLs in the respective fractions. ATPases possibly present inside the substrate fractions were preinactivated by incubation with 5 mM VaO_4. *B*, thin layer chromatography of extracts of complemented mutants $DR74^{DevB}$ and $DR74^{DevB\_N333A}$, and purified HGLs. *WT*, $DR74^{DevB}$; *MT*, $DR74^{DevB\_N333A}$; *VCE*, vegetative cell extract; *HCE*, heterocyst cell extract; *HCM*, heterocyst cytoplasmic membranes; *HCW*, heterocyst cell walls; *HGL*, purified HGLs. *Arrows* indicate HGLs. *C*, SPR analysis of the interaction of either immobilized TolC ($TolC^{sol}$_i8H; ~730 RU; *black curves*) or DevAC (DevAC_i8H; ~510 RU; *gray curves*) to DevB ($DevB^{sol}$; *solid lines*) or $DevB^{N333A}$ ($DevB^{sol}$_N333A; *dashed lines*). DevB was injected in the reaction buffer at 2.0 μM. *D*, electron micrograph of a heterocyst of strain $DR74^{DevB}$. *HEP*, heterocyst envelope polysaccharide layer; *HGL*, glycolipid layer. *Error bar*, 1 μm. *E*, electron micrograph of a heterocyst of strain $DR74^{DevB\_N333A}$. *Bar*, 1 μm.

described as adaptors for different exporters specialized on their respective substrates (7, 8, 10). It can be assumed that TolC, the only OMF predicted from the *Anabaena* sp. PCC 7120 genome sequence (20), must complete further heterocyst development related (and unrelated) tasks after 9 h of nitrogen depletion. At least six close homologues of *devB* can be found in the *Anabaena* sp. PCC 7120 genome (*all0809*, *all2652*, *alr3647*, *alr4280*, *alr4973*, and *all5347*). They, and MFPs of other export systems, could also interact with TolC, and some of them had expression patterns similar to that of *devB* (data not shown). A mutant of *all5347* (*hgdB*) could not fix N_2 and showed aberrant HGL layers (29). To focus on TolC-DevBCA and to minimize the influence of other MFPs and the respective exporters, cross-linking studies were performed using filaments that had experienced 9 h of nitrogen deprivation because TolC seems to play a promiscuous role in cyanobacteria.

Glycolipid Export by an ATP-driven Efflux Pump—The correlation between the enrichment of HGLs (Fig. 3*B*) and the response of the ATPase activity of DevAC (Fig. 3*A*) clearly shows that HGLs are a substrate of DevBCA-TolC. Moieties of HGLs or proteins/other compounds, suspected to possibly be exported by DevBCA-TolC (20), could not be identified as substrates. Any impairment of TolC-DevBCA caused the accumulation of entire HGLs, but not of their moieties, in the cytoplasmic membrane fraction (Fig. 3*B*, *MT*, shown for the *devB* mutant $DR74^{DevB\_N333A}$). The moieties would have to be assembled after or during translocation to the cell surface (compare Lipid A (44, 45)). Other HGL components or intermediates have never been detected in *Anabaena* sp. PCC 7120 heterocysts in past studies (20, 29, 36, 46–49). Involvement of DevBCA-TolC in protein export was not observed; the response of DevAC did not differ for untreated and proteinase K-treated or boiled fractions. Nevertheless, the substrate specificity of DevBCA-TolC presented in this work must not necessarily reflect all substrates and functions *in vivo*. It is known that the homologous system MacAB-TolC, where MacA corresponds to DevB and MacB to DevAC, is involved in the export of macrolides but does not show any response in ATPase activity toward their presence, indicating that additional factors could be required for activity (38). Because DevBCA is tightly regulated at the stages of expression/degradation (Fig. 1*A*) and seems to export a specific substrate at a specific stage in heterocyst differentiation, putative accessory factors may not be required for translocation/ATPase activity response.

Involvement of ABC exporters, *e.g.* the LolCDE- and MsbA systems, in lipoprotein/glycolipid export has been reported previously (50–54). The IMF DevAC does not show remarkable sequence similarities to MsbA but has higher homologies to the Gram-negative ABC exporter LolCDE, where LolCE corresponds to DevC and LolD to DevA. DevAC also shows high similarities to FtsEX (55, 56), where FtsX corresponds to DevC and FtsE to DevA. FtsEX is involved in cell division and is assumed to export salts. MsbA, LolCDE, and FtsEX are not known to interact with an OMF such as TolC. Taken together, no known ABC exporter involved in cell division/differentiation and in glycolipid transfer resembles the DevBCA-TolC export machinery of *Anabaena* sp. PCC 7120.

Prerequisites of Cyanobacterial Glycolipid Efflux Pump—Although *Anabaena* prefers a freshwater environment (pH 7.8 or higher), the optimal pH for TolC-DevB interaction appears to be 6.2 and is therefore similar to that required for MacA-TolC interaction in *E. coli* (pH 5.8 (Ref. 10)). The periplasm of Gram-negative bacteria is known to be more acidic than the cytoplasm and, in most cases, is more acidic than the surrounding medium (57). So far, there are no data showing a complete respiratory chain in the cytoplasmic membrane of any cyanobacteria. Consequently, there are no data on H^+ accumulation in the cyanobacterial periplasm (58). Cyanobacteria usually maintain a photosynthesis-driven H^+ gradient over the thylakoid membrane. Nevertheless, a heterocyst-specific acidification of the periplasm could be caused by increase in the respiratory rate in the cytoplasmic membrane of heterocysts to consume harmful oxygen (23) All0809, a close homologue of DevB, was localized in all cells of the filament and showed a binding optimum to TolC at higher pH.[3] Lower pH in the periplasm of heterocysts could favor the binding of DevB to TolC, simply because the complex is needed in this state of heterocyst development.

A "bridging model" was proposed for the TolC-DevBCA homologue TolC-MacAB, with a MacA hexamer fitting to the tip of TolC in a cogwheel-like manner (9, 40, 41). It was derived from *in silico* protein models based on MacA crystals resolved to hexamers and electron micrographs showing a barrel-like hexameric assembly. Furthermore, the IMF MacB was proposed to form dimers (37, 39) and the OMF TolC trimers (7, 8). Hence, a TolC:MacA:MacB ratio of 3:6:2 could be assumed. Our data on DevBCA-TolC support exactly this stoichiometry (Fig. 2). DevB_N333A does not seem to form stable hexamers (Fig. 3*C* and supplemental Fig. S3) and cannot make DevAC recognize the presence of HGLs *in vitro* (Fig. 3*A*). This mutant does not rescue the phenotype of a *devB* knock-out (Fig. 3*E*). These observations imply the importance of a hexameric bridge between IMF and OMF even *in vivo* (Fig. 3*E*). However, details on the connecting structures of DevB to TolC either bridging to or wrapping around the OMF (like that modeled for the resistance-nodulation-division exporter AcrAB (6, 8, 59)), cannot be predicted from our data. ABC exporters such as DevAC are anchored compactly into the cytoplasmic membrane and do not contact TolC directly (37–39). Therefore, a hexameric DevB tunnel separating the transport pathway from the periplasm could provide a distinct milieu for HGL export.

Evaluation of SPR and ITC data predicted two binding events of DevB to both TolC and DevAC (Fig. 2). Both affinities seem to be largely based on MFP behavior. Although the interaction of free DevB with immobilized TolC or DevAC is reproducible for a wide range of surface protein densities, the kinetics of the immobilized DevB with its ligands strongly depend on the concentration of DevB on the chip surface. The reaction parameters were comparable only when a high surface density of DevB was used. This could be due to the resulting enhanced possibility of surface-bound DevB forming one of the preferred states in solution, *i.e.* a hexamer (supplemental Fig. S3). The oligomerization pattern of DevB indicates that more binding events, including those involving the binding of MFP to MFP, could be expected. The reason for there being only two dominant (and therefore detectable) binding events could be a very stringent interaction behavior in the presence of OMF or IMF ligands and reflect either hexamer formation with subsequent ligand binding or an additional but yet unknown intermediate binding state.

In summary, our results suggest that TolC-DevBCA form an efflux pump required for the export of HGLs of the heterocyst cell wall in *Anabaena* sp. PCC 7120. DevB connects the IMF DevAC to the OMF TolC by forming a hexamer throughout the acidic periplasm. It can provide a separate lipophilic tunnel for the transport of lipophilic HGLs beyond the outer membrane. TolC-DevBCA can be considered as a uniquely adjusted system for the formation of an extracellular glycolipid layer in heterocysts. It is the first reported ATP-driven efflux pump that provides a novel pathway for glycolipid export.

Acknowledgments—We thank Claudia Menzel for preparing the electron microscopy samples and Oleksandra Fokina and Dr. Javier Espinosa for introduction into and support with SPR and ITC. Furthermore, we thank Professor Enrico Schleiff for critical discussion and helpful suggestions. We thank Professor C. Peter Wolk for pRL plasmids and Dr. A. Muro-Pastor for pCSEL24.

REFERENCES

1. Piñero-Fernandez, S., Chimerel, C., Keyser, U. F., and Summers, D. K. (2011) *J. Bacteriol.* **193,** 1793–1798
2. Martins, M., Viveiros, M., Couto, I., Costa, S. S., Pacheco, T., Fanning, S., Pagès, J. M., and Amaral, L. (2011) *In Vivo* **25,** 171–178
3. Deininger, K. N., Horikawa, A., Kitko, R. D., Tatsumi, R., Rosner, J. L., Wachi, M., and Slonczewski, J. L. (2011) *PLoS ONE* **6,** e18960
4. Ferhat, M., Atlan, D., Vianney, A., Lazzaroni, J. C., Doublet, P., and Gilbert, C. (2009) *PLoS ONE* **4,** e7732
5. Hantke, K., Winkler, K., and Schultz, J. E. (2011) *J. Bacteriol.* **193,** 1086–1089
6. Symmons, M. F., Bokma, E., Koronakis, E., Hughes, C., and Koronakis, V. (2009) *Proc. Natl. Acad. Sci. U.S.A.* **106,** 7173–7178
7. Koronakis, V., Eswaran, J., and Hughes, C. (2004) *Annu. Rev. Biochem.* **73,** 467–489
8. Koronakis, V., Sharff, A., Koronakis, E., Luisi, B., and Hughes, C. (2000) *Nature* **405,** 914–919
9. Yum, S., Xu, Y., Piao, S., Sim, S. H., Kim, H. M., Jo, W. S., Kim, K. J., Kweon, H. S., Jeong, M. H., Jeon, H., Lee, K., and Ha, N. C. (2009) *J. Mol. Biol.* **387,** 1286–1297

[3] P. Staron, K. Forchhammer, and I. Maldener, unpublished data.

10. Tikhonova, E. B., Dastidar, V., Rybenkov, V. V., and Zgurskaya, H. I. (2009) *Proc. Natl. Acad. Sci. U.S.A.* **106,** 16416–16421
11. Mikolosko, J., Bobyk, K., Zgurskaya, H. I., and Ghosh, P. (2006) *Structure* **14,** 577–587
12. Eswaran, J., Koronakis, E., Higgins, M. K., Hughes, C., and Koronakis, V. (2004) *Curr. Opin. Struct. Biol.* **14,** 741–747
13. Higgins, M. K., Bokma, E., Koronakis, E., Hughes, C., and Koronakis, V. (2004) *Proc. Natl. Acad. Sci. U.S.A.* **101,** 9994–9999
14. Lobedanz, S., Bokma, E., Symmons, M. F., Koronakis, E., Hughes, C., and Koronakis, V. (2007) *Proc. Natl. Acad. Sci. U.S.A.* **104,** 4612–4617
15. Holland, I. B., Schmitt, L., and Young, J. (2005) *Mol. Membr. Biol.* **22,** 29–39
16. Saier, M. H., Jr., Beatty, J. T., Goffeau, A., Harley, K. T., Heijne, W. H., Huang, S. C., Jack, D. L., Jähn, P. S., Lew, K., Liu, J., Pao, S. S., Paulsen, I. T., Tseng, T. T., and Virk, P. S. (1999) *J. Mol. Microbiol. Biotechnol.* **1,** 257–279
17. Tseng, T. T., Gratwick, K. S., Kollman, J., Park, D., Nies, D. H., Goffeau, A., and Saier, M. H., Jr. (1999) *J. Mol. Microbiol. Biotechnol.* **1,** 107–125
18. Fiedler, G., Arnold, M., and Maldener, I. (1998) *Biochim. Biophys. Acta* **1375,** 140–143
19. Fiedler, G., Arnold, M., Hannus, S., and Maldener, I. (1998) *Mol. Microbiol.* **27,** 1193–1202
20. Moslavac, S., Nicolaisen, K., Mirus, O., Al Dehni, F., Pernil, R., Flores, E., Maldener, I., and Schleiff, E. (2007) *J. Bacteriol.* **189,** 7887–7895
21. Maldener, I., Hannus, S., and Kammerer, M. (2003) *FEMS Microbiol. Lett.* **224,** 205–213
22. Kaneko, T., Nakamura, Y., Wolk, C. P., Kuritz, T., Sasamoto, S., Watanabe, A., Iriguchi, M., Ishikawa, A., Kawashima, K., Kimura, T., Kishida, Y., Kohara, M., Matsumoto, M., Matsuno, A., Muraki, A., Nakazaki, N., Shimpo, S., Sugimoto, M., Takazawa, M., Yamada, M., Yasuda, M., and Tabata, S. (2001) *DNA Res.* **8,** 205–213; 227–253
23. Wolk, C. P., Ernst, A., and Elhai, J. (1994) *The Molecular Biology of Cyanobacteria* (Bryant, D.A., ed.), pp. 769–823, Kluwer Academic, Dudrecht, The Netherlands
24. Fay, P. (1992) *Microbiol. Rev.* **56,** 340–373
25. Cardemil, L., and Wolk, C. P. (1976) *J. Biol. Chem.* **251,** 2967–2975
26. Haury, J. F., and Wolk, C. P. (1978) *J. Bacteriol.* **136,** 688–692
27. Gambacorta, A., Romano, I., Sodano, G., and Trincone, A. (1998) *Phytochemistry* **48,** 801–805
28. Campbell, E. L., Cohen, M. F., and Meeks, J. C. (1997) *Arch. Microbiol.* **167,** 251–258
29. Fan, Q., Huang, G., Lechno-Yossef, S., Wolk, C. P., Kaneko, T., and Tabata, S. (2005) *Mol. Microbiol.* **58,** 227–243
30. Awai, K., and Wolk, C. P. (2007) *FEMS Microbiol. Lett.* **266,** 98–102
31. Rippka, R., Dereules, J., Waterbury, J. B., Herdman, M., and Stanier, R. Y. (1979) *J. Gen. Microbiol.* **111,** 1–61
32. Wolk, C. P., Vonshak, A., Kehoe, P., and Elhai, J. (1984) *Proc. Natl. Acad. Sci. U.S.A.* **81,** 1561–1565
33. Olmedo-Verd, E., Muro-Pastor, A. M., Flores, E., and Herrero, A. (2006) *J. Bacteriol.* **188,** 6694–6699
34. Candiano, G., Bruschi, M., Musante, L., Santucci, L., Ghiggeri, G. M., Carnemolla, B., Orecchia, P., Zardi, L., and Righetti, P. G. (2004) *Electrophoresis* **25,** 1327–1333
35. Fokina, O., Chellamuthu, V. R., Zeth, K., and Forchhammer, K. (2010) *J. Mol. Biol.* **399,** 410–421
36. Winkenbach, F., Wolk, C. P., and Jost, M. (1972) *Planta* **107,** 69–80
37. Lin, H. T., Bavro, V. N., Barrera, N. P., Frankish, H. M., Velamakanni, S., van Veen, H. W., Robinson, C. V., Borges-Walmsley, M. I., and Walmsley, A. R. (2009) *J. Biol. Chem.* **284,** 1145–1154
38. Tikhonova, E. B., Devroy, V. K., Lau, S. Y., and Zgurskaya, H. I. (2007) *Mol. Microbiol.* **63,** 895–910
39. Xu, Y., Sim, S. H., Nam, K. H., Jin, X. L., Kim, H. M., Hwang, K. Y., Lee, K., and Ha, N. C. (2009) *Biochemistry* **48,** 5218–5225
40. Xu, Y., Song, S., Moeller, A., Kim, N., Piao, S., Sim, S. H., Kang, M., Yu, W., Cho, H. S., Chang, I., Lee, K., and Ha, N. C. (2011) *J. Biol. Chem.* **286,** 13541–13549
41. Xu, Y., Sim, S. H., Song, S., Piao, S., Kim, H. M., Jin, X. L., Lee, K., and Ha, N. C. (2010) *Biochem. Biophys. Res. Commun.* **394,** 962–965
42. Kim, H. M., Xu, Y., Lee, M., Piao, S., Sim, S. H., Ha, N. C., and Lee, K. (2010) *J. Bacteriol.* **192,** 4498–4503
43. Nicolaisen, K., Hahn, A., and Schleiff, E. (2009) *J. Basic Microbiol.* **49,** 5–24
44. Raetz, C. R., Ulevitch, R. J., Wright, S. D., Sibley, C. H., Ding, A., and Nathan, C. F. (1991) *FASEB J.* **5,** 2652–2660
45. Raetz, C. R., Reynolds, C. M., Trent, M. S., and Bishop, R. E. (2007) *Annu. Rev. Biochem.* **76,** 295–329
46. Black, K., Buikema, W. J., and Haselkorn, R. (1995) *J. Bacteriol.* **177,** 6440–6448
47. Ramírez, M. E., Hebbar, P. B., Zhou, R., Wolk, C. P., and Curtis, S. E. (2005) *J. Bacteriol.* **187,** 2326–2331
48. Shi, L., Li, J. H., Cheng, Y., Wang, L., Chen, W. L., and Zhang, C. C. (2007) *J. Bacteriol.* **189,** 5075–5081
49. Bauersachs, T., Compaoré, J., Hopmans, E. C., Stal, L. J., Schouten, S., and Sinninghe Damsté, J. S. (2009) *Phytochemistry* **70,** 2034–2039
50. Narita, S., and Tokuda, H. (2006) *FEBS Lett.* **580,** 1164–1170
51. Narita, S., and Tokuda, H. (2010) *Methods Mol. Biol.* **619,** 117–129
52. Siarheyeva, A., and Sharom, F. J. (2009) *Biochem. J.* **419,** 317–328
53. Kaul, G., and Pattan, G. (2011) *Indian J. Biochem. Biophys.* **48,** 7–13
54. Eckford, P. D., and Sharom, F. J. (2010) *Biochem. J.* **429,** 195–203
55. Garti-Levi, S., Hazan, R., Kain, J., Fujita, M., and Ben-Yehuda, S. (2008) *Mol. Microbiol.* **69,** 1018–1028
56. Schmidt, K. L., Peterson, N. D., Kustusch, R. J., Wissel, M. C., Graham, B., Phillips, G. J., and Weiss, D. S. (2004) *J. Bacteriol.* **186,** 785–793
57. Wilks, J. C., and Slonczewski, J. L. (2007) *J. Bacteriol.* **189,** 5601–5607
58. Schultze, M., Forberich, B., Rexroth, S., Dyczmons, N. G., Roegner, M., and Appel, J. (2009) *Biochim. Biophys. Acta* **1787,** 1479–1485
59. Touzé, T., Eswaran, J., Bokma, E., Koronakis, E., Hughes, C., and Koronakis, V. (2004) *Mol. Microbiol.* **53,** 697–706

4. Additional experiments (I)

4.1 Control of *devBCA* and *tolC* expression by NtcA and HetR

4.1.1 Background and experimental design

It was shown that *devBCA* is differentially expressed in the course of heterocyst maturation. The expression of this operon depends on the heterocyst development master regulators NtcA and HetR. Mutants in *ntcA* or *hetR* were not able to induce *devBCA*-expression during heterocyst maturation (Fiedler *et al.* 2001; Olmedo-Verd *et al.* 2005). There was no data on the transcription of *tolC* in these mutants. The upstream region of *tolC* is expressed in NO_3-grown filaments, and it is also upregulated during heterocyst maturation (Moslavac *et al.* 2007). So, a direct or indirect regulation of *tolC* trough NtcA and/or HetR is likely, although *tolC* does not contain a typical NctA binding site (Su *et al*. 2005). In the following chapter, this will be investigated.
In addition, the transcription level must not necessarily reflect the amount of protein. To relate the transcription to the amount of protein, DevB and TolC were monitored during combined nitrogen starvation. Since *devB* is the first gene of the *devBCA* operon, DevB represents the proteins encoded by the entire operon.

4.1.2 Materials and Methods

Used strains and growth conditions

All used strains and the applied antibiotics are listed in Tab. 1 (wild type PCC7120, CSE2, and 216 in appendix 11.2, page 124). To induce heterocyst formation, combined nitrogen was removed by washing the filaments at least 3 subsequential times with medium free of ammonia as described.

Expression analysis

Total RNA was purified from cells of 50 ml samples of *Anabaena* strain PCC 7120, mutant CSE2 (mutant in *ntcA*), and mutant 216 (mutant in *hetR*) at different states of combined nitrogen deprivation (before and at 3, 6, 9, 12 and 24 h after nitrogen step-down) by using the High Pure RNA Isolation Kit (Roche, Manheim, Germany) according to the manufacturer's instructions. Prior to RNA purification, the cells were washed with PBS buffer (10 mM Na_2HPO_4; 2 mM KH_2PO_4, pH 7.4; 120 mM NaCl; 2.5 mM KCl; and 10 µl/ml β-mercaptoethanol), and total RNA was derived by a conventional phenol-chloroform extraction (Chomczynski and Sacchi 2006). A mixture of 50% phenol, 48% chloroform, and 2% isoamyl alcohol was added to equal volumes of cell lysates prepared by incubation of PBS-washed filaments with lysis buffer (4 M guanidiniumthiocyanate; 20 mM Na-acetate, pH 5.2; 0,1 mM dithiotreitol; and 0.5% w/v N-lauroyl-sarcrosine). After centrifugation (20,800 *g*, 4 °C, 2 min), the aqueous phase was washed with chloroform, and subsequently total RNA was precipitated with 96% ethanol.

8-10 ng of the respective RNA samples were reverse transcribed and amplified using the One Step RT-PCR Kit (Qiagen), according to the manufacturer's instructions. For *rnpB* amplification, the RNA samples were boiled at 95 °C for 5 min prior to amplification. The primers used for RT-PCR of *devB*, *tolC*, and *rnpB* are listed in Tab. 4 (appendix 11.4, page 127). The products were analyzed on a 2 % agarose gel stained with 0.05 % ethidium bromide.

Immunodetection

For immunodetection of DevB and of TolC, total membrane proteins were extracted from *Anabaena* strains PCC7120, CSE2, and 216. Therefore, cells of the respective cultures at different states of combined nitrogen deprivation (before and at 3, 6, 9, 12 and 24 h after nitrogen step-down) were broken by at least five passes through a French Pressure cell (24,000 psi), and total membranes were collected by centrifugation (60,000 *g*, 4 °C, 30 min) . Prior to cell disruption, a few crystals of DNase I (from bovine pancreas, Roche) and 0.2 mM of the protease-inhibitor phenylmethylsulfonylfluorid (PMSF) were added to the cell suspension. Twenty µg of each sample was separated on a 10 % SDS-PAGE (Laemmli 1970), and the proteins were subsequently transferred to a PVDF membrane by semi-dry-blotting at 2.0 mA/cm^2 using the Towbin buffer system (Towbin *et al*. 1979). Membranes were blocked for 10 min with TBS buffer (20 mM Tris-HCl, pH 7.5; 150 mM NaCl) containing 1% powdered milk and then incubated with primary antibody solution (in TBS containing 0.1% powdered milk) at 4°C overnight. After 3 consecutive washes with TBS, the membrane was incubated with horseradish peroxidase-conjugated secondary α-rabbit antibody for 1 h at room temperature (1:100,000; POD-α-rabbit; Sigma-Aldrich, Munich). The signals were captured using a Kodak Gel Logic 1500 imaging system. The primary antibodies used for western blotting were α-TolC (1:10,000; Pineda, Berlin) and α-DevB (1:2,500; Pineda).

4.1.3 Results

Similar to the transcription level of *devB* in filaments of *Anabaena* wild type, DevB was most abundant at 9 h after combined nitrogen deprivation (Fig. 19A). It was detectable in a time slot of 6 h only (6-12 h after N-stepdown). *Anabaena* mutants CSE2 (mutant in *ntcA* (Frías *et al*. 1994)) and 216 (mutant in *hetR* (Buikema and Haselkorn 1991)) did not show transcription of *devB*. In agreement, DevB was hardly detectable (Fig. 19A).

Similar to *devB,* the amount of *tolC* transcript reached a maximum at 9h and decreased afterwards (Fig. 19B). In contrast, the protein TolC stayed in nearly equal amounts at an elevated level after 9h (Fig. 19B). In the *ntcA*-mutant CSE2, *tolC* transcripts were present at all states of nitrogen step-down in equal amounts. The TolC protein was detectable and increased after 9h (Fig. 19B). In the *hetR*-mutant 216, upregulation of *tolC* was delayed showing the maximum level of *tolC* transcripts and of TolC protein after 12h of nitrogen deprivation (Fig. 19B).

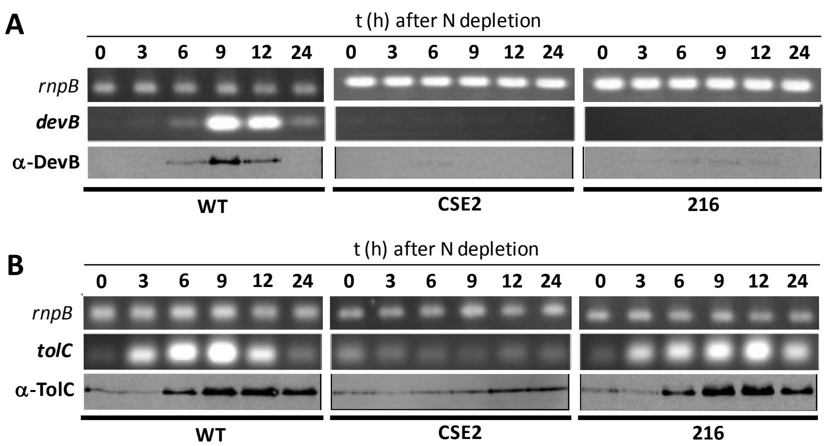

Figure 19. NtcA- and HetR-dependent expression of DevB and TolC

The time-dependent expression of *devB* **(A)** and *tolC* **(B)** *was* analyzed by RT-PCR (italic) or immunoblots (α). RNA or cell extracts were obtained from the same culture after indicated time points of nitrogen starvation (4.1.2). RT of *devB* = 18 PCR cycles; RT of *tolC* = 20, RT of *rnpB* = 15.

4.1.4 Summary

In contrast to DevB, TolC was stable and did not decrease after the transcription level of *tolC* reached its maximum. As already shown (Fiedler *et al.* 2001; Olmedo-Verd *et al.* 2005), mutations in *ntcA* or *hetR* abolished transcriptional induction of *devB*. Although *tolC* is not predicted to be under transcriptional control of NtcA (Su *et al*. 2005), the induction of *tolC* was depending on NtcA. HetR seemed to be involved in temporal coordination of *tolC* expression, since the upregulation of *tolC* during heterocyst formation was delayed.

4.2. Substrate specificity of DevBCA

4.2.1 Background and experimental design

As shown in this work (3. publication), DevBCA react toward the presence of HGLs by increasing the ATP hydrolysis rate of DevA. The intensity of the reaction seemed to depend on the batch and the age of purified glycolipids. The older purified HGLs were the less ATP hydrolysis was observed. This effect was investigated systematically in the following chapter. Four different samples of purified HGLs (1-(O-α-D-glucopyranosyl)-3,25-hexacosanediol and the 3-keto-tautomer) were used to check the reaction of DevBCA toward them. They differed in the age of the culture the HGLs were purified from, and in the intervening time between purification and ATPase assay.

4.2.2 Materials and Methods

Protein design and overexpression

DevB and DevCA were overexpressed as glutathione S-transferase (GST) fusions using the respective pET42a constructs listed in Tab. 3 (pIM381/409, appendix 11.3, page 126) in *E. coli* strain Rosetta-gami (Merck, Darmstadt), and they were purified according to the manufacturer`s instructions (e.g. Fig. 48, appendix 11.6, page 129).

HGL purification and preparation

HGLs were purified by a continuous sucrose gradient as described for *Anabaena cylindrica* (Winkenbach *et al.* 1972). Sample 1 was purified from a young wild type culture deprived from combined nitrogen for 72 h, while sample 3 was purified from an older culture deprived from combined nitrogen for ~2 weeks. Evaporated aliquots of lipids from both samples were kept for ~1 week at room temperature and under air to create samples 2 (from sample 1) and 4 (from sample 3).

Thin layer chromatography

TLC was performed as described (Winkenbach *et al*. 1972). Lipids were dissolved in 100 µl of chloroform and chromatographed on silica gel thin-layer plates (Kieselgel 60, Merck) in 170 ml chloroform, 30 ml methanol, 20 ml acetic acid, and 7.4 ml distilled water. To visualize lipids, the plates were sprinkled with 25% sulfuric acid and exposed to 200°C for 90-120 s.

Densitometry of TLC plates

The percentage of the reduced HGL 1-(O-α-D-glucopyranosyl)-3,25-hexacosanediol in mixtures of both HGLs was determined by evaluating lipids spots on the thin-layer plate by ImageJ 1.4.5 (Abramoff *et al.* 2004).

ATPase assay

ATPase activity was measured as described (3. publication). In brief, 0.1 µg/ml DevAC, 0.2 µg/ml DevB, and 8 µg (dry weight) of the respective HGL samples described above were mixed in reaction buffer (50 mM MES-NaOH, pH 6.5; 1.5 mM DTT; and 0.05% Triton X-100) supplemented with standard ATP-regeneration and NAD-detection ingredients (e.g. 3. publication). The coupled enzyme assay was monitored at 340 nm, and the rate of ATP hydrolysis in U was calculated as moles of ATP hydrolyzed per min and per mg of DevAC.

4.2.3 Results

The different HGLs samples influenced ATP-hydrolysis rates of DevBCA. The more of the 3-enol form 1-(O-α-D-glucopyranosyl)-3,25-hexacosanediol was exposed to DevBCA (Fig. 20A) the higher was the ATP-hydrolyzing reaction (Fig. 20B). The shorter purified samples have been kept under air or the younger the formed heterocysts were the more of the reduced 3-enol tautomer could be detected (Fig. 20A).

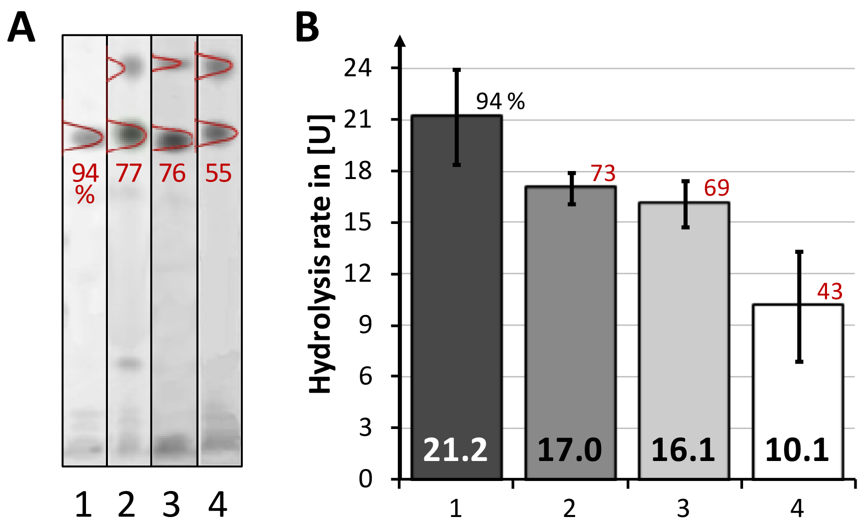

Figure 20. Substrate specificity of DevBCA

(A) TLCs of different samples of HGLs (4.2.2). Samples 1 and 3 refer to different batches of HGL preparations, while samples 2 and 4 were derived by exposing samples 1 and 3 to air for ~1 week (4.2.2). Numbers indicate the percentage of the reduced (and more slowly migrating) 3-enol form. The percentage was derived from densitometric evaluation with ImageJ (lines crossing the lipid spots). **(B)** ATP hydrolysis rates of DevBCA in presence of samples 1-4. Numbers indicate the percentage of U compared to sample 1. The 94 % of sample 1 correspond to the 94 % of the reduced HGL present in sample 1 (A).

4.2.4 Summary

Freshly isolated HGLs from young cultures contained more of the reduced diol-form, which was a better substrate for DevBCA than the oxidized 3-keto-tautomer formed in older cultures or after aerobic incubation.

4.3 Reconstitution of DevBCA and TolC in proteoliposomes

4.3.1 Background and experimental design

DevB and the fused protein DevAC were shown to respond to the presence of HGLs by ATP hydrolysis of DevA (3. publication and previous chapter 4.2). Together with this observation and the phenotype of mutants in genes encoding this EP (1.6; Maldener *et al.* 1994; Fiedler *et al.* 1998; Moslavac *et al.* 2007), it was concluded that HGLs are a substrate of DevBCA-TolC. However, direct evidence of HGL-translocation across the Gram-negative cell wall was missing. The basic idea was to demonstrate translocation of HGLs by using proteoliposomes. This technique was successful to show substrate transport by ABC transporters not participating in EP/T1SS (Geertsma *et al.* 2008). Since DevBCA-TolC form a *trans*-envelope EP, those experiments had to be adjusted accordingly. To simulate both membranes (CM and OM), two types of proteoliposomes had to be created (Fig. 21).

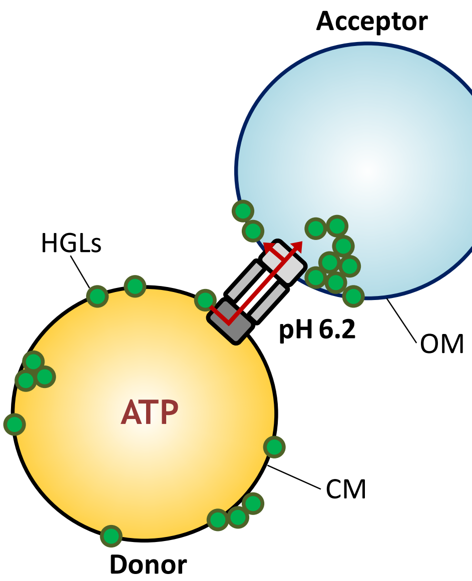

Figure 21. Reconstitution of DevBCA and TolC in proteoliposomes

Schedule for the reconstitution of DevBCA and of TolC in proteoliposomes to demonstrate translocation of HGLs.

The so-called donor proteoliposome (referred to as donor in the following text) should contain the IMF DevAC and the MFP DevB embedded in CM lipids of *Anabaena*. In addition, it should contain HGLs. The so-called acceptor proteoliposome (referred to as acceptor in the following text) should contain the OMF TolC solubilized in OM lipids of *Anabaena* sp. PCC 7120. It should not contain HGLs. In the *devA* transposon mutant M7 (Maldener *et al.* 1994), HGLs remain in the cytoplasmic membrane fraction and are not exported beyond the OM (3. publication). So, this mutant was chosen for the preparation of both lipid mixes.

4.3.2 Material and Methods

Protein design and overexpression

To incorporate widely native proteins into the proteoliposomes, no membrane integral parts have been removed, and no internal tags have been introduced. For discrimination of the proteoliposomes, DevB was fused to a C-terminal StrepII tag, and TolC was fused to a C-terminal His tag. DevA and DevC were fused to one polypeptide joined by 4 repeats of GS. In analogy to the ABC-type IMF MacB from *E. coli*, and to simulate the supposed *in vivo* interaction of the NBD and the SBD, DevA was fused to the N-terminus of DevC. All proteins were overexpressed as GST fusions using the respective pET42a constructs listed in Tab. 3 (pIM407/408/409, appendix 11.3, page 126) in *E. coli* strain Rosetta-gami (Merck, Darmstadt), and they were purified according to the manufacturer`s instructions (e.g. Fig. 48, appendix 11.6, page 129).

Cell fractioning and lipid extraction

To purify the CM and the OM for proteoliposome construction, enriched premature heterocysts (Moslavac *et al*. 2007) of mutant M7 (Maldener *et al.* 1994) were broken by at least five passes through a French Pressure cell (24,000 psi) and separated into a soluble cytoplasmic and an insoluble membrane fraction by centrifugation (60,000 × g, , 4 °C, 30 min). The pellet was loaded on the bottom of a discontinuous sucrose gradient (10/30/40/55 %) to separate CM, TM and OM for 16h at 130,000 *g* and 4 °C according to Moslavac *et al.* (2007). HGLs were purified from the insoluble membrane fraction by a continuous sucrose gradient as described above (4.2.2). Total lipids from the CM or the OM or HGLs were methanol/chloroform-extracted as described above (4.2.2).

Reconstitution of DevBCA and TolC in proteoliposomes

The reconstitution of DevBCA and TolC in proteoliposomes was performed as described by Geertsma *et al.* (2008). To adjust the experiment for simulating *trans*-envelope efflux pumps, DevBCA were incorporated into 2 different proteoliposomes. The donor should contain DevB, DevCA, and CM of *Anabaena* mutant M7, while the acceptor should contain TolC and OM of *Anabaena* mutant M7.

(A) Construction of lipid vesicles

For the construction of the donors, 19.2 mg (dry weight) of total lipids of the CM of the mutant M7 have been purified. For the construction of the acceptors, 15.7 mg (dry weight) of total lipids of the OM of the mutant M7 have been purified. To form liposomes, lipids of the CM or lipids of the OM were suspended in 1 ml 50 mM KP_i-NaOH pH 7.0 and sonicated in six cycles (15s on/45s off) at an intensity of 4 µm on ice water. Subsequently, the suspension was frozen in liquid N_2, and thawed at room temperature. This procedure was repeated five times. The thawed suspensions were extruded eleven times trough a 400 nm polycarbonate filter, and they were subsequently diluted to 3 mg/ml lipid in 50 mM KP_i-NaOH pH 7.0 and 20% glycerol. 5 ml of each liposomes were titrated with 13 aliquots of 10 µl of 10% Triton X-100 wt/vol (donor) or 9 aliquots (acceptor), to reach maximal saturation of the liposomes with the detergent (a maximum OD_{540} of 0,94/0,80). Subsequently, further 5 aliquots of 10% Triton X-100 were added to both liposomes.

(B) Construction of proteoliposomes

Purified DevB and DevAC (1mg/ml in 50 mM KP_i, pH 7.8; 20% glycerol wt/vol; 200 mM NaCl, and 500 mM imidazole) were added to 5 ml of the donors in a ratio of 1:75 DevB-to-lipid (wt/wt) and 1:150 DevAC-to-lipid (wt/wt). The applied molecular DevB-to-DevAC ratio of ~3:1 reflects the ratio demonstrated to be crucial for *in vivo* interaction (3. publication). Purified TolC (1mg ml^{-1} in 50 mM KPi, pH 7.8; 20% wt/vol glycerol; 200 mM NaCl; and 500 mM imidazole) was added to 5 ml of the acceptors in a ratio of 1:150 TolC-to-lipid (wt/wt). The resulting molecular ratio of DevB-to-TolC (donor to acceptor) of ~2:1 reflects the ratio demonstrated to be crucial for *in vivo* interaction (3. publication). The protein-lipid mixtures were incubated for 15 min at room temperature with gentile agitation. After the formation of proteoliposomes, 200 mg of Bio-Beads SM2 (BioRad, Munich) were added 4 subsequential times to 5 ml of the proteoliposome suspensions, and incubated with gentile agitation for 30 min at room temperature, for 60 min at 4 °C, overnight at 4 °C, and for additional 120 min at 4 °C. This step was performed to dilute Triton X-100 below its CMC. Afterwards, Bio-Beads SM2 (binding Triton X-100) were removed by filtration of the mixtures trough sintered glass. To decrease to amount of glycerol, both types of proteoliposomes were diluted ten-fold. Subsequently, proteoliposomes were collected by centrifugation (20 min; 267,000 *g*; room temperature) and suspended with 50 mM KP_i-NaOH, pH 6.2 to a final lipid concentration of 15 mg/ml.

Substrate translocation assay

(A) Inclusion of ATP or medium into proteoliposomes

To include ATP into the donor proteoliposomes, 0.1 ml of 50 mM Na_2-ATP and 50mM $MgSO_4$ in 50 mM KPi-NaOH, pH 7.0 was mixed with 0.5 ml of proteoliposomes of 20 mg ml^{-1} lipid. The mixture was frozen two times in liquid nitrogen, and thawed at 4 °C. By this step, unilamellar proteoliposomes became multilamellar (enveloping parts of the prior surrounding solution). To restore unilamellar vesicles (= final inclusion process), the proteoliposome solution was extruded 11 times trough a 200 nm polycarbonate filter.

To include $BG11_0$-medium into the acceptor proteoliposomes (to simulate growth conditions), 0.5 ml of usual $BG11_0$ medium (Rippka *et al.* 1988) was mixed with 0.5 ml of acceptor proteoliposomes of 20 mg ml^{-1} lipid. The inclusion process was performed as described above.

(B) Translocation assay

Donors and acceptors were mixed in equal parts (5 mg CM lipid to 5 mg OM lipid) in 50 mM MES-NaOH, pH 6.2, and 150 mM NaCl. For HGL translocation, the mixture was incubated for 3h at room temperature. To separate donors from acceptors, the mixture, *i.e.* TolC (acceptor), was purified via Ni-NTA columns according to the manufacturer`s recommendations (Qiagen). Due to the pH of the washing buffer (8.0), the interaction of TolC (acceptor) with DevB (donor) was abolished (3. publication).

Protein interaction assay

Donor and acceptor proteoliposomes were incubated in a lipid ratio of 1:1 in 50 mM MES-NaOH pH 6.2, and 150 mM NaCl. The mixture, *i.e.* TolC (acceptor) was purified via Ni-NTA columns according to the manufacturer`s recommendations (Qiagen). To maintain DevB-TolC interaction, the pH of the washing buffer was adjusted to 6.3.

ATPase assay

ATPase activity was measured as described (3. publication and previous chapter 4.2.2), but by modifying the concentrations of the ATP regeneration system to 60 mM PEP and 0.3 µg/ml pyruvate kinase (were at 6 mM PEP and 3µg/ml pyruvate kinase before; 3. publication).

4.3.3 Results

A complex of DevCA and Strep II-tagged DevB (that has not been used in other ATPase assays) was able to react toward the presence of purified HGLs (Fig. 22A), and all 3 proteins were incorporated into their respective liposomes (Fig. 22B).
Nevertheless, a translocation of the glycolipids did not occur (Fig. 22C). Translocation did also not occur, when (i) the lumen of the donor was filled with an modified ATP regeneration system (60 mM PEP and 0.3 µg/ml pyruvate kinase) and the according buffer, or (ii) 0.1 µg/ml cytoplasm of *Anabaena* wild type and M7 (blue supernatant after centrifugation at 60,000 *g*, 30 min, 4 °C) starved for 9 h and mixed with the ATP regeneration system in the according buffer have been incorporated into the donors, and (iii) CM membranes containing proteins (and not only extracted lipids) were used for proteoliposome construction, or (iv) the translocation was done overnight (all not shown). In any case, the HGLs remained in the donor proteoliposomes (with no remarkable difference in amount), and no HGLs could be detected in acceptor proteoliposomes.
However, donor and acceptor proteoliposomes were able to bind to each other by specific interactions of DevB and TolC. Acceptor vesicles bound to Ni-NTA columns were able to retain donor vesicles at pH 6.3 (Fig. 23), while they were not able to do so at pH 8.0 (Fig. 23). This is consistent with the pH-dependence of DevB-TolC interaction (3. publication).

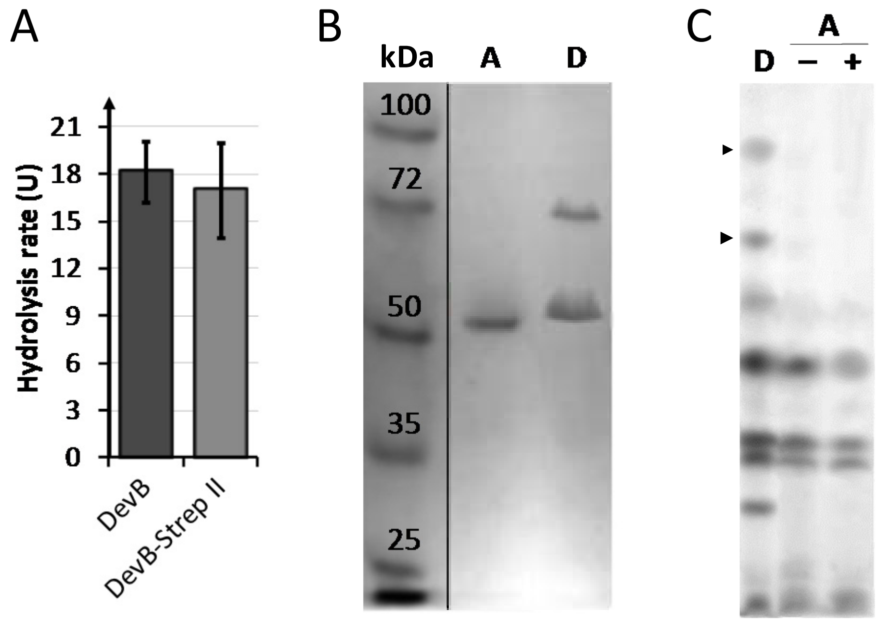

Figure 22. Substrate translocation from donor to acceptor proteoliposomes

(A) ATP hydrolysis rates of DevAC with non-tagged DevB and in complex with DevB-Strep II. The modified ATP regeneration system described in 4.3.2 was used here. **(B)** SDS-PAGE separation of acceptor (A) and donor proteoliposomes (D). The band of higher MW in lane D is DevAC, the lower band is DevB. The band in lane A is TolC. kDa = protein standard. **(C)** TLC (4.2.2) of donor (D) and acceptor (A) proteoliposomes before (-) and after (+) incubation for 3 h together. Arrowheads indicate HGLs.

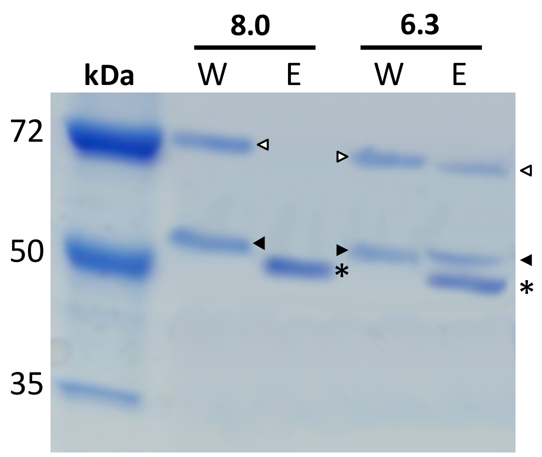

Figure 23. Interactions between acceptor and donor proteoliposomes

kDa = protein standard **(8.0)** Washing fraction (W) and eluant (E) of mixed donors and acceptors purified for His-tagged TolC. The pH of the washing buffer was 8.0. **(6.3)** Washing fraction (W) and eluant (E) of mixed donors and acceptors purified for His-tagged TolC. The pH of the washing buffer was 6.3. White arrowheads = DevAC; black arrowheads = DevB; stars = TolC.

4.3.4 Summary

DevBCA and TolC were incorporated into different liposomes. The resulting proteoliposomes were able to interact via DevB and TolC, but translocation of HGLs did not occur.

5. Manuscript I: Structure-function analysis of the ATP-driven glycolipid efflux pump DevBCA reveals the complex organization with TolC

STRUCTURE-FUNCTION ANALYSIS OF THE ATP-DRIVEN GLYCOLIPID EFFLUX PUMP DEVBCA REVEALS THE COMPLEX ORGANIZATION WITH TOLC

Peter Staron, Karl Forchhammer and Iris Maldener
From Department of Microbiology/Organismic Interactions, IMIT –Institute of Microbiology and Infection Medicine Tübingen
University of Tübingen, 72076 Tübingen

Running Head: Structure-function analysis of an ATP-driven efflux pump

Address correspondence to: Iris Maldener, Department of Microbiology/Organismic Interactions, Auf der Morgenstelle 28, 72076 Tübingen, Phone: +49 (7071) 29-78847, Fax: +49 (7071) 29-5843, E-mail: iris.maldener@uni-tuebingen.de

Background: DevBCA-TolC form an ATP-driven glycolipid trans-envelope efflux pump.
Results: A DevB hexamer interacts tip-to-tip with TolC, and it promotes substrate recognition of DevAC.
Conclusion: A central periplasmic hexamer coordinates the formation of an ATP-driven efflux pump.
Significance: Mechanistic details of efflux pumps are important for understanding various bacterial processes like cell differentiation, acclimatization processes or drug resistance.

SUMMARY

In Gram-negative bacteria, each trans-envelope efflux pump has a periplasmic membrane fusion protein (MFP) as an essential periplasmic component. In general, MFPs act as mediators between an outer membrane factor (OMF) and an inner membrane factor (IMF). In this study, structure-function relations of the ATP-driven glycolipid efflux pump DevBCA-TolC from the cyanobacterium *Anabaena* sp. PCC 7120 were analyzed. Modified variants of the MFP DevB were generated, and their interaction with the OMF TolC and the IMF DevAC were investigated. The binding of DevB to TolC absolutely required the tip-regions of the respective α-helical domains. The interaction of DevB to DevAC mainly involved the β-barrel and the lipoyl domain of the MFP. Efficient binding to DevAC and TolC was depending on stable DevB hexamers. Except for the distal part of the α-helical domain, all domains of DevB contributed to stable hexamers. DevB variants inhibited in hexamerization, as well as a DevB variant lacking the N-terminal cytoplasmic tail, were not able to promote substrate recognition of DevAC.

INTRODUCTION

Gram-negative bacteria use tripartite trans-envelope efflux pumps to export a wide variety of proteins and other molecules (1-3). These exporters span the cytoplasmic membrane, the periplasm, and the outer membrane. They are composed of inner membrane factors (IMFs) and of outer membrane factors (OMFs), and both are connected by central periplasmic membrane fusion proteins (MFPs) (2,3).
IMFs can either be ATP-driven (ATP-binding cassette (ABC) superfamily, also known as type I secretion systems) or proton gradient-driven (resistance-nodulation-division (RND) or major facilitator superfamily), while the same TolC-like OMF can be used by all IMFs (1-6). The

periplasmic MFPs differ from each other in sequence, molecular mass and biochemical properties, but are structurally similar (7). A typical ABC-type MFP consists of the following structural elements: an N-terminal cytoplasmic tail, an anchor in the cytoplasmic membrane, a cytoplasmic membrane proximal β-roll, a β-barrel domain, a lipoyl domain and an α-helical domain protruding toward the OMF (2,8,9).

Up to now, most of our knowledge on structure, complex formation and transport mechanism of efflux pumps is based on studies on the RND-type multidrug efflux pump AcrAB-TolC, and on studies on the ABC-type efflux pump MacAB-TolC of *Escherichia coli* (1,2,6). In the AcrAB-TolC-exporter the IMF AcrB assembles to a trimer, and utilizes a proton-gradient as driving force for the export of various drugs, salts, and antibiotics in *E. coli* (2,10,11). AcrB has large periplasmic domains that presumably are in direct contact with the OMF TolC (12,13). Evaluation of cross-link data indicated a trimer of the MFP AcrA wrapping its α-helical domain around TolC (14-17). The proposed model for the ABC-type efflux pump MacAB suggests a completely different pump topology. Here, a hexameric MFP MacA is assumed to connect the IMF MacB and the OMF TolC (18-20). In this model, MacA and TolC interact in a cogwheel-like assembly between both tip-regions of the respective α-helical domains.

Our previous work on DevBCA-TolC supported the model proposed for MacAB-TolC. DevBCA and TolC from the filamentous cyanobacterium *Anabaena* sp. PCC 7120 were shown to form an ATP-driven efflux pump to export glycolipids in the course of heterocyst maturation (21). Heterocysts are formed during depletion of combined nitrogen in a semi regular pattern along the filaments. Whilst the vegetative cells, from which they differentiate, perform oxygenic photosynthesis, the heterocysts are specialized for fixation of nitrogen by nitrogenase. They provide an micro-oxic environment suitable for nitrogenase and exchange metabolites and signals with the vegetative cells (22-24). Among other adaptations, heterocyst deposit two additional layers on the top of the Gram-negative cell wall to reduce the entrance of oxygen from the aerobic environment. The innermost layer is made up of heterocyst specific glycolipids, and represents the actual barrier for O_2 (25). It is stabilized by a thick polysaccharide layer. The DevBCA-TolC efflux pump was shown to export this heterocyst glycolipids. The crucial stoichiometric relations of DevBCA-TolC for export were found to be in line with the ones postulated for MacAB-TolC: the IMF-to-MFP-to-OMF ratio of DevAC-to-DevB-to-TolC was shown to be 2:6:3 (21).

To contribute to a better understanding of the structure and assembly of an ATP-driven efflux pump, we took a closer look on DevBCA-TolC. We investigated modified variants of the MFP DevB. By this, we could clarify the relevance of different structural elements in formation and function of the efflux pump machinery via size exclusion chromatography (SEC), surface plasmon resonance (SPR) and ATP hydrolysis assays. We could show that a hexameric MFP plays a key role in the functional assembly of ATP-driven efflux pumps. This oligomeric state allowed high affinity binding to the OMF TolC, and to the IMF DevAC. Interaction of DevB with DevAC involved the MFP`s β-barrel and lipoyl domain, whereas the binding to TolC absolutely required the tip regions of the respective α-helical domains. Hexameric DevB allowed the IMF DevAC to react to its substrate, while any impairment in hexamerization abolished this ability. In addition, a DevB variant lacking the N-terminal cytoplasmic tail was also not able to promote substrate recognition.

EXPERIMENTAL PROCEDURES

Construction, overexpression, and purification of recombinant proteins-

DevB variants, TolC variants, and DevAC were overexpressed and purified as described previously (21). All protein constructs were overexpressed as glutathione-S-transferase tag fusions in *E. coli* strain Rosetta-Gami^{TM} DE3 using pET42a (Merck, Darmstadt, Germany). Recombinant proteins were purified according to the manufacturer's instructions. Depending on the respective experiment, some of the proteins carried an additional C-terminal octahistidine tag (8H). A register of the variants used in this study can be found in Table 1. The created plasmid constructs are listes in Table S1, the oligonucleotides used for amplification are listed in Table S2.

Gel filtration chromatography-

Recombinant proteins were analyzed via size-exclusion chromatography (SEC) as described previously (21). In brief, 1 mg/ml of variant DevB proteins were separated on a Superdex 200 HR 10/30 gel-filtration column (GE Healthcare) in running buffer (25 mM MES-NaOH, pH 6.2; 150 mM NaCl and 0.05% Triton X-100). The flow rate was decreased to 0.5 ml/min.

Surface plasmon resonance-

Surface plasmon resonance (SPR) experiments were performed by using a Biacore X biosensor system (Biacore AB, Uppsala, Sweden) as described previously (21). His-tagged ligands were immobilized in flow cell 2 (FC2) of an Ni^{2+}-loaded NTA sensor chip, and His tag-free analytes in reaction buffer (25 mM MES-NaOH at pH 6.2; 150 mM NaCl; and 0.05% Triton X-100) were injected into FC1 and FC2 at a flow rate of 0.5 ml/min. Specific interactions were captured as response difference between FC2 and FC1.

Cell fractionation and glycolipid purification-

Cell fractions (26) and pure heterocyst glycolipids (27) were prepared as described. In brief, enriched heterocysts (26) were broken by at least five passes through a French Pressure cell (24,000 psi) and separated into a soluble cytoplasmic and an insoluble membrane fraction by centrifugation (45,000 × g, 30 min, 4°C). The pellet was separated by the respective gradients to purify cell fractions (26) or heterocyst glycolipids (27).

ATP hydrolysis assay-

The assay was performed as described previously (21). 0.1 µg/ml DevAC and 0.2 µg/ml of the respective DevB variant, and 8 µg of purified heterocyst glycolipids were mixed in reaction buffer. Absorbance data of the coupled ATPase assay were collected at a wavelength of 340 nm, and rate of hydrolysis in units was calculated as moles of ATP hydrolyzed per minute and per milligram of the ATPase.

RESULTS

All domains of DevB contribute to hexamerization-

A DevB hexamer is crucial for the *in vivo*-function of DevBCA-TolC (21). A mutation of N^{333} to A, located in the proximal α-helical domain (Fig. 1A), prevented the MFP from forming stable hexamers. This inability resulted in the loss of function to export glycolipids across the Gram-negative cell wall.

To clarify how the domains of DevB contribute to this important oligomeric state, we investigated the hexamerization behavior of different variants of DevB via SEC and SPR, and compared it to full-length reference DevB (Fig. 1A, Tab. 1). The variants used in this approach where lacking either parts of the α-helical domain, the entire α-helical domain, or the β-barrel domain (Fig. 1E-F, Tab. 1). To maintain the MFP`s overall structure, the lipoyl domain was not deleted, but central parts were replaced by repeats of GGS or SSG. DevB is not predicted to encode a (full) β-roll, so this structural feature was not considered in this work.

In SEC, the majority of full-length DevB (Fig. 1A; reference B) was eluted as hexamers (Fig. 2A; upper solid line). In contrast, DevB lacking the entire α-helical domain (B-αHD) was massively impaired in hexamer formation (Fig. 2A; lower solid line). In agreement with this result, SPR analysis showed that B-αHD was highly impaired in binding to immobilized full-length DevB (Fig. 2B). By removing the distal part of DevB`s α-helical domain (B-DαHD), no remarkable change in hexamer levels could be observed in SEC (Fig. 2A; dashed line). In line with this results, B-DαHD was not remarkably impaired in binding to immobilized full-length DevB (Fig. 2B). Instead, a deletion of the proximal part of DevB`s α-helical domain had a severe effect. This DevB variant (B-PαHD) was massively impaired in hexamerization (Fig. 2A; dotted line), and the interaction with immobilized full-length DevB was remarkably decreased (Fig. 2B).

Deleting the β-barrel domain (B-βBD) led to a moderate impairment in hexamer formation (Fig. 2A; dot-dot-dashed line). Replacing central parts of the lipoyl domain (B_xLipD) had a more severe effect (Fig. 2A; dot-dashed line). In line with the remaining ability to form hexamers, the affinity of B-βBD to immobilized full-length DevB in SPR is higher than the one of B_xLipD (Fig. 2B).

In summary, all domains of DevB contribute to hexamerization. Only the distal part of the α-helical domain was dispensable in this context.

The α-helical tip regions of both proteins are crucial for sufficient binding of hexameric DevB to trimeric TolC-

It was proposed that a MacA hexamer binds to trimeric TolC in a cogwheel-like manner (18-20). The interaction interface was shown to be formed by the α-helical tip of MacA and by the α-helical tips of TolC. To investigate whether this is also true for the DevBCA-TolC, we quantified the interaction of DevB lacking the α-helical tip region with reference TolC via SPR (Fig. 1 and Tab. 1). This approach is also suitable to address the influence of DevB hexamerization affecing the binding to TolC. Therefore, the native α-helical tips of DevB variants shown to be impaired in hexamerization were modified. The interaction of DevB variants carrying both types of tip regions, native and replaced ones, was quantified towards reference TolC by using SPR.

Regardless of the remaining structure, all DevB variants lacking the native α-helical tips (B*, B-DαHD*, B-PαHD*, B_xLipD*, B-βBD*) could hardly interact with immobilized reference TolC in SPR (Fig. 3A). The affinities of native α-helical tip variants of DevB toward TolC were almost in line with the ability to hexamerize observed before.

We also investigated structural criteria of TolC in binding to DevB. Therefore, we quantified the interaction of TolC variants lacking the native α-helical tips with immobilized reference DevB via SPR analysis.

In agreement to the binding of tip-mutated variants of DevB with TolC, tip-mutated TolC could not efficiently interact with surface-bound reference DevB in SPR (Fig. 3B; D^{*}).

Furthermore, we analyzed if the proposed model of the RND-type exporter AcrAB-TolC could be applied to DevB-TolC interaction (14-17). In this model, TolC helices 3/4 and 7/8 provide binding pockets for the α-helical domain of AcrA. Therefore, the respective regions of *Anabaena*`s TolC have been mutated to helix-conserving AL-repeats, and the interaction with immobilized DevB was quantified via SPR.

As compared to reference TolC, mutations in TolC`s helices 3/4 (D_xαH3/4; Fig. 1H) or helices 7/8 (D_xαH7/8; Fig. 1I) did not remarkably impair the interaction with DevB (Fig. 3B).

Our results for DevB-TolC interaction are in line with the cogwheel-like tip-to-tip interface formed by MacA and TolC. This interface is made up by the respective tip-regions. In agreement with results shown previously for the DevB variant N^{333}A (21), the second crucial factor for efficient interaction with TolC is the ability of DevB to form hexamers.

A DevB hexamer promotes substrate dependent reaction of the IMF DevAC-

Complete formation of an ATP-driven efflux pump also includes interactions between the MFP and the substrate recognizing and exporting motor, the IMF. Therefore, we took a closer look on the interplay of DevB variants with the immobilized IMF DevAC in SPR.

As compared to the interaction with TolC, DevB variants lacking parts or the entire α-helical domain were less impaired in interaction with DevAC (Fig. 4A; B-αHD, B-DαHD, B-PαHD). Mutating the lipoyl domain or deleting the β-barrel domain resulted in severely descreased responses (Fig. 4A; B_xLipD, B-βBD). Once again, an influence of DevB`s hexamerization ability can be observed. The order of response strength implies i) a contact interface of DevB to DevAC involving both the lipoyl and the β-barrel domain, and it reflects ii) a stabilizing effect of DevB hexamers on the binding to DevAC. Latter is similar to the binding of DevB to TolC (Fig. 2A and 2B).

A single-site mutation in the proximal α-helical domain of DevB (N^{333} to A) prevented the formation of stable hexamers (21). This mutation also abolished the ability of DevB to promote a substrate-dependent increase in ATPase activity of DevAC. In line, all DevB variants impaired in hexamerization failed to promote an ATP-hydrolizing reaction of DevAC toward the substrate (Fig. 4B). In contrast, DevB-DαHD was not remarkably impaired in forming hexamers (Fig. 2A and 2B), and it retained the ability to activate DevAC. Interestingly, a deletion of DevB`s N-terminal cytoplasmic tail also completely abolished the recognition of the glycolipid substrate by DevAC (Fig. 4B; B-N), although this variant was not remarkably impaired in binding to DevAC (Fig. 4A; B-N).

Our results confirm and further extend the earlier postulated importance of the hexameric state of DevB. An MFP hexamer is required for the binding binding to the IMF DevAC. It plays a crucial role in promoting recognition and export of the substrate.

DISCUSSION

DevB and TolC form a tip-to-tip interface-

It was proposed that a hexameric MacA binds to trimeric TolC in a cogwheel-like manner (18-20). Our previous data on DevBCA-TolC indirectly supported this model by predicting a 3:6:2 stoichiometry of TolC:DevB:DevAC (21). This study unambiguously demonstrates a cogwheel-like tip-to-tip interface between DevB and TolC. Whenever that interface had been modified, the interaction of the MFP with the OMF was remarkably impaired (Fig. 3A and 3B).

The regions claimed to be crucial for the interaction of the RND-type MFP AcrA to TolC did not seem to be important for the ABC-type MFP DevB. *In vivo* cross-linking revealed contact sites in the α-helical domain of AcrA and in the α-helical barrel of TolC, and therefore it implied a 3:3:3 stoichiometry of AcrB:AcrA:TolC. It was proposed that the α-helical domain of AcrA docks into pockets provided by helices 3/4 and 7/8 of TolC`s α-helical barrel. Thus, three molecules of AcrA would wrap around TolC, and TolC is in direct contact to the IMF AcrB (14-17). For DevB-TolC interaction, the corresponding region of helices 3,4,7, and 8 of TolC were not crucial for binding DevB (Fig. 3B). If the proposed wrapping model was true for DevB and TolC, a more severe effect on the interaction should be expected. So, a coiled-coil interaction of DevB and TolC is not likely. The upper subdomain of the periplasmic core of MacB, an ABC exporter like DevC, shows similarities to AcrB`s TolC-docking domain (28), and therefore it could interact with the tips of TolC. DevAC did neither interact with TolC carrying native tips nor with TolC carrying mutated tips in SPR (Fig. S3; green line). Taken together, DevBCA-TolC did not reflect the organization of AcrAB-TolC. It has to be noted, that more recent studies predict a hexameric AcrA/AcrA-homologue MtrC to interact with TolC (29,30). The proposed 3:3:3 model could reflect the functional state of AcrA-TolC, a 3:6:3 model an intermediate state (or *vice versa*).

Appropriate binding of DevB to TolC requires a stable DevB hexamer-

A DevB hexamer is a prerequisite for the *in vivo* function of DevBCA-TolC. A mutation in the proximal α-helical domain of DevB (N^{333} to A) prevented the formation of stable hexamers, and therefore it abolished the export of the glycolipid substrate (21). As already implied by this mutation, DevB-PαHD is not able to form stable hexamers (Fig. 2A and 2B), and it is also not able to cause a DevAC reaction toward the glycolipid substrate (Fig. 4B). In contrast, almost no influence on hexamerization could be observed when the distal part of the α-helical domain was deleted. It seems that inter-MFP-interactions in the proximal α-helical domain of DevB are involved in stabilization of hexamers, while residues in the distal α-helical domain have a minor effect.

The crystal structure of MacA (18) could be interpreted to allow several possible inter-MFP bridges in the α-helical domain -but- not being restricted to the proximal part only. Anyway, comparing the α-helical domains of MacA and DevB is challenging, since both show only minor homologies in sequence. In addition, DevB is predicted to form a much longer α-helical domain containing coiled-coil extensions (26). This might be an adaptation to the large cyanobacterial periplasm (approx. 46 nm (31)). Nevertheless, it seems that the proximal α-helical domain is more conserved: besides showing slightly higher homologies to MacA, two large insets appear to be conserved in all DevB-like MFPs from *Anabaena* (as compared to MacA; Fig. S5). In contrast, the distal α-helical domain includes extensions not conserved in all close DevB homologues (and also not in MacA). So, while the more conserved proximal helices seem to be responsible for hexamer stabilization, the specific extensions in the distal α-helical domain could reflect an individual modification of the respective MFP.

The crystal structure of MacA also implies some possible inter-MFP bridges between the lypoil domains. Replacing those regions, including the loop of Q^{209} conserved in MacA systems (18), with GS repeats remarkably impaired DevB in forming hexamers. A similar mode to inter-MacA-bridging can be assumed here.

As shown for MacA (18), the β-barrel domain of DevB was involved in providing hexamer stability (Fig. 2A). The variant used in this study lacks most of the β-barrel domain, including the regions of MacA`s E^{231}, Y^{275}, and T^{293}. These residues have been shown to have a skriking effect on hexamer formation by MacA (18). The hexamer stabilization method of DevB seems to slightly differ to MacA systems, since only E^{231} is conserved in DevB and its *Anabaena* sp. PCC 7120 homologues (as E^{391}).

Taken together, all three domains of DevB contribute to the oligomerization process.

Proper substrate recognition of DevAC requires a hexameric DevB-

An interface between DevB and DevAC cannot be exactly predicted from our data. Both DevB`s β-barrel domain and the lipoyl domain had a severe effect on the interaction with DevAC (Fig. 4A). Regarding the response strenght, it was comparable to that of mutations in the DevB-TolC interface. Several crucial contact sites to DevC seem to be absent here.

Interestingly, the binding behavior did not match with the ability of the DevBCA complex to recognize the substrate and thereupon, to enhance ATP hydrolysis in the presence of the substrate. Besides reference DevB and B-DαHD, none of the MFP variants could mediate substrate-dependent ATPase activity (Fig. 4B). So, a DevB hexamer is also crucial for promoting the ability of substrate recognition of DevAC. This is supported by a DevB mutant in N^{333}, a residue important for stable hexamerization. DevB N^{333}A fails to promote substrate-dependent reaction of DevAC, as reported earlier (21).

Interestingly, the DevB variant lacking the first 22 residues (variant B-N) was also not able to promote a substrate-dependent reaction in ATPase activity of DevAC, although was not noticeably impaired in binding to the IMF. This short cytoplasmic tail seems to be involved in the IMF`s substrate recognition mechanism. Six close homologues of the MFP DevB predicted from the genome of *Anabaena* sp. PCC 7120 (encoded by the genes *all0809*, *all2675*, *alr3647*, *alr4280*, *alr4973*, and *all5347*) also have cytoplasmic tails of 10-18 aa`s, but totally different in sequence. All0809 is not able to promote a substrate-dependent reaction of the ATPase activity of DevAC, although All0809 binds to DevAC (unpublished data). So, the cytoplasmic tail might add an additional binding-specificity control of the MFP to the IMF and *vice versa*.

In summary, our results confirm the central role of MFP hexamers in ABC-driven efflux pumps. A DevB hexamer does not only form a cogwheel-like tip-to-tip interface to the OMF TolC, it also promotes activation and substrate recognition of the IMF DevAC. Any impairment regarding the hexamerization of DevB consequently inhibits the formation of the whole secretion machinery.

REFERENCES

1. Zgurskaya, H. I., Krishnamoorthy, G., Ntreh, A., and Lu, S. (2011) *Front. Microbiol.* **2**, 189
2. Zgurskaya, H. I. (2009) *Future Microbiol.* **4**, 919-932
3. Koronakis, V., Eswaran, J., and Hughes, C. (2004) *Annu. Rev. Biochem.* **73**, 467-489
4. Holland, I. B., Schmitt, L., and Young, J. (2005) *Mol. Membr. Biol.* **22**, 29-39
5. Saier, M. H., Jr., Beatty, J. T., Goffeau, A., Harley, K. T., Heijne, W. H., Huang, S. C., Jack, D. L., Jahn, P. S., Lew, K., Liu, J., Pao, S. S., Paulsen, I. T., Tseng, T. T., and Virk, P. S. (1999) *J. Mol. Microbiol. Biotechnol.* **1**, 257-279
6. Nikaido, H. (2011) *Adv. Enzymol. Relat. Areas Mol. Biol.* **77**, 1-60
7. Tikhonova, E. B., Dastidar, V., Rybenkov, V. V., and Zgurskaya, H. I. (2009) *Proc. Natl. Acad. Sci. U.S.A.* **106**, 16416-16421
8. Johnson, J. M., and Church, G. M. (1999) *J. Mol. Biol.* **287**, 695-715
9. Zgurskaya, H. I., Yamada, Y., Tikhonova, E. B., Ge, Q., and Krishnamoorthy, G. (2009) *Biochim. Biophys. Acta* **1794**, 794-807
10. Murakami, S., Nakashima, R., Yamashita, E., and Yamaguchi, A. (2002) *Nature* **419**, 587-593
11. Tikhonova, E. B., Yamada, Y., and Zgurskaya, H. I. (2011) *Chem. Biol.* **18**, 454-463
12. Tamura, N., Murakami, S., Oyama, Y., Ishiguro, M., and Yamaguchi, A. (2005) *Biochemistry* **44**, 11115-11121
13. Tikhonova, E. B., and Zgurskaya, H. I. (2004) *J. Biol. Chem.* **279**, 32116-32124
14. Lobedanz, S., Bokma, E., Symmons, M. F., Koronakis, E., Hughes, C., and Koronakis, V. (2007) *Proc. Natl. Acad. Sci. U S A* **104**, 4612-4617
15. Bavro, V. N., Pietras, Z., Furnham, N., Perez-Cano, L., Fernandez-Recio, J., Pei, X. Y., Misra, R., and Luisi, B. (2008) *Mol. Cell* **30**, 114-121
16. Symmons, M. F., Bokma, E., Koronakis, E., Hughes, C., and Koronakis, V. (2009) *Proc. Natl. Acad. Sci. U.S.A.* **106**, 7173-7178
17. Touze, T., Eswaran, J., Bokma, E., Koronakis, E., Hughes, C., and Koronakis, V. (2004) *Mol. Microbiol* **53**, 697-706
18. Yum, S., Xu, Y., Piao, S., Sim, S. H., Kim, H. M., Jo, W. S., Kim, K. J., Kweon, H. S., Jeong, M. H., Jeon, H., Lee, K., and Ha, N. C. (2009) *J. Mol. Biol.* **387**, 1286-1297
19. Xu, Y., Sim, S. H., Song, S., Piao, S., Kim, H. M., Jin, X. L., Lee, K., and Ha, N. C. (2010) *Biochem. Biophys. Res. Commun*. **394**, 962-965
20. Xu, Y., Song, S., Moeller, A., Kim, N., Piao, S., Sim, S. H., Kang, M., Yu, W., Cho, H. S., Chang, I., Lee, K., and Ha, N. C. (2011) *J. Biol. Chem.* **286**, 13541-13549
21. Staron, P., Forchhammer, K., and Maldener, I. (2011) *J. Biol. Chem.* **286**, 38202-38210
22. Flores, E., and Herrero, A. (2010) *Nat. Rev. Microbiol.* **8**, 39-50
23. Flores, E., Herrero, A., Wolk, C. P., and Maldener, I. (2006) *Trends Microbiol.* **14**, 439-443
24. Kumar, K., Mella-Herrera, R. A., and Golden, J. W. (2010) *Cold Spring Harb. Perspect. Biol.* **2**, a000315
25. Wolk, C. P., Ernst, A., and Elhai, J. (1994) *The Molecular Biology of Cyanobacteria, Bryant, D.A. (ed.)*, 769-823, Kluwer Academic, Dudrecht, The Netherlands
26. Moslavac, S., Nicolaisen, K., Mirus, O., Al Dehni, F., Pernil, R., Flores, E., Maldener, I., and Schleiff, E. (2007) *J. Bacteriol.* **189**, 7887-7895
27. Winkenbach, F., Wolk, C. P., Jost M. (1972) *PLANTA* **107**, 69-80
28. Xu, Y., Sim, S. H., Nam, K. H., Jin, X. L., Kim, H. M., Hwang, K. Y., Lee, K., and Ha, N. C. (2009) *Biochemistry* **48**, 5218-5225
29. Janganan, T. K., Bavro, V. N., Zhang, L., Matak-Vinkovic, D., Barrera, N. P., Venien-Bryan, C., Robinson, C. V., Borges-Walmsley, M. I., and Walmsley, A. R. (2011) *J. Biol. Chem.* **286**, 26900-26912
30. Xu, Y., Lee, M., Moeller, A., Song, S., Yoon, B. Y., Kim, H. M., Jun, S. Y., Lee, K., and Ha, N. C. (2011) *J. Biol. Chem.* **286**, 17910-17920
31. Wilk, L., Strauss, M., Rudolf, M., Nicolaisen, K., Flores, E., Kuhlbrandt, W., and Schleiff, E. (2011) *Cell Microbiol.* **13**, 1744-1754

FOOTNOTES

This work was supported by Deutsche Forschungsgemeinschaft (DFG-Ma1359/5-1).

ABBREVIATIONS

OMF, outer membrane factor; MFP, membrane fusion protein; IMF, inner membrane factor; ABC, ATP- binding cassette; SEC, size exclusion chromatography; SPR, surface plasmon resonance

TABLES

Table 1: Protein constructs used in this study.

A graphical representation is shown in Fig. 1. The respective plasmid constructs are listed in Table S1, the primers used for construction are listed in Table S2.

Construct	Modification
Full-length DevB	DevB with replaced membrane anchor (4GS instead).
B*	The α-helical tip of B-DαHD was replaced with GGS.
B-αHD	DevB lacking the α-helical domain.
B-DαHD	DevB lacking the distal α-helical domain.
B-DαHD*	The α-helical tip of B-DαHD was replaced with GGS.
B-PαHD	DevB lacking the proximal α-helical domain.
B-PαHD*	The α-helical tip of B-PαHD was replaced with GGS.
B_xLipD	DevB with replaced parts of the (ascending) lipoyl domain.
B_xLipD*	The α-helical tip domain of B_xLipD was replaced with GGS.
B-βBD	DevB lacking most parts of the β-barrel domain.
B-βBD*	The α-helical tip domain of B-βBD was replaced with GGS.
B-N	DevB lacking the cytoplasmic N-terminus.
Reference TolC	TolC lacking the beta barrels (2x 4GS or 8H instead).
D*	The α-helical tips of D were replaced with GGS/SSG.
D_xαHD3/4	Central parts of TolC helices 3 and 4 were replaced with 4AL.
D_xαHD3/4*	The α-helical tips of D_xαHD3/4 were replaced with GGS/SSG.
D_xαHD7/8	Central parts of TolC helices 7 and 8 were replaced with 4AL.
D_xαHD7/8*	The α-helical tips of D_xαHD7/8 were replaced with GGS/SSG.
DevAC	The stop codon of DevA was removed, and DevC was fused to the C-terminus of DevA by 8H.

DevB, DevC, and DevA are also referred to as Alr3710, Alr3711, and Alr3712. TolC is also referred to as HgdD or Alr2887.

FIGURE LEGENDS

FIGURE 1: Variants of DevB and TolC used in this study.
The shown protein variants reflect illustrating models of DevB and TolC. They are based on resolved crystals of MacA (DOI: 10.2210/pdb3fpp/pdb) and TolC (DOI: 10.2210/pdb1ek9/pdb) of *E. coli.* For simplicity, the α-helical domain of DevB is shortened. Additional information is given in Tab. 1. **(A)** Full-length DevB. In green: tip region. **(B)** DevB lacking the α-helical domain (in grey; B-αHD). **(C)** DevB lacking the distal part of the α-helical domain (in grey; B-DαHD). **(D)** DevB lacking the proximal part of the α-helical domain (in grey; B-PαHD). **(E)** DevB with replaced parts in the (ascending) lipoyl domain (in red; B_xLipD). **(F)** DevB lacking most of the β-barrel domain (in grey; B-βBD). **(G)** Reference TolC. In green: tip regions of the α-helical hairpins. Numerics indicate the helix number. **(H)** TolC with replaced parts in helices 3 and 4 (in red; D_xαHD3/4). **(I)** TolC with replaced parts in helices 7 and 8 (in red; D_xαHD7/8).

FIGURE 2: Influence of DevB subdomains on oligomerization.
(A) SEC profile of different DevB variants (Fig. 1). All variants of DevB were aligned to the hexamer peak of full-length DevB. The raw data are shown in Fig. S1. Upper solid line = Full-length DevB; lower solid line = B-αHD; dashed line = B-DαHD; dotted line = B-PαHD; dot-dashed line = B_xLipD; dot-dot-dashed line = B-βBD. **(B)** Evaluated SPR analysis of the interaction of immobilized full-length DevB with different variants of DevB (indicated). The raw data are shown in Fig. S2, and they were evaluated after 118s in the association phase respecting the molecular weight of each variant.

FIGURE 3: Stable DevB hexamers interact tip-to-tip with TolC.
(A) Evaluated SPR analysis of the interaction of immobilized reference TolC with different variants of DevB (indicated). The raw data are shown in Fig. S3A, and they were evaluated after 118s in the association phase respecting the molecular weight of each variant**.**
(B) Evaluated SPR analysis of the interaction of immobilized full-lenght DevB with different variants of TolC (indicated). The raw data are shown in Fig. S3B, and they were evaluated after 118s in the association phase respecting the molecular weight of each variant**.**

FIGURE 4: Stable DevB hexamers promote the substrate recognition of DevAC.
(A) Evaluated SPR analysis of the interaction of immobilized DevAC with different variants of DevB (indicated). The raw data are shown in Fig. S4 and were evaluated after 177s in the association phase respecting the molecular weight of each variant.
(B) ATP hydrolysis rates of DevAC in presence of different constructs of DevB (indicated) and the HGL substrate. CA = DevAC alone; -S = no glycolipid substrate.

FIGURES

Figure 1

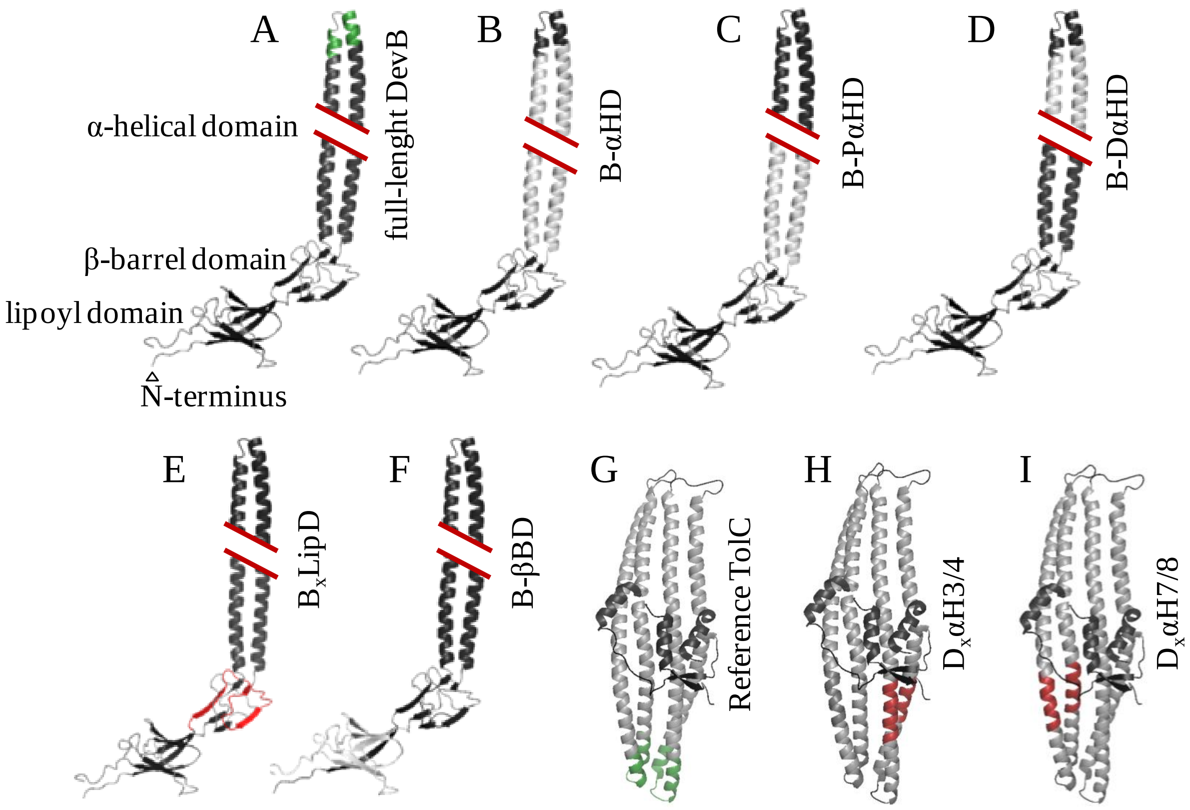

Figure 2

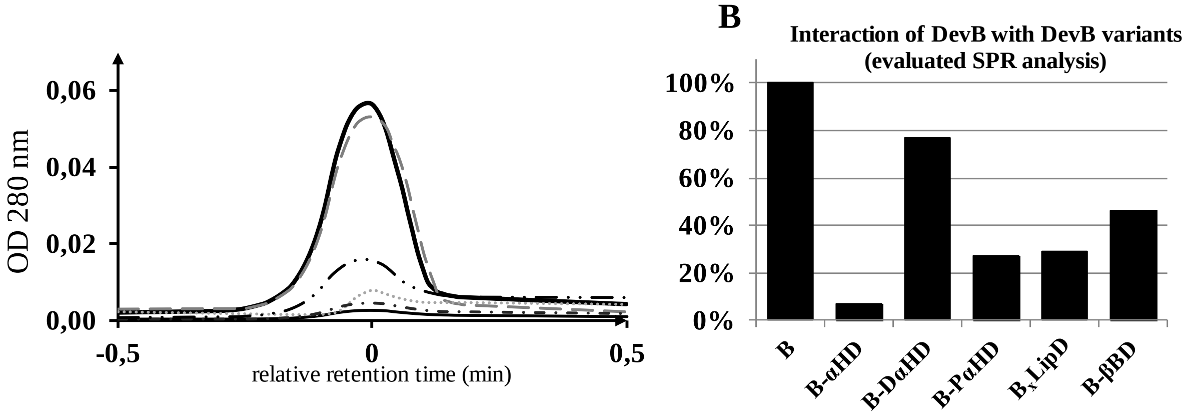
0,06
0,04
0,02
0,00
OD 280 nm
-0,5
0
0,5
relative retention time (min)
B
Interaction of DevB with DevB variants
(evaluated SPR analysis)
100%
80%
60%
40%
20%
0%
B
B-αHD
B-DαHD
B-PαHD
BxLipD
B-βBD

Figure 3

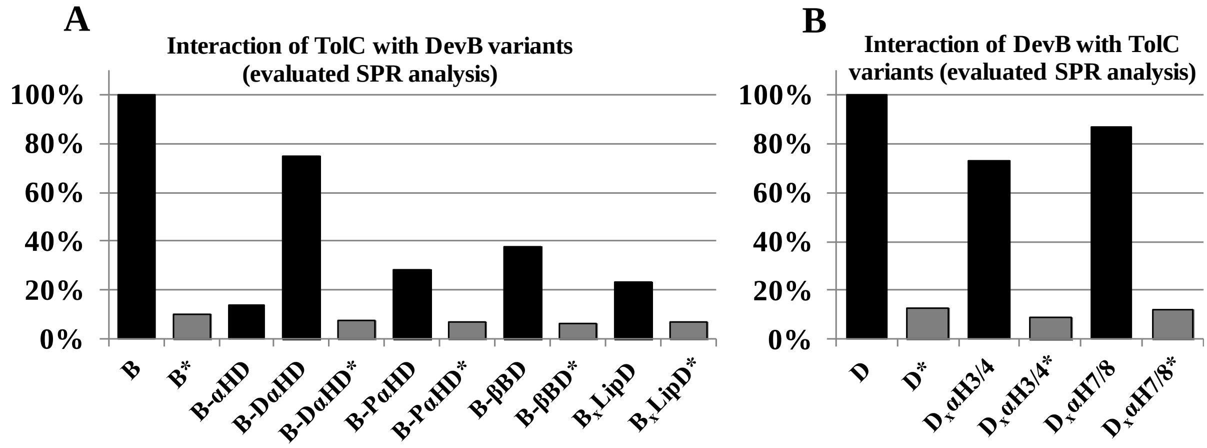
A
Interaction of TolC with DevB variants (evaluated SPR analysis)
100%
80%
60%
40%
20%
0%
B
B*
B-αHD
B-DαHD
B-DαHD*
B-PαHD
B-PαHD*
B-βBD
B-βBD*
BxLipD
BxLipD*
B
Interaction of DevB with TolC variants (evaluated SPR analysis)
100%
80%
60%
40%
20%
0%
D
D*
DxαH3/4
DxαH3/4*
DxαH7/8
DxαH7/8*

Figure 4

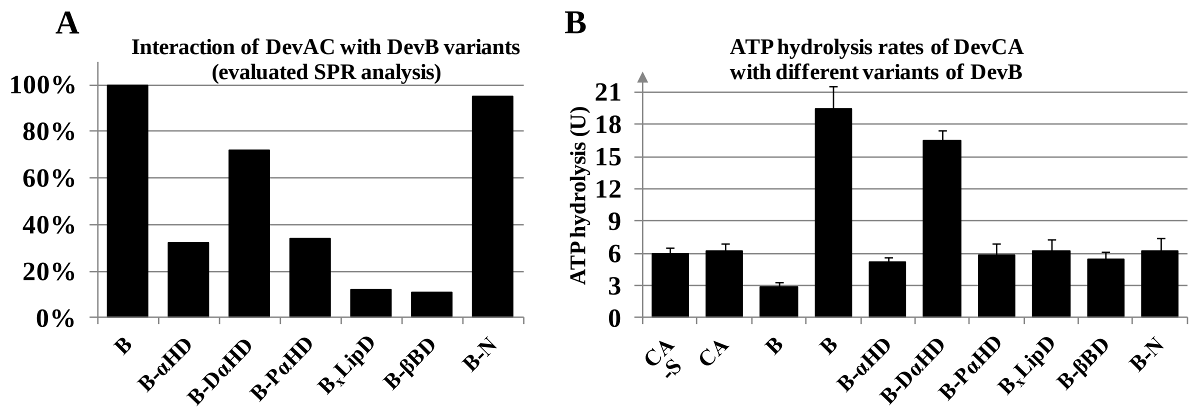

A
Interaction of DevAC with DevB variants (evaluated SPR analysis)
100%
80%
60%
40%
20%
0%
B
B-αHD
B-DαHD
B-PαHD
BxLipD
B-βBD
B-N
B
ATP hydrolysis rates of DevCA with different variants of DevB
ATP hydrolysis (U)
21
18
15
12
9
6
3
0
CA -S
CA
B
B
B-αHD
B-DαHD
B-PαHD
BxLipD
B-βBD
B-N

SUPPLEMENTARY DATA*

Tab. S1 (Plasmids constructed in this study) and Tab. S2 (Oligonucleotides used in this study) were integrated into Tab. 3 (Generated constructs, Appendix 11.3, page 126) and Tab. 4 (Used oligonucleotides, Appendix 11.4, pages 127 and 128) that comprise the data of the whole work.

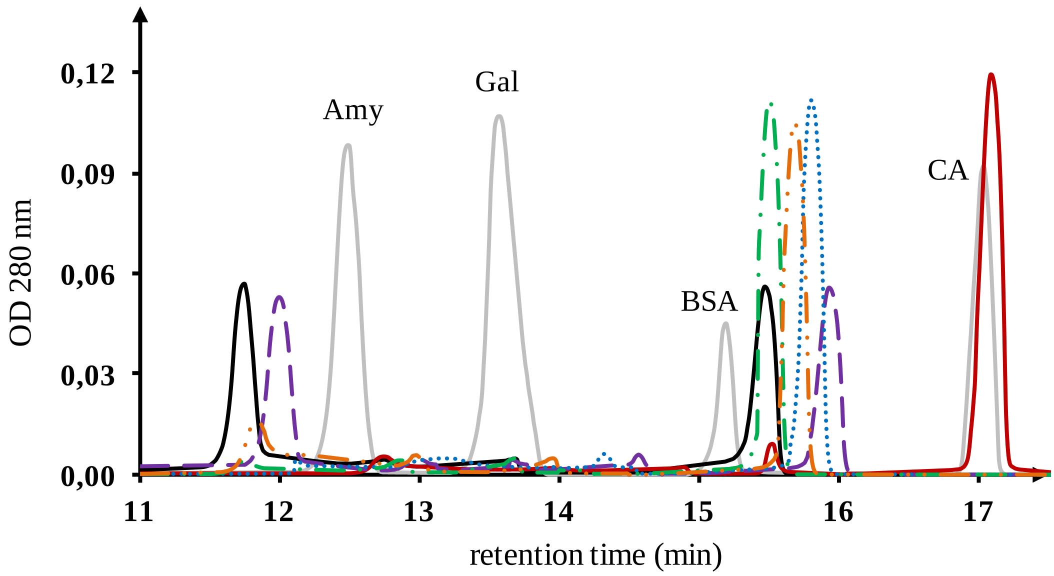

Figure S1: Influence of DevB domains on hexamerization (raw SEC data)
SEC profile of different DevB variants. Solid black line = Full-length DevB; solid red line = B-αHD; dashed purple line = B-DαHD; dotted blue line = B-PαHD; dot-dashed green line = B_xLipD; dot-dot-dashed orange line = B-βBD; solid grey line = standard. Amy = β-amylase (200 kDa), Gal = β-galactosidase (116 kDa), BSA = bovine serum albumin (66 kDa), CA = carbonic anhydrase (29 kDa).

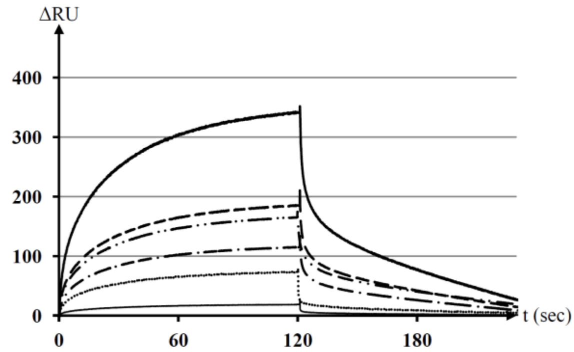

Figure S2: Influence of DevB domains on hexamerization (raw SPR data)
SPR analysis of the interaction of immobilized full-lenght DevB with different variants of DevB. Latter were injected at 3.2 μM. Solid line = full-lenght DevB; thin solid line = B-αHD; dashed line = B-DαHD; dotted line = B-PαHD; dot-dashed line = B_xLipD; dot-dot-dashed line = B-βBD. For full-length DevB, B-αHD, B-PαHD and B-βBD ~80RU of full-length DevB were immobilized on the chip surface, for B-DαHD and B_xLipD the surface was coated with ~65 RU.

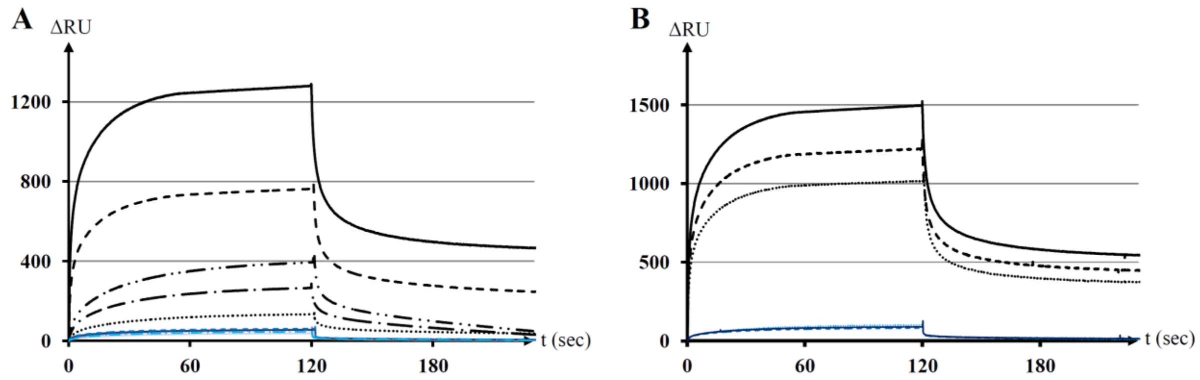

Figure S3: Stable DevB hexamers interact tip-to-tip with TolC (raw SPR data)
(A) SPR analysis of the interaction of immobilized reference TolC (~550 RU) with different variants of DevB. Variants were injected at 3.2 μM. Black lines = native α-helical tip; blue lines = modified α-helical tip. Solid line = reference DevB; thin solid line = B-αHD; dashed line = B-DαHD; dotted line = B-PαHD; dot-dashed line = B_xLipD; dot-dot-dashed line = B-βBD. **(B)** SPR analysis of the interaction of immobilized reference DevB (~910 RU) towards different constructs of TolC. The constructs were injected at 3.2 μM. Black lines = native α-helical hairpins; blue lines = modified α-helical hairpins. Solid line = reference TolC; dotted line = DxαHD3/4; dashed line = DxαHD7/8.

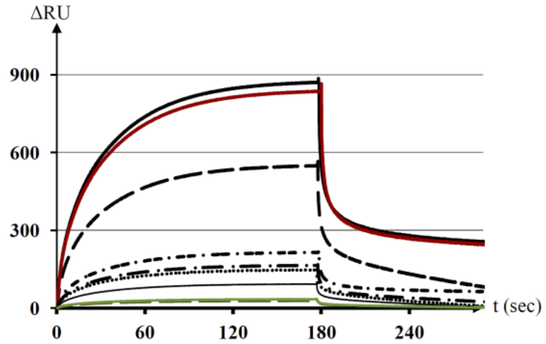

Figure S4: Stable DevB hexamers promote substrate recognition of DevAC

SPR analysis of the interaction of immobilized DevAC (~440 RU) with different variants of DevB. Variants were injected at 3.2 μM. Solid line = reference DevB; thin solid line = B-αHD; dashed line = B-DαHD; dotted line = B-PαHD; dot-dashed line = B_xLipD; dot-dot-dashed line = B-βBD; red line = B-N; green line = reference TolC; dashed green line = D*.

```
                                                   ... proximal <-> distal ...
DevB        DNHDTQLAAVEEAKAKLLESRANLAQVRVG-S-PRDIQAQTAVIARLQAQLVGEMGAQQA
All0809     DSRDRLKAALKEAQEQVKVAQANLNRTQAG-AKGGEIAAQMATIAKLEA-----------
All2652     QGIDQLEADLRDAEANVRLHEAELLKVEQGEAKQGEMAAQRATIARLEA-----------
Alr3647     DSRARLQTAVLQAEKQIRVAQAKLNQVKAG-AKTGDIRAQQASVERLQAQSQGDRTGQQQ
Alr4280     DNRDRLEAAYQEAQEAVKVAQVNLEKVREG-AKVGEINAQKAEIARVQAQTTGDGREQQE
Alr4973     DNRDTRLAALNRAKQQVAVAQSQLAQVKAG-AKQGEIAAQQATIAELAA-----------
All5347     EDYSRATAALEQALDKLQIAKIKLAQVKAG-AKPGDIDAQKATVARLES-----------
MacA_Ec     DPEQAEN----------------------------QIKEVEATLMELRA-----------
            :                                   :    * :    :

                                                      ... distal <-
DevB        SITRIASQLSGEKVAQQALVNRLEAELVGQQDSLRATLNRIRAEQRNAQVDAGRYDFLYR
All0809     -------EGRGNIAA------------------QLATVARLQAEVRNATAENQRYQTLYQ
All2652     -------QLKAETTQ------------------KQAAINSAEATLQEAQLTYQRRQDLST
Alr3647     TIARIEAQWQGDRIA------------------QEATIRKLEAELKNAEAEYQRYQQLYS
Alr4280     TVARLEAQWQGEKSA------------------QQATVKRLEAELKNAQSEWERYQKLYA
Alr4973     -------ELRQEVAA------------------RVATVRRLEAEVRNAQIEYQRYQSLQA
All5347     -------QLKGEVAT------------------QQATINRIKAELNNAQTENDRYQKLFK
MacA_Ec     ------------------------------------QRQQAEAELKLARVTYSRQQRLAQ
                                                     .:    *     * : *

            tip region       -> distal ...
DevB        EGAISQQERDRRRLTATTANQQVIESQAALRQALATLRQQVAEARANQMKTLASLQQQLI
All0809     QGAVSASEGDRQRLNLETAQKTLQEAQADLQRIQTTSQQQ--------------------
All2652     EGAISIADADTAKRELATAEATLMERQAELEKTITTLQAQ--------------------
Alr3647     EGAISSSAIDTRRLSVETAKEQLDEAKAVLNRINSTASKELAEA----------------
Alr4280     DGAISQSSYDTKRLSLDTITQQLSEAQANLQRIDSTGRKQISEA----------------
Alr4973     DGAVSVSIRDSKKLTLETAEESLREALANRSQTSETLQER--------------------
All5347     EGAVSASVFDSKALQLKTVEQQLTEAKASLSRSQNTLADQ--------------------
MacA_Ec     TQAVSQQDLDNAATEMAVKQAQIGTID---------------------------------
              * *    :            :

                ... distal <-> proximal ...
DevB        EARVTRDKTITTLQRQIDEEKARLKRLVEVSPTDVQMAQAQVSNAIANVRRAEAELKLSY
All0809     ----------------LQQAKATLAQITEVRGVDVEAAKAEVNRAIAAMNQAKVHLQQAY
All2652     ----------------ITQEEATLAQLKEIRPVDVRISKVHLEKAKIAVIQRKAQLENAK
Alr3647     --KVALNRINATSNKQISEAKATLTSIAEVRPVDVQAAQTEVEEAIASLKRATTDLEAAY
Alr4280     --KTALYRINATGSKQVSAAAATLNKIAEVRPIDVQAAKVEVNRAVAAAKQAKANLDQVY
Alr4973     ----------------LRQAKATLNQIAEVRPTDVQAAQAEVESAKAAVQEAQANLNLTY
All5347     ----------------IKEAKATLSSVKEVRAVDVDLAQMEVRSAVTAVKQAKADQELTY
MacA_Ec     ---------------------------------------AQIKRNQASLDTAKTNLDYTR
                                                    ::            ..
```

Figure S5: Sequence alignment of the α-helical domains of DevB, close homologues of DevB, and MacA
The sequence alignment was done with ClustalOmega (http://www.ebi.ac.uk/Tools/msa/clustalo/). Prediction of DevB`s sec. structure (thicker tubes = α-helix) was performed by using MINNOU (http://minnou.cchmc.org/). Highlighted = N^{333} (21).

6 Additional experiments (II)

6.1 DevB`s involvement in substrate recognition

6.1.1 Background and experimental design

The hexameric crystal structure of MacA implies a barrier for the substrates between the lipoyl domain (mouth) and the α-helical domain (stem). This barrier is composed of a loop from each of the 6 lipoyl domains (Fig. 24). Assuming this barrier is formed *in vivo*, it could be related to substrate recognition of MacAB, at least as an additional mechanism of substrate discrimination.

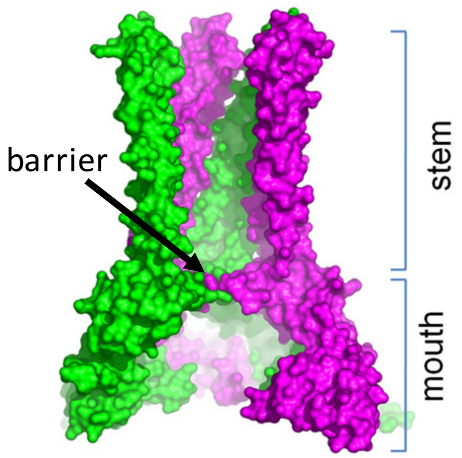

Figure 24. Cross-section of a hexameric MacA crystal

This figure was taken from Yum *et al.* (2009) and modified.

DevB containing a largely replaced lipoyl domain was not able to promote a substrate-dependent reaction of DevAC (5. manuscript I). In this variant, the ascending part of DevB`s lipoyl domain was replaced, while the mentioned barrier loop is encoded by the descending lipoyl domain (in the case of MacA). In the following chapter, the possible funnel-closing loops of DevB were more extensively investigated. DevB`s loop region was determined by aligning DevB to MacA and to close homologues of DevB predicted from the genome of *Anabaena* (8.1.3), and the respective region was modified. This DevB variant was investigated on the binding affinity to DevAC and on the promotion of an ATP-hydrolyzing reaction toward the presence of HGLs.

6.1.2 Materials and Methods

Protein sequences, prediction of secondary structure, and sequence alignment

All protein sequences were obtained from the NCBI protein database. The accession numbers were NP_487750.1 for DevB and BAB72766.1/BAB74351.1/BAB75346.1/BAB75979.1/BAB77046.1 for the DevB-homologues All0809/All2652/Alr3647/Alr4280/All5347 (8.1.3). For MacA from *E. coli* the accession number was 3FPP_A. The secondary structure was predicted by using MINNOU (2.2), and the respective sequences were aligned by using ClustalOmega (2.2).

Protein design and overexpression

The supposed loop sequence of DevB was replaced with 4GS or the respective sequence from All0809 (pIM533/534; Tab. 3 in appendix 11.3, page 126). The primers for construction are listed in Tab. 4 (appendix 11.4, page 127). DevB, GS-loop DevB (B_{4GS}Loop), All0809-loop DevB (BG_{0809}Loop), and DevCA were overexpressed as N-terminal GST tag fusions and purified as described (3. Publication; e.g. Fig. 48, appendix 11.6, page 129).

HGL purification and ATPase assay

HGLs were purified via a continuous sucrose gradient as described above (4.2.2). ATPase activity was measured as described (3. Publication, 4.2.2). The rate of ATP hydrolysis in U was calculated as moles of ATP hydrolyzed per min and per mg of DevAC.

6.1.3 Results

DevB and its homologues presumably have a smaller (or no) loop as compared to MacA (Fig. 25). In agreement, a replacement of this region with non-sense GS repeats or the respective region of All0809 did neither influence the binding to DevAC in SPR (Fig. 26A) nor the ATPase activity of DevAC in combination with B_{4GS}Loop or B_{0809}Loop (Fig. 26B).

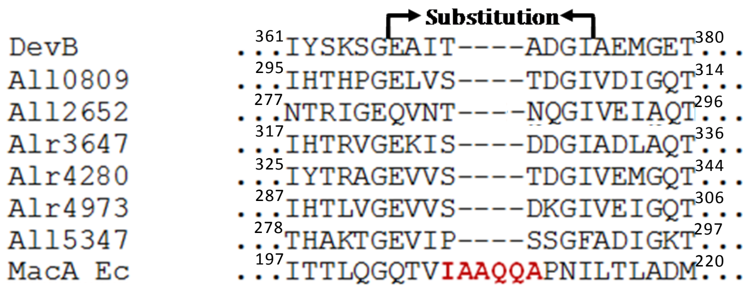

Figure 25. Alignment of the loop region in the lipoyl domain of DevB, its close *Anabaena* homologues, and MacA

The alignment was done with ClustalOmega (2.2.). Red = loop region from MacA as derived from the crystal structure. Numbers indicate the aa position in the respective protein. Compare Fig. 32 and Fig. 36-41 in appendix 11.1, pages 117-120.

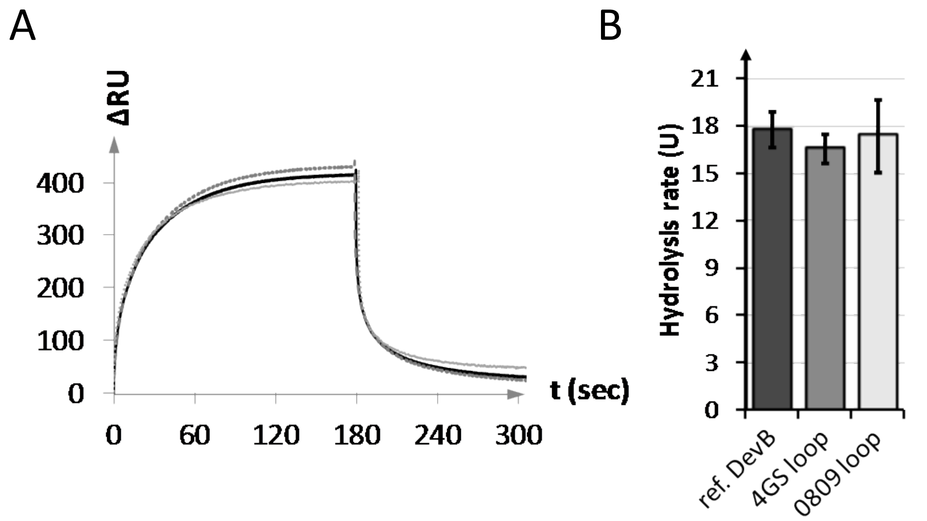

Figure 26. ATPase activity promotion and SPR analysis of DevB loop variants

(A) Response of immobilized DevAC (~180 RU) toward reference DevB (solid line), B_{4GS}Loop (dashed line), and B_{0809}Loop (dotted line; 3,2 μM each). **(B)** ATP hydrolysis rates of DevAC in complex with B_{4GS}Loop and B_{0809}Loop.

6.1.4 Summary

The funnel-closing loops of MacA are not present (or shorter) in DevB-like MFPs from *Anabaena*, and maybe therefore they are not important for the substrate recognition mechanism of DevBCA.

7. Manuscript II: All0809/8/7 is a DevBCA-like ABC-type efflux pump required for diazotrophic growth of *Anabaena* sp. PCC 7120

All0809/8/7 is a DevBCA-like ABC-type efflux pump required for diazotrophic growth in *Anabaena* sp. PCC 7120

Peter Staron and Iris Maldener
From Department of Microbiology/Organismic Interactions, IMIT - Institute of Microbiology and Infection Medicine Tübingen
University of Tübingen, 72076 Tübingen

Running Head: The All0809/8/7-TolC efflux pump of *Anabaena* sp. PCC7120

Address correspondence to: Iris Maldener, Department of Microbiology/Organismic Interactions, Auf der Morgenstelle 28, 72076 Tübingen, Phone: +49 (7071) 29-78847, Fax: +49 (7071) 29-5843, E-mail: iris.maldener@uni-tuebingen.de

SUMMARY

Efflux pumps export a wide variety of proteinaceous and non-proteinaceous substrates across the Gram-negative cell wall. For the filamentous cyanobacterium *Anabaena* sp. PCC 7120, the ATP-driven glycolipid efflux pump DevBCA-TolC was shown to be crucial for the differentiation of N_2-fixing heterocysts from photosynthetic active vegetative cells to. In this study, a homologous system was described. All0809/8/7-TolC form a typical ATP-driven efflux pump as shown by surface plasmon resonance. This putative exporter is also involved in diazotrophic growth of *Anabaena* sp. PCC 7120. A mutant in *all0809* encoding the periplasmic membrane fusion protein of the pump was not able to grow without combined nitrogen. Although heterocysts of this mutant were not distinguishable from those of the wild type in light and electron micrographs, they were impaired in providing the microoxic environment necessary for N_2-fixation. RT-PCR of *all0809* transcripts and localization studies on All0807-GFP revealed that All0809/8/7 was initially downregulated during heterocyst maturation and upregulated at later stages of heterocyst formation in all cells of the filament. A substrate of the efflux pump could not be identified in ATP hydrolysis assays so far. We discuss a role for All0809/8/7-TolC in maintaining the continous periplasm by expulsing used-up substances and how this would be of special importance for heterocyst differentiation.

INTRODUCTION

Anabaena sp. strain PCC 7120 is a filamentous cyanobacterium that differentiates N_2-fixing cells upon nitrogen starvation. These heterocysts provide the photosynthetic filament with fixed nitrogen, and in return they obtain metabolites to fix N_2 (Wolk, 1994). Heterocysts protect the oxygen-labile N_2-fixing nitrogenase system by inactivating and degrading the oxygen-producing photosystem II, by increasing the respiratory O_2 consumption, and by forming two additional envelope layers outside the gram-negative cell wall to avoid O_2-diffusion into the heterocyst (Kumar *et al.*, 2010; Zhao, 2008). The laminated layer consists of heterocyst specific glycolipids (HGL) and envelops the outer membrane; it represents the barrier for O_2-diffusion. The outermost layer of heterocyst envelope polysaccharides (HEPs) protects the laminated layer from mechanical and chemical damage.

The method by which HGLs traverse the Gram-negative cyanobacterial cell wall has been demonstrated recently (Staron *et al.*, 2011). The ATP-binding cassette (ABC)-exporter DevBCA and the outer membrane protein TolC form an ATP-driven *trans*-envelope efflux pump to export HGLs across the Gram-negative cell wall. Like any typical Gram-negative *trans*-envelope pump, *Anabaena*`s HGL-exporter consists of an inner membrane factor (IMF; comprising DevA as nucleotide binding domain and DevC as substrate binding domain), a periplasmic membrane fusion protein (MFP; DevB) and an outer membrane factor (OMF; TolC). Knockout mutations of *devBCA* or *tolC* -or mutations impairing the correct stoichiometric assembly of the efflux pump (2:6:3 of IMF:MFP:OMF)- lead to immature heterocysts lacking the laminated layer (Fiedler *et al.*, 1998a; Fiedler *et al.*, 1998b; Moslavac *et al.*, 2007a; Staron *et al.*, 2011).

To further investigate the role of ATP-driven efflux pumps in *Anabaena* sp. PCC7120, particularly with regard to heterocyst maturation, we started to analyze gene clusters homologous to DevBCA. Mutants in *all5346* (*hgdC*) or *all5347* (*hgdB*) have been shown to be unable to fix N_2 aerobically, and to aberrantly assemble HGL layers (Fan *et al.*, 2005). In this work we have investigated the function of the gene cluster *all0809/8/7*. By *in vitro* protein-protein interaction studies, we could show that All0809/8/7-TolC form a typical ATP-driven efflux pump. A knock-out mutant of *all0809* encoding the central periplasmic MFP was not able to grow diazotrophically under aerobic conditions. All0809/8/7-TolC were neither restricted to heterocysts in localization studies nor were they directly involved in formation of the additional heterocyst cell wall layers. A disctinct substrate of the IMF All0807/8 could not be identified in ATP hydrolysis assays. Therefore, this efflux pump could play a general but important maintaining role in the periplasm of mature heterocysts.

METHODS

Anabaena strains and growth conditions

All *Anabaena* strains used in this study are listed in Tab. 1, the respective plasmids are listed in Tab. 2. Wild-type *Anabaena* sp. PCC 7120 grew photoautotrophically at 28°C in liquid $BG11_0$ medium (Rippka, 1979). Mutants unable to fix N_2 grew in $BG11_0$ medium supplemented with 5 mM NH_4Cl and 5 mM TES-NaOH buffer, pH 7.8. Respective mutant strains were cultivated in the presence of appropriate antibiotics listed in Tab. 1 (for applied concentrations see (Fiedler *et al.*, 1998a; Fiedler *et al.*, 1998b; Maldener *et al.*, 2003; Moslavac *et al.*, 2007a)). Media were solidified with 1.5% agar (Difco, Heidelberg, Germany). Induction of heterocyst formation and isolation was performed as described earlier (Moslavac *et al.*, 2007a).

Generation of mutant *Anabaena* strains

Anabaena mutants were generated by triparental mating and double recombination by using pRL277 (Black *et al.*, 1993) as described earlier (Elhai & Wolk, 1988; Wolk *et al.*, 1984). Double recombinants were selected by the use of *sacB* as described (Cai & Wolk, 1990). The *C.K3*-cassette

was derived from pRL442 (Elhai & Wolk, 1988), and it was inserted into a central *Eco47*III-site of *all0809* in (mutant M0809F in Tab. 1; plasmid pIM391 in Tab. 2) and against gene orientation (mutant M0809R; plasmid pIM392). The respective oligos (KO) are listed in Table 3.
Mutant M0809R was complemented via single recombination of pRL271 containing *all0809* and $P_{all0809}$ (plasmid pIM450) into the downstream part of the disrupted chromosomal *all0809::C.K3* resulting in mutant C0809 (Table 1). The respective oligos (CP) are listed in Table 3.
Mutants encoding GFP-fusions were generated by single recombination of pRL271 containing translational fusions of either *all0807* (plasmid pIM521) or *devA* (plasmid pIM522) to GFP amplified from pCSEL19 (Muro-Pastor *et al.*, 2006) into the respective wild-type gene. Fusions of GFP to the C-terminus of the respective genes were generated by long flanking homology PCR. The respective oligos (GFP) are listed in Table 3.

Microscopic visualization

Light micrographs were captured by a DM 5500B microscope (Leica) using a DFC420C camera (Leica). Reduction of INT (2-(4-Iodophenyl)-3-(4-nitrophenyl)-5-phenyl-2*H*-tretrazolium-chloride) to Formazan crystals (1-(4-Iodphenyl)-3-(phenyl)-5-(4-nitrophenyl)-formazan) was performed by incubating culture aliquots with 2 mM INT for 10 min prior to microscopy (Fay & Kulasooriya, 1972). GFP was excited at 480 nm, and fluorescence was captured at 525 nm.
Samples for transmission electron microscopy were prepared as described previously (Fiedler *et al.*, 1998b). Fixation and post-fixation were performed using glutaraldehyde and potassium permanganate. Ultrathin sections were stained with uranyl acetate and lead citrate. Micrographs of the samples were taken with a Tecnai electron microscope (Philips) at 80 kV.

Expression analysis

Total RNA was extracted from 50 ml samples of *Anabaena* cultures before and at 3, 6, 9, 12, and 24 h after combined nitrogen step-down and RT-PCR was performed as described (Staron *et al.*, 2011). The respective oligos (RT) are listed in Table 3.

Construction, overexpression, and purification of recombinant proteins

Recombinant proteins were overexpressed and purified as described (Staron *et al.*, 2011). In brief, proteins were overexpressed as glutathione-S-transferase tag fusions in *E. coli* strain Rosetta-Gami™ DE3 using the vector pET42a (Merck). GST fusions were purified, and the N-terminal GST was cleaved off the respective protein. The respective oligos (OEX) are listed in Table 3. Internal modifications of the protein variants or protein-protein fusions (like of All0807 with All0808, or of DevA with DevC) were generated by long flanking homology PCR. The respective oligos are listed in Table S1.

Surface plasmon resonance

Surface plasmon resonance (SPR) experiments were performed using a Biacore X biosensor system (Biacore AB, Uppsala, Sweden), as described earlier (Fokina *et al.*, 2010; Staron *et al.*, 2011).

Binding assays were done in reaction buffer (25 mM MES-NaOH at indicated pH from 6.0-6.6 or HEPES-NaOH at pH 7.0; 150 mM NaCl; and 0.05% Triton X-100) at 25°C. Samples were injected into both flow cells (FC1 and FC2) of the sensor chip at a flow rate of 20 µl/min, and the response difference (FC2−FC1) was recorded. FC1 was chosen as reference cell free of immobilized protein. The reaction was evaluated from received data using BiaEvaluation (Biacore AB) and Excel 2010 (Microsoft).

Cell fractionation and glycolipid purification

Cell fractions (Moslavac *et al.*, 2007a) and heterocyst glycolipids (Winkenbach, 1972) were prepared as described. In brief, enriched heterocysts were broken by at least five passes through a French Pressure cell (24,000 psi) and separated into a soluble cytoplasmic and an insoluble membrane fraction by centrifugation (45,000 × g, 30 min, 4°C). To obtain cytoplasmic membrane, thylakoid membrane and outer membrane according the pellet was separated by a discontinuous sucrose gradient (Moslavac *et al.*, 2007a). To obtain heterocyst glycolipids the pellet was separated by continous sucrose gradient (Winkenbach, 1972).

ATP hydrolysis assay

The assays were performed as described earlier (Staron *et al.*, 2011). In brief, 0.1 µg/ml DevAC or All0807/8, and 0.2 µg/ml DevB or All0809, and 2 µg of the respective cell fractions or 8 µg of heterocyst glycolipids at indicated concentrations were mixed in ATPase reaction buffer supplemented with an ATP regeneration system, and an reaction detection system. The rate of hydrolysis in units (U) was calculated as moles of ATP hydrolyzed per minute and per milligram of the ATPase DevAC or the ATPase All0808/7.

RESULTS

The MFP encoding gene *all0809* is essential for diazotrophic growth of *Anabaena* sp. PCC7120

At least six gene clusters closely homologuos to *devBCA* (also referred to as *alr3710-3712*) can be predicted from the genome sequence of *Anabaena* sp. PCC7120: (i) *all0809-0807*, (ii) *all2652-2651*, (iii) *alr3647-3649*, (iv) *alr4280-4282*, (v) *alr4973-alr4975* and (vi) *all5347-5346* (Fig. S1). Clusters ii and vi do not encode a DevA-like protein. All clusters are predicted to encode MFPs, so their gene products presumably form an ATP-driven efflux pump together with the only one OMF encoded in the genome of *Anabaena* sp. PCC7120: TolC (also referred to as Alr2887 or HgdD (Moslavac *et al.*, 2007a). Like *devBCA*, *all0809/8/7* are predicted to encode subunits of an ABC exporter. In the same order as *devBCA*, *all0809* encodes an DevB-like MFP, *all0808* the substrate binding domain of an DevAC-like IMF, and *all0807* the nucleotide binding domain of the same IMF (Fig. 1a).
To elucidate the function of *all0809/8/7* in *Anabaena* sp. PCC7120, we mutated the MFP-encoding gene *all0809*, and therefore we prevented a possible assembly of a hypothetic All0809/8/7-TolC efflux pump. The knock-out mutants of *all0809* (M0809F and M0809R, F and R refers to the orientation of the *C.K3*-cassette with respect to the gene, Tab. 1) did not obviously have a visible

phenotype, when grown on NH_4^+ (Fig. 1b, +N). In contrast, the mutants were not able to grow without combined nitrogen (Fig. 1b, -N). Although the filaments of both M0809F and M00809R bleached and fragmented after several days of combined nitrogen-starvation, heterocysts and vegetative cells were indistinguishable from the wild type with respect to their ultrastructure (Fig. 1 d, e). Mutant heterocysts contained a laminated HGL-layer (Fig. 1d; HGL) synthesis was not impaired (data not shown)) and an ordinary appearing HEP-layer (Fig. 1d; HEP). The poles were reduced to the polar neck containing the cyanophycin granulum (Fig. 1d) and the thylakoid membranes rearranged as in wild type heterocysts (Fig. 1d; see e.g. (Merino-Puerto *et al.*, 2011)).

When compared to the wild-type, heterocysts of M0809 reduced INT to insoluble formazan crystals less frequently (Fig. 1e). This indicates a partial inability to provide a microoxic environment inside the mutant heterocysts. Furthermore, M0809 was able to survive combined nitrogen deprivation ~three times as long, when it was kept under microoxic conditions (data not shown). The mutant phenotype could be rescued by complementation with a wild-type copy of *all0809* (C0809 in Tab. 1). C0809 is able to grow in absence of combined nitrogen (Fig. 1c).

The MFP-encoding gene *all0809* is essential for diazotrophic growth of *Anabaena* sp. PCC7120. M0809 is not able to survive the absence of combined nitrogen under aerobic conditions, and this phenotype can be rescued by a copy of *all0809*. Although light or electron micrographs do not reveal abnormalities in cell morphology, heterocysts of M0809 are impaired in providing microxic conditions necessary to fix N_2.

The expression pattern of *all0809-7* is different to *devBCA*

Since the ABC-type exporter formed by All0809/8/7 is necessary for the function of heterocysts, we analyzed the expression pattern of *all0809* under different nitrogen supply, as representative of the entire cluster. The homologous heterocyst glycolipid ABC-exporter DevBCA was shown to be upregulated during nitrogen stepdown in single cells, presumably maturing heterocyst, showing maximum abundance at 9-12h (Fiedler *et al.*, 2001; Maldener *et al.*, 1994; Staron *et al.*, 2011).

Transcripts of *all0809* could be detected in comparable amounts in filaments grown on NH_4^+ and after 24h of nitrogen-step down (Fig. 2a). However during the first 9h of N deprivation the expression level dropped clearly with a minimum at 6h.

Furthermore, we could localize the nucleotide binding protein All0807 by fusion to GFP in filaments of *Anabaena* sp. PCC7120. Since the nucleotide binding protein is predicted to be localized at the inner site of the cytoplasmic membrane, the GFP fusion to this part of the efflux pump was reasonable. GFP cannot fold to an active fluorescent protein outside the cell and a C-terminal fusion at All0807 does not seem to lead to a loss of function as shown for the homologue DevA previously (Staron *et al.*, 2011).

Before depletion of combined nitrogen, All0807-GFP was localized in all cells of the filament (Fig. 2b, All0807-eGFP 0h). In agreement with the expression data of *all0809*, the amount of All0807-GFP decreased after 12h of combined nitrogen-stepdown, and was hardly detectable in both vegetative cells and heterocysts (Fig. 2b, All0807-GFP 12h). After 24h. when heterocysts usually have completed maturation, All0807-GFP had returned to the initial level of expression in all cell types (Fig. 2b All0807-GFP 24h). DevA-GFP was not detectable before nitrogen stepdown (Fig. 2B, DevA-eGFP 0h). In agreement to *devBCA* expression analysis, DevA-GFP showed maximal abundance after 12h of nitrogen-stepdown, and it was localized to heterocysts only (Fig. 2B, DevA-eGFP 12h).

From this data we could conclude that the DevBCA homologue All0809/8/7 is not restricted to heterocysts. The expression pattern of *all0809/8/7* is contradictionary to that of *devBCA* and is not localized to heterocysts specifically.

All0809/8/7 and TolC form a typical ATP-driven efflux pump

DevBCA and TolC were shown to form an ATP-driven efflux pump to export glycolipids across the Gram-negative cell wall. In prescence of the substrate, the MFP DevB promoted an increase in ATP hydrolysis of the IMF DevAC (Staron *et al.*, 2011). The products of *all0809/8/7* are also predicted to encode a DevBCA-like ABC-exporter, and due to the presence of the MFP All0809, they are also assumed to form an efflux pump with TolC.

In contrast to mutants in DevB (and DevC, DevA, and TolC (Fiedler *et al.*, 1998a; Fiedler *et al.*, 1998b; Moslavac *et al.*, 2007a)), the observed phenotype of M0809 did not provide evidence on the function of the hypothetic efflux pump All0809/8/7-TolC. Before testing All0809/8/7 for possible substrates, the formation of an All0809/8/7-TolC efflux pump had to be demonstrated. For this purpose, the interaction of the MFP All0809 with the OMF TolC, and the interaction of All0809 with the IMF All0807/8 fusion protein, was measured via SPR in analogy to DevB, TolC, and DevAC (Staron *et al.*, 2011).

In contrast to DevB (pH 6.2), the highest response of the surface-bound OMF TolC towards the free MFP All0809 was observed at a pH of 6.5. As already shown for the interaction of DevB with TolC and for MFPs in *E. coli* (Tikhonova *et al.*, 2009), higher pH values remarkably impaired the binding of All0809 to TolC (Fig. 3a). Saturation response at pH 6.5 predicted an All0809-to-TolC-ratio of 1.8:1 (Fig. 3b). The ratio of DevB to TolC was calculated to be 2:1 (Staron *et al.* 2011). Saturation response predicted an All0809-to-All0808/7-ratio of 2.7:1 (Fig. 3b). The ratio of DevB to DevAC was calculated to be 3:1 (Staron *et al.* 2011).

Taken together, All0809/8/7 and TolC form a typical ATP-driven efflux pump. The overall molar ratio appears to be 3:6:2 (OMF TolC to MFP All0809 to IMF All0808/7), and it therefore is the same as the ratio for DevBCA-TolC (Staron *et al.*, 2011).

All0809/8/7 do not react towards heterocyst glycolipids

The efflux pump DevBCA-TolC was shown to be responsive towards the presence of heterocyst glycolipids via changes in the ATP hydrolysis rate of the nucleotide binding protein DevA (Staron *et al.*, 2011). The phenotype of M0809 did not provide precise informations about the function and the putative substrates of All0809/8/7-TolC. To identify possible substrates, All0809/8/7 were exposed to different cell fractions, and the ATPase activity of All0807 was recorded.

In contrast to DevBCA, All0809/8/7 did not react to any fraction via changes in ATPase activity (Fig. 4). No remarkable differences could be recorded when All0809/8/7 were assayed for basal activity or in presence of soluble or any membrane fractions from NH_4^+-grown filaments (Fig. 4, V-fractions) or 12h N-starved filament (Fig. 4, H-fractions). All0809/8/7 did also not respond towards the presence of HGLs, even when All0809 was replaced with DevB, or when All0808/7 was replaced with DevAC. The subunits are not interchangeable.

Assaying All0809/8/7 for a substrate did not provide any information about the function of All0809/8/7-TolC, and therefore no further indications on the reason for the loss of diazotrophy of *Anabaena* sp. PCC7120.

DISCUSSION

All0809/8/7-TolC form a typical ATP-driven efflux pump

DevBCA was the first ABC exporter described for cyanobacteria. It was shown to form an ATP-driven efflux pump with TolC and to export glycolipids necessary for the formation of an additional layer of the heterocyst cell wall (Staron *et al.*, 2011). In this work, we investigated All0809/8/7, another ABC exporter from *Anabaena* sp. PCC7120 necessary for heterocyst function.

As shown for DevBCA-TolC, All0809/8/7 and TolC also assemble a typical ATP-driven efflux pump. Since the molar ratio of the OMF TolC to the MFP All0809 to the IMF All0808/7 was determined to be 3:6:2, it exactly resembles the molar ratio of TolC:DevB:DevAC, or the (theoretically combined) molar ratio of TolC:MacA:MacB (Staron *et al.*, 2011; Yum *et al.*, 2009; Zgurskaya *et al.*, 2011). So, similar to other described ATP-driven efflux pumps, a central MFP All0809 hexamer seems to play a key role in the physiological function of All0809/8/7-TolC. Consequently, a tip-to-tip cogwheel-like interaction of the MFP with the OMF in ATP-driven efflux pumps also seems to be true for All0809 and TolC.

In contrast to DevB interaction with TolC, All0809 interaction with TolC has a higher pH optimum. Since TolC (Alr2887) is the only TolC-like outer membrane protein predicted from the genome of *Anabaena*, several TolC-depending exporters have to compete with each other for the binding of the respective MFP to the OMF. Different pH optima for the affinity of the MFP to TolC could determine the selection of the MFP needed for a specific purpose. This would add a physiological manner of regulation by differential expression. DevB, formed in the middle of the maturation process, could more easily banish competing MFPs present in undifferentiated filaments (e.g. All0809). The expression pattern of *all0809* (Fig. 2a) and the localization of All0807-GFP (Fig. 2b) would confirm this assumption. This concept could also be true for further heterocyst-related functions: among adjustments of the efflux pump portfolio, heterocyst maturation involves a plenty adjustments in the membrane/periplasmic proteome (Moslavac *et al.*, 2007b; Nicolaisen *et al.*, 2009a) or remarkable modifications of the cell wall (e.g. the murein layer (Lazaro *et al.*, 2001; Lehner *et al.*, 2011; Zhu *et al.*, 2001)). It remains to be shown in future wether developing heterocysts locally and temporally change their periplasmic pH values (or the pH value of the continuous periplasm of the whole filament) to discriminate between heterocyst-specific and heterocyst-unspecific functions.

Homologues of DevBCA are crucial for aerobic diazotrophic growth of *Anabaena* sp. PCC7120

Due to missing or aberrant laminated layer, mutants in *devB* (Fiedler *et al.*, 1998a) or *all5347*/*hgdb* (Fan *et al.*, 2005) are not able to fix N_2 aerobically. Heterocyst of M0809 show a wild type-like laminated HGL-layer (Fig. 1d). In addition, All0809/8/7 did not react in ATP hydrolysis rate towards the presence of HGLs (Fig. 4). So, specific contribution of All0809/8/7-TolC into export and/or formation of the laminated layer appears to be unlikely.

Nevertheless, an impairment in providing a microoxic environment for N_2-fixation can be deduced. When compared to the wild-type, heterocysts of M0809 reduced INT to insoluble formazan crystals less frequently (Fig. 1E). Consequently, the wild type-like appearing laminated layer M0809 seems to be partially functional only, or the mutant is impaired in other mechanisms providing a microoxic environment as exemplified in the following chapter. A functional relation to the nearby *hglK* gene (*all0813* (Black *et al.*, 1993)) seems unlikely, since a *hglK* mutant is not able to deposit a laminated layer.

Like mutants in *devB* or *hgdB*, M0809 does not appear to be impaired in synthesis, export or assembly of the outermost polysaccharide layer. Heterocysts of all mentioned mutants show a wild-type like HEP-layer (Fig. 1d, (Fan *et al.*, 2005; Fiedler *et al.*, 1998b; Moslavac *et al.*, 2007a)).

All0809/8/7-TolC may play a role in maintaining the heterocyst periplasm

The efflux pump All0809/8/7-TolC either seems to indirectly affect heterocyst maturation, or to adopt a heterocyst-specific function. An indirect effect on heterocyst formation could be explained in the same manner as the proposed function of an H^+-driven efflux pump in *E. coli*: during cell division, AcrEF-TolC were supposed to act as a cleaner for the periplasm from proteins and products of murein and membrane recycling. Overproduction of a periplasmic protein in an *acrEF* mutant resulted in filamentous *E. coli* (Lau & Zgurskaya, 2005). Analogously, All0809/8/7-TolC could also play a role in maintaining the periplasm of *Anabaena* sp. PCC7120. A lack of this function could produce unforeseen -and maybe unseen- artefacts in the cell wall of developing heterocysts, and therefore somehow allow the entrance of O_2 into the heterocyst or prohibit (impede) supply of reductants to the mature heterocyst by periplasmic diffusion (Flores *et al.*, 2006; Flores & Herrero, 2010; Mariscal & Flores, 2010; Nicolaisen *et al.*, 2009b).

On the other hand a heterocyst specific role of All0809/8/7-TolC could also be explained by this means: as already mentioned above, heterocyst maturation involves a plenty of modifications of the cell wall or adjustments in the membrane/periplasmic proteome. If All0809/8/7-TolC would function as a specific cleaner of the periplasm of developing heterocysts, its absence would impair the formation of a fully functional heterocyst cell wall. Then, proteins or other compounds could not be removed from the periplasm and would accumulate to concentrations maybe inhibiting crucial heterocyst cell wall functions. Regarding a hypothetic cleaning of the periplasm from DevB not needed anymore, the opposed expression pattern of *all0809*(*/8/7*) would answer expectations: the amount of All0809/8/7-TolC decreases, when the amount of DevBCA-TolC increases, and *vice versa*. Since DevBCA are massively induced in developing heterocysts, and DevB may have structural advantages to occupy the binding sites of TolC (e.g. a longer α-helical domain or a shifted pH optimum in binding to TolC), it would be necessary to remove DevBCA after they have fulfilled their stage-specific function in exporting HGLs. All0809/8/7-TolC could address this task, and therefore it could allow other exporters to occupy TolC. These possible explanations could also account for the absence of All0809/8/7-ATP activity towards the exposed cell fractions. Since the ABC-exporter was not exposed towards enriched periplasm, potential substrates could have been too strongly diluted (in the soluble fraction used) to promote a detactable increase in ATPase activity. On the other hand, it is not clear, if the efflux pump would be able to recognize all periplasmic proteins/substrates, a disctinct part of them, or even only specifically modified ones.

All0809/8/7-TolC is the second characterized ABC-type efflux pump of cyanobacteria and, as its homologues DevBCA and HgdBC, essential for diazotrophic growth of *Anabaena*. Future studies on the other homologues will underline the importance of this broadly distributed class of exporter systems in cyanobacteria and in Gram-negative bacteria in general.

ACKNOWLEDGEMENT

We thank Karl Forchhammer for access to BIACORE-facility, Claudia Menzel for preparing the electron microscopy samples, and Josef Lehner for help at the fluorescence microscope. We thank Regine Rahmer, Steffen Sigle, and Sabrina Rohrer for practical helps. We thank Prof. C. Peter Wolk for pRL plasmids and Dr. A. Muro-Pastor for pCSEL19. This work was supported by Deutsche Forschungsgemeinschaft (DFG-Ma1359/5-1).

REFERENCES

Black, T. A., Cai, Y. & Wolk, C. P. (1993). Spatial expression and autoregulation of hetR, a gene involved in the control of heterocyst development in *Anabaena*. *Mol Microbiol* **9**, 77-84.

Cai, Y. & Wolk, C. P. (1990). Use of a conditionally lethal gene in *Anabaena* sp. strain PCC 7120 to select for double recombinants and to entrap insertion sequences. *J Bacteriol* **172**, 3138-3145.

Elhai, J. & Wolk, C. P. (1988). A versatile class of positive-selection vectors based on the nonviability of palindrome-containing plasmids that allows cloning into long polylinkers. *Gene* **68**, 119-138.

Fan, Q., Huang, G., Lechno-Yossef, S., Wolk, C. P., Kaneko, T. & Tabata, S. (2005). Clustered genes required for synthesis and deposition of envelope glycolipids in *Anabaena* sp. strain PCC 7120. *Mol Microbiol* **58**, 227-243.

Fay, P. & Kulasooriya, S. A. (1972). Tetrazolium reduction and nitrogenase activity in heterocystous blue-green algae. *Arch Mikrobiol* **87**, 341-352.

Fiedler, G., Arnold, M., Hannus, S. & Maldener, I. (1998a). The DevBCA exporter is essential for envelope formation in heterocysts of the cyanobacterium *Anabaena* sp. strain PCC 7120. *Mol Microbiol* **27**, 1193-1202.

Fiedler, G., Arnold, M. & Maldener, I. (1998b). Sequence and mutational analysis of the devBCA gene cluster encoding a putative ABC transporter in the cyanobacterium *Anabaena variabilis* ATCC 29413. *Biochim Biophys Acta* **1375**, 140-143.

Fiedler, G., Muro-Pastor, A. M., Flores, E. & Maldener, I. (2001). NtcA-dependent expression of the *devBCA* operon, encoding a heterocyst-specific ATP-binding cassette transporter in *Anabaena* spp. *J Bacteriol* **183**, 3795-3799.

Flores, E., Herrero, A., Wolk, C. P. & Maldener, I. (2006). Is the periplasm continuous in filamentous multicellular cyanobacteria? *Trends Microbiol* **14**, 439-443.

Flores, E. & Herrero, A. (2010). Compartmentalized function through cell differentiation in filamentous cyanobacteria. *Nat Rev Microbiol* **8**, 39-50.

Fokina, O., Chellamuthu, V. R., Zeth, K. & Forchhammer, K. (2010). A novel signal transduction protein P(II) variant from *Synechococcus elongatus* PCC 7942 indicates a two-step process for NAGK-P(II) complex formation. *J Mol Biol* **399**, 410-421.

Kumar, K., Mella-Herrera, R. A. & Golden, J. W. (2010). Cyanobacterial heterocysts. *Cold Spring Harb Perspect Biol* **2**, a000315.

Lau, S. Y. & Zgurskaya, H. I. (2005). Cell division defects in *Escherichia coli* deficient in the multidrug efflux transporter AcrEF-TolC. *J Bacteriol* **187**, 7815-7825.

Lazaro, S., Fernandez-Pinas, F., Fernandez-Valiente, E., Blanco-Rivero, A. & Leganes, F. (2001). *pbpB*, a gene coding for a putative penicillin-binding protein, is required for aerobic nitrogen fixation in the cyanobacterium *Anabaena* sp. strain PCC7120. *J Bacteriol* **183**, 628-636.

Lehner, J., Zhang, Y., Berendt, S., Rasse, T. M., Forchhammer, K. & Maldener, I. (2011). The morphogene AmiC2 is pivotal for multicellular development in the cyanobacterium *Nostoc punctiforme*. *Mol microbiol* **79**, 1655-1669.

Maldener, I., Fiedler, G., Ernst, A., Fernandez-Pinas, F. & Wolk, C. P. (1994). Characterization of *devA*, a gene required for the maturation of proheterocysts in the cyanobacterium *Anabaena* sp. strain PCC 7120. *J Bacteriol* **176**, 7543-7549.

Maldener, I., Hannus, S. & Kammerer, M. (2003). Description of five mutants of the cyanobacterium *Anabaena* sp strain PCC 7120 affected in heterocyst differentiation and identification of the transposon-tagged genes. *FEMS Microbiol Lett* **224**, 205-213.

Mariscal, V. & Flores, E. (2010). Multicellularity in a heterocyst-forming cyanobacterium: pathways for intercellular communication. *Adv Exp Med Biol* **675**, 123-135.

Merino-Puerto, V., Mariscal, V., Schwarz, H., Maldener, I., Mullineaux, C. W., Herrero, A. & Flores, E. (2011). FraH is required for reorganization of intracellular membranes during heterocyst differentiation in *Anabaena* sp. strain PCC 7120. *J Bacteriol* **193**, 6815-6823.

Moslavac, S., Nicolaisen, K., Mirus, O., Al Dehni, F., Pernil, R., Flores, E., Maldener, I. & Schleiff, E. (2007a). A TolC-like protein is required for heterocyst development in *Anabaena* sp. strain PCC 7120. *J Bacteriol* **189**, 7887-7895.

Moslavac, S., Reisinger, V., Berg, M., Mirus, O., Vosyka, O., Ploscher, M., Flores, E., Eichacker, L. A. & Schleiff, E. (2007b). The proteome of the heterocyst cell wall in *Anabaena* sp. PCC 7120. *Biol Chem* **388**, 823-829.

Muro-Pastor, A. M., Olmedo-Verd, E. & Flores, E. (2006). All4312, an NtcA-regulated two-component response regulator in *Anabaena* sp. strain PCC 7120. *FEMS microbiology letters* **256**, 171-177.

Nicolaisen, K., Hahn, A. & Schleiff, E. (2009a). The cell wall in heterocyst formation by *Anabaena* sp. PCC 7120. *J Basic Microbiol* **49**, 5-24.

Nicolaisen, K., Mariscal, V., Bredemeier, R., Pernil, R., Moslavac, S., López-Igual, R., Maldener, I., Herrero, A., Schleiff, E. & Flores, E. (2009b). The outer membrane of a heterocyst-forming cyanobacterium is a permeability barrier for uptake of metabolites that are exchanged between cells. *Mol Microbiol* **74**, 58-70.

Rippka, R., J. Dereules, J. B. Waterbury, M. Herdman, and R. Y. Stanier (1979). Generic assignments, strain stories and properties of pure cultures of cyanobacteria. *J Gen Appl Microbiol* **111**, 1-61.

Staron, P., Forchhammer, K. & Maldener, I. (2011). Novel ATP-driven pathway of glycolipid export involving TolC protein. *J Biol Chem* **286**, 38202-38210.

Tikhonova, E. B., Dastidar, V., Rybenkov, V. V. & Zgurskaya, H. I. (2009). Kinetic control of TolC recruitment by multidrug efflux complexes. *Proc Natl Acad Sci U S A* **106**, 16416-16421.

Winkenbach, F., Wolk, C. P., Jost M. (1972). Lipids of membranes and of the cell envelope in heterocysts of a blue-green alga. *PLANTA* **107**, 69-80.

Wolk, C. P., Vonshak, A., Kehoe, P. & Elhai, J. (1984). Construction of shuttle vectors capable of conjugative transfer from *Escherichia coli* to nitrogen-fixing filamentous cyanobacteria. *Proc Natl Acad Sci U S A* **81**, 1561-1565.

Wolk, C. P., Ernst, A., and Elhai, J. (1994). Heterocyst metabolism and development *The Molecular Biology of Cyanobacteria, Bryant, DA (ed)*, 769-823, Kluwer Academic, Dudrecht, The Netherlands.

Yum, S., Xu, Y., Piao, S., Sim, SH., Kim, HM., Jo, WS., Kim, KJ., Kweon, HS., Jeong, MH. & other authors (2009). Crystal structure of the periplasmic component of a tripartite macrolide-specific efflux pump. *J Mol Biol* **387**, 1286-1297.

Zgurskaya, H. I., Krishnamoorthy, G., Ntreh, A. & Lu, S. (2011). Mechanism and function of the outer membrane channel TolC in multidrug resistance and physiology of enterobacteria. *Front Microbiol* **2**, 189.

Zhao, J. and Wolk C. P. (2008). Developmental biology of heterocysts, 2006. *Whitworth DE (ed) Myxobacteria: Multicellularity and Differentiation, Washington, DC: ASM Press*, 397-418.

Zhu, J., Jäger, K., Black, T., Zarka, K., Koksharova, O. & Wolk, C. P. (2001). HcwA, an autolysin, is required for heterocyst maturation in *Anabaena* sp. strain PCC 7120. *J Bacteriol* **183**, 6841-6851.

TABLES*

*Tab. 1 (*Anabaena* strains used in this study), Tab. 2 (Constructs used in this study), and Tab. 3 (Oligonucleotides used in this study) of this manuscript were integrated into Tab. 1 (Used *Anabaena* strains, appendix 11.2, page 124), Tab. 3 (Generated constructs, appendix 11.3, page 126), and Tab. 4 (Used oligonucleotides, appendix 11.4, pages 127 and 128) that comprise the data of the whole work.

FIGURE LEGENDS

Fig. 1 Phenotype of mutant M0809

(A) Genetic organization of the *devBCA* operon (also referred to as *alr3710-12*) and the *all0809/8/7* gene cluster. **(B)** Samples of liquid cultures of wild-type *Anabaena* sp. PCC 7120 (WT), the *all0809* knock-out mutant (M0809), and the *devB* knock-out mutant (DR74). Cultures were either grown in presence of 5 mM NH_4Cl (+N), or they were starved for combined nitrogen for one week (-N). **(C)** Cultures of wild-type *Anabaena* sp. PCC7120 (WT), a complementation mutant of M0809 (C0809), and the mutant M0809. Cultures were starved for combined nitrogen for one week. **(D)** Electron micrograph of a terminal heterocyst (H) and a vegetative cell (V) of M0809. HGL = heterocyst glycolipid layer, HEP = heterocyst envelope polysaccharide layer. **(E)** Light micrographs of wild-type *Anabaena* sp. PCC7120 (WT) or the *all0809* knock-out mutant (M0809) starved for combined nitrogen for ~40h, after preincubation with INT. H = heterocysts, stars = crystals inside the heterocysts (reduced INT). The percentage refers to heterocysts containing formazan crystals. Inlays = 3x magnification of a heterocyst.

Fig. 2 Expression of the DevBCA-like efflux pump encoding genes *all0809/8/7*

(A) Time-dependent expression pattern of *devB* (taken from Staron *et al*. 2011) and *all0809* analyzed by RT-PCR. *rnpB* refers to the loading control used for RT-PCR of *all0809*. RNA was obtained from a wild-type culture before (0) and after indicated time points of nitrogen starvation. **(B)** Micrographs of filaments bearing translational fusions of DevA-GFP and of All0807-GFP. 0h refers to unstarved filaments, 12h to N-starved filaments. BF = bright field, AF = autofluorescence, GFP = GFP fluorescence

Fig. 3 Binding of the All0809/8/7-TolC complex

(A) Evaluated SPR analysis of the interaction of immobilized TolC with free DevB or with free All0809 in dependence of indicated pH values. The raw data were taken from Staron *et al.* (2011) for DevB. The raw data for All0809 are shown in Fig. S1.

(B) Evaluated SPR analysis of the interaction of immobilized TolC or immobilized All0808/7 with free All0809 in dependence of indicated MFP concentrations. The raw data are shown in Fig. S2.

Fig. 4 Activity of All0809/8/7 towards different substrate-mixes

ATP hydrolysis rates of the IMF All0808/7 in presence of indicated substrate mixes. The term “heterocyst” refers to *Anabaena* filaments starved for 12 h, while “vegetative cell” refers to unstarved filaments. **BAS** = basal activity of All0809/8/7; **HCE** = heterocyst whole-cell extract; **HSF** = heterocyst soluble fraction; **HMF** = heterocyst whole membrane fraction; **HCM** = heterocyst cytoplasmic membrane; **HCW** = heterocyst cell wall; **MHCM** = heterocyst cytoplasmic membrane of mutant M0809, **MHCW** = heterocyst cell wall of mutant M0809; **VCE** = vegetative whole-cell extract; **VSF** = vegetative cell soluble fraction; **VMF** = vegetative cell whole membrane fraction; **VCM** = vegetative cell cytoplasmic membrane; **VCW** = vegetative cell cell wall; **HGL** = heterocyst glycolipids; **B HGL** = All0808/7 with DevB instead of All0809 and heterocyst glycolipids; **CA HGL** = DevCA instead of All0808/7 with All0809 and heterocyst glycolipids.

FIGURES

Figure 1

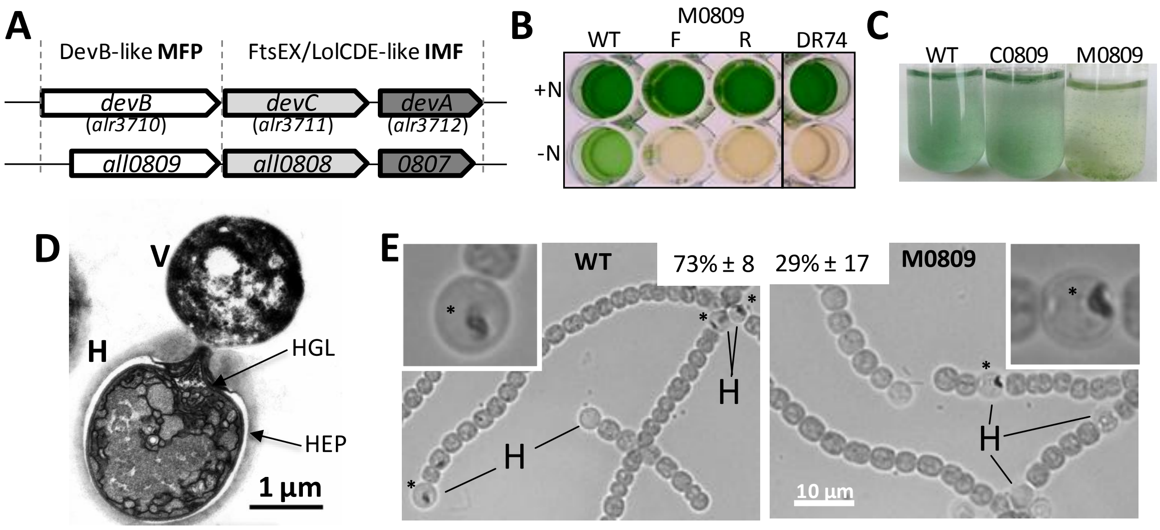

.

Figure 2

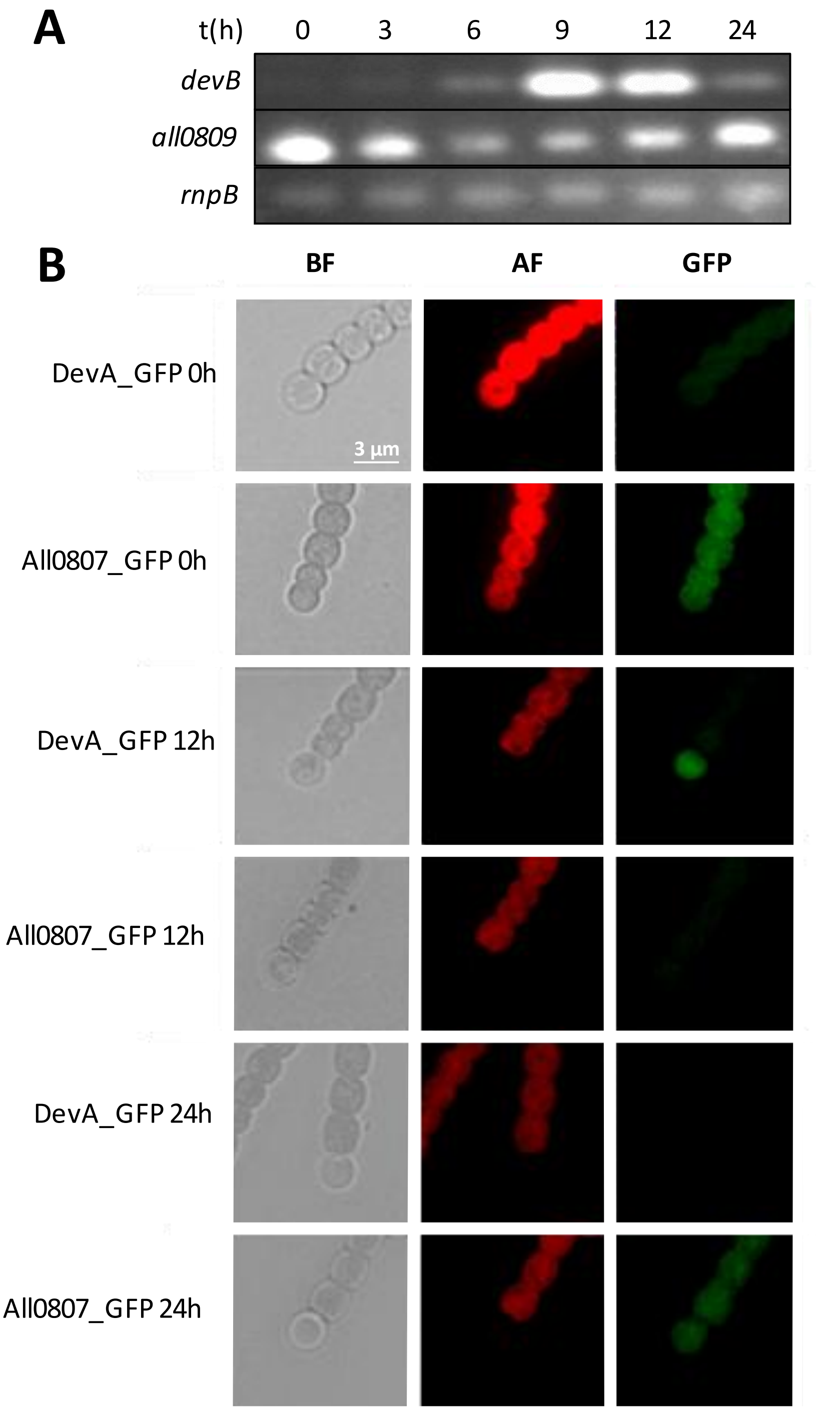
A
t(h)
0
3
6
9
12
24
devB
all0809
rnpB
B
BF
AF
GFP
DevA_GFP 0h
3 µm
All0807_GFP 0h
DevA_GFP 12h
All0807_GFP 12h
DevA_GFP 24h
All0807_GFP 24h

Figure 3

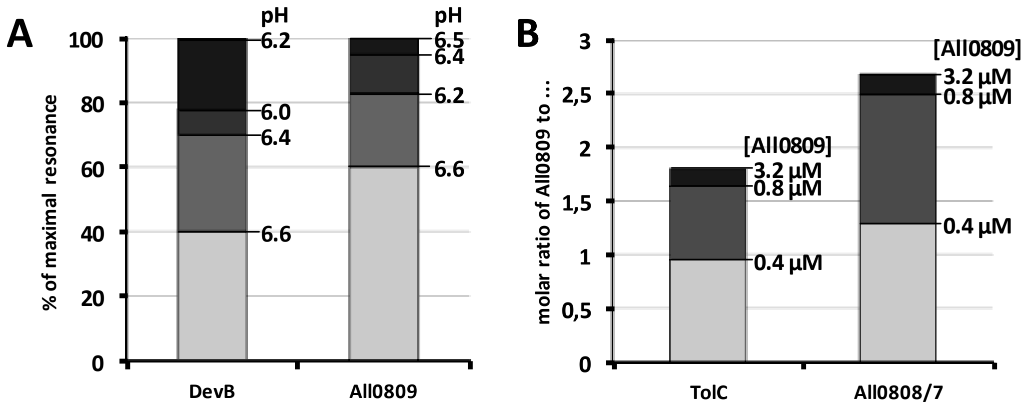

A
% of maximal resonance
100
80
60
40
20
0
pH
6.2
6.0
6.4
6.6
pH
6.5
6.4
6.2
6.6
DevB
All0809
B
molar ratio of All0809 to ...
3
2,5
2
1,5
1
0,5
0
[All0809]
3.2 µM
0.8 µM
0.4 µM
[All0809]
3.2 µM
0.8 µM
0.4 µM
TolC
All0808/7

Figure 4

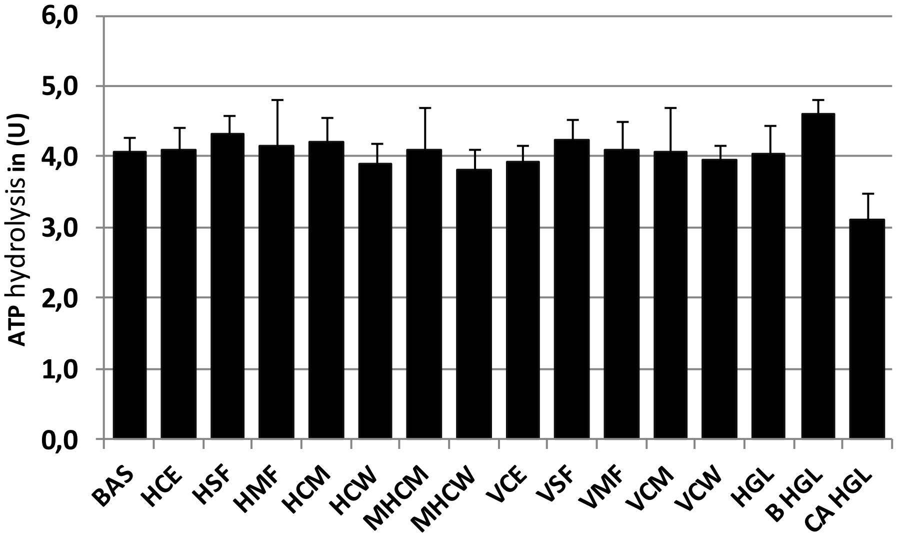
ATP hydrolysis in (U)
6,0
5,0
4,0
3,0
2,0
1,0
0,0
BAS
HCE
HSF
HMF
HCM
HCW
MHCM
MHCW
VCE
VSF
VMF
VCM
VCW
HGL
B HGL
CA HGL

8. Additional experiments (III)

8.1 Homologues of DevBCA: expression and functional analysis

8.1.1 Background and experimental design

One major objective of this work was to determine further TolC-dependent systems potentially involved in heterocyst maturation and function. The described EP DevBCA-TolC involved in export of heterocyst glycolipids and a potential HgdBC(NBD)-TolC system involved in spatial and temporal deposition or assembly of the laminated layer show high sequence homologies to each other (*hgdB* and *hgdC* are described in Fan *et al.* 2005). Although the NBD of HgdBC-TolC was not defined yet, this system is predicted to form an ATP-driven EP/T1SS very similar to DevBCA-TolC. Further DevBCA-TolC-like systems may be involved in heterocyst maturation or function. In the following chapter, *devB*, *devC*, and *devA* were analyzed concerning potential homologues encoded by the *Anabaena* genome, and the function of those homologues was investigated.

8.1.2 Methods

Determination of homologous proteins and prediction of secondary structures

Homologues of DevB, DevC, or DevA were determined by using NCBI`s protein BLAST as mentioned above (2.2). Secondary structures and transmembrane helices of DevB homologues were predicted by using MINNOU and TMHMM as mentioned above (2.2).

Used strains and growth conditions

Generated mutants that could not fix N_2 were grown in $BG11_0$ medium supplemented with 5 mM NH_4Cl and 5 mM TES-NaOH buffer, pH 7.8. All generated mutants and the applied antibiotics are listed in Tab. 1 (Appendix 11.2, page 124). To induce heterocyst formation, NH_4Cl was removed by washing the culture at least 3 subsequential times with medium free of combined nitrogen as described.

Generation of knock-out mutants in homologous genes to *devB*

All mutants were generated by triparental mating using RP4 as conjugal plasmid and pRL528 as helper plasmid as described (Wolk *et al*. 1984; Elhai and Wolk 1988b). Knock-out mutants were generated by double-recombination of the mutated gene with the wild type copy in the *Anabaena* genome, and double recombinants were selected by the use of *sacB* as described (Cai and Wolk 1990). Genes were mutated by inserting a C.K3 cassette derived from pRL442 (Elhai and Wolk, 1988a) into blunt restriction sites encoded by the respective genes. Blunt restriction sites were *Eco47*III for *all0809*, *alr4973*, and *all5347*, *Hinc*II for *all2652*, *BsaB*I for *alr3647*, and *EcoR*V for *alr4280*. Genes or gene fragments containing each a C.K3 cassette in both directions were ligated to the cargo vector pRL277 via *Xho*I. All received plasmids and mutants are listed in Tab. 1 and Tab. 3 (appendices 11.2 and 11.3, pages 124 and 126).

Expression analysis

Total RNA was extracted from filaments of 50 ml samples of an *Anabaena* wild type culture in different states of combined nitrogen deprivation (before and at 3, 6, 9, 12 and 24 h after nitrogen step-down) and reverse transcribed as described above (4.1.2).

8.1.3 Results

Close homologues of *devBCA* in *Anaebana*

BLAST analysis with each DevB, DevC, and DevA predicted six homologous gene clusters in the genome of *Anabaena* sp. PCC 7120 (Fig. 27). With exception of gene clusters ii and vi (*all2652*+*all2651* and *all5347*+*all5346*), all operons encode a DevB-type MFP, a DevC-type substrate binding domain of an IMF and a nucleotide binding domain of an IMF in the same order as *devBCA* does (Fig. 27). Genes in closer proximity (+/- 5) to operons ii and vi did not encode a *devA*-like NBD. The genes *all5346* and *all5347* are also known as *hgdC* and *hgdB*, respectively (Fan *et al.* 2005).

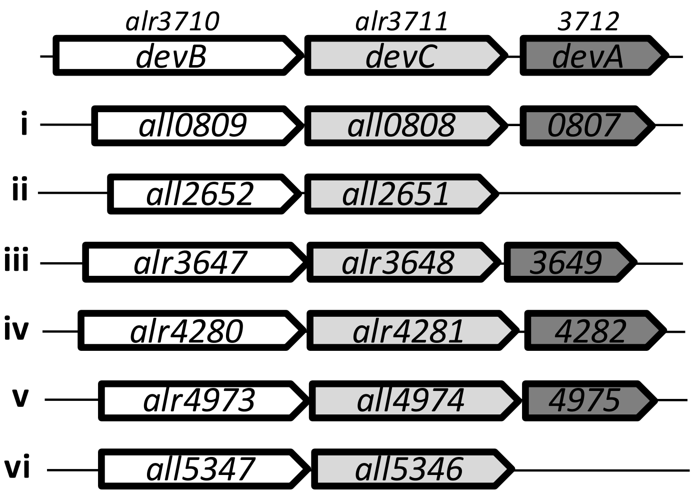

Figure 27. Gene clusters homologous to *devBCA*

Organization of 6 gene clusters homologous to *devBCA*.

Despite some minor and irregular differences in the size of some secondary structures, the overall appearance of the IMFs (or the SBDs in the case of operons ii and vi) is similar. The α-helical domain of the MFPs differs in length (Fig. 28). Like DevB, all homologous MFPs predicted from the respective genes in Fig. 27 lack the C-terminal β-roll present in other described MFPs (Fig. 28 and 5. manuscript I).

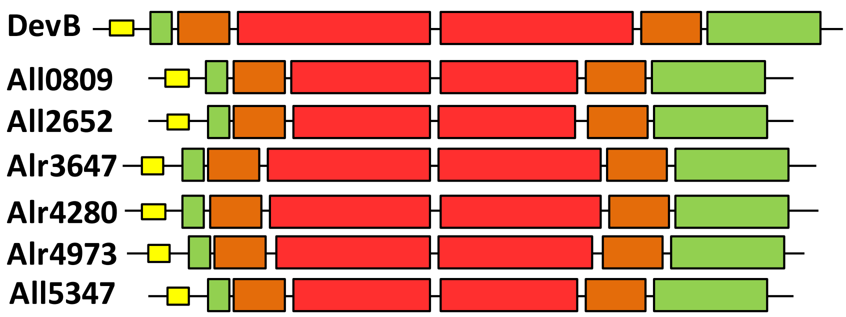

Figure 28. Structural elements of DevB in comparison to its close *Anabaena* homologues

Secondary structures and transmembrane helices were predicted by using MINNOU. Yellow = transmembrane helix; green = β-barrel domain; brown = lipoyl domain; red = α-helical domain. The NBCI protein accession no. are listed in 6.1.2.

Expression of *devB* homologues during heterocyst formation

To get an idea of a potential involvement of the *devBCA* homologues in heterocyst maturation, the expression of each homologous MFP encoding gene was determined via semiquantitative RT-PCR.

With exception of *alr4280* and *alr4973* that did not show remarkable changes in their expression rate (Fig. 29), two types of responses to nitrogen stepdown could be observed. Similar to *devB*, the expression of *all2652*, *alr3647*, and *all5347* (*hgdB*) was upregulated in the first 9 h, and it was downregulated to a barely elevated initial transcription level after 24 h (Fig. 29). The expression of *all0809* was contrary to the other responding genes. *All0809* was downregulated to a minimum at 6 to 9h, and the transcription increased to the initial level after 24 h (Fig. 29).

With the exception of *all3647* and *all5347*, the transcription data risen on the homologues of *devB* roughly agrees with a whole RNA transcription study of Ehira *et al*. (2003). In contrast, a recent study of Flaherty *et al*. (2011) predicts a steady increase of *all0809* until 21 h after nitrogen deprivation. Also, the transcription of *all2652* is reported to remain constant, while the induction of *all5347* takes place at 21h. The reported transcription rates of *all3647* match to the ones risen in this study.

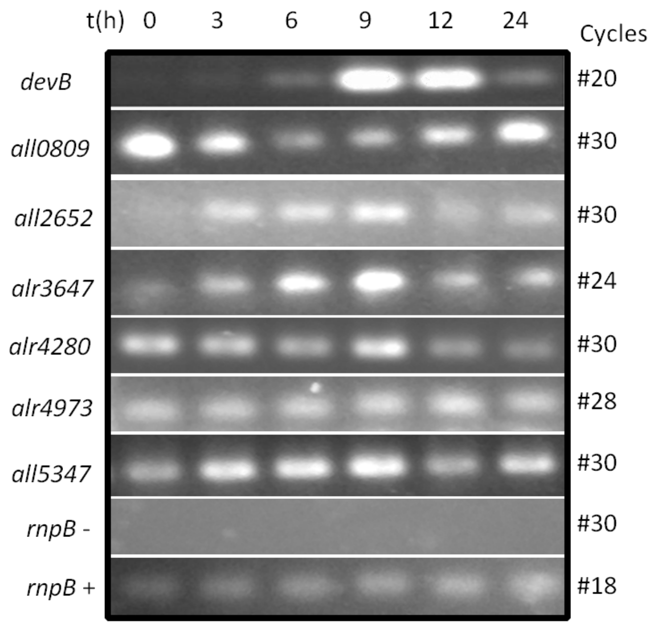

Figure 29. Expression of genes encoding heterocyst_DevB-like MFPs

The time-dependent expression of *all0809*, *all2652*, *alr3647*, *alr4280*, *alr4973* and *all5347* was analyzed by RT-PCR (8.1.2). RNA was obtained from the same wild type culture after indicated time points of nitrogen starvation (8.1.2). *RnpB* refers to the loading control of *devB* homologues.

Site-directed mutagenesis of six close homologues of *devB*

To check an influence of the respective homologues on diazotrophic growth, each MFP gene was attempted to be inactivated by site-directed mutagenesis.
Only mutants in *all0809*, *alr3647*, *alr4973*, and *all5347* (*hgdB*) could be segregated (the mutation could be established in all chromosomal copies of *Anabaena*; see Fig. 47 in appendix 11.5, page 129). Mutants in *all2652* and *alr4280* could not be completely segregated, even when much higher concentrations of antibiotics were applied. Both (partial) mutants were not impaired in diazotrophic growth (not shown).
Mutants in *alr3647* and *alr4973* did not show any obvious impairment in growing without combined nitrogen (Fig. 30). In contrast, mutants in *all0809* and in *all5347* (*hgdB*) were not able to perform diazotrophic growth (Fig. 30). In any mutant, the orientation of the inserted C.K3 cassette did not influence the phenotype. So, polar effects could be excluded.

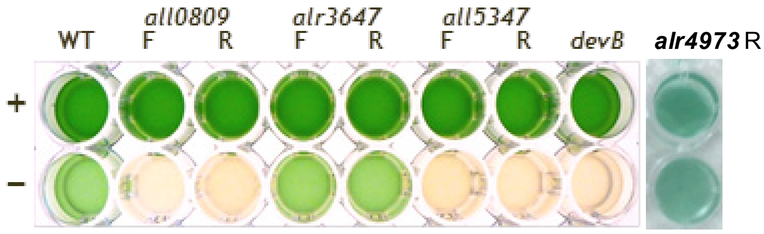

Figure 30. Diazotrophic phenotype of mutants in heterocyst_DevB-like homologues

+ = *Anabaena* cultures grown for ~1 week in presence of NH_4^+. - = *Anabaena* cultures grown for ~1 week without combined nitrogen. WT = wild type, F = forward-orientation of the C.K3 cassette, R = reverse-orientation

8.1.4 Summary

Two out of 6 MFPs homologous to DevB are crucial for diazotrophic growth: All0809 and All5347. *All0809* is downregulated during heterocyst formation, and upregulated when heterocyst maturation is about to finish. *All5347* (also known as *hgdB* (Fan *et al.* 2005)) is regulated contrary to *all0809* and similar to *devB*.

9. Discussion

9.1 Glycolipid export by an ATP-driven efflux pump

The participation of the ABC exporter DevBCA in heterocyst-specific glycolipid deposition was assumed since the first detailed description of *devBCA*`s gene function in 1998 (Fiedler *et al.*). The formation of a T1SS involving DevBCA was suggested in 2003 (Maldener et al.), and a complex of DevBCA-TolC in particular was predicted in 2007 (Moslavac *et al.*). This complex was proven in this work: DevBCA and TolC form an ATP-driven *trans*-envelope EP for the translocation of HGLs as building blocks of the laminated heterocyst layer. DevBCA-TolC represent the second T1SS known besides MacAB-TolC not exclusively exporting proteins. Other described T1SS like HlyBD-TolC (exports hemolysin; Holland *et al.* 2005), CvaAB-TolC (exports a colicin; Gilson *et al.* 1990), or PrtCDE-PtrF (exports a protease; Delepelaire 1994) were shown to be involved in exporting proteins. For these T1SS, metabolites or drugs have not been identified as substrates yet. Even MacAB-TolC is believed to have a proteinaceous physiological substrate: heat stable enterotoxin II (Yamanaka et al. 2008). However, DevBCA-TolC and MacAB-TolC can be considered as ATP-driven EP too, instead of being classified as T1SS. It has to be noted that the clinical relevance of all T1SS (and MF-type EPs) is inferior to that of the RND-type EP AcrAB that even outshines all other RND-type EPs. Therefore, in Gram-negative bacteria T1SS -and ABC exporters in general- are less investigated than their RND counterparts (Zgurskaya 2009).

Up to date, translocation of glycolipids by a T1SS/ATP-driven EP -or any EP in general- has not been described. In Gram-negative bacteria, most glycolipids can be found in the outer leaflet of the OM. Therefore, Gram-negative bacteria evolved distinct systems for the transport of glycolipids that are formed in the cytoplasmic membrane (Doerrler 2006).
The best known pathway for glycolipid export comprises the ABC exporters MsbA and LptFGB, and the periplasmic chaperones LptC and LptA, as well as the OM- lipoprotein LptE and β-barrel protein LptD (Fig. 31, page 102 and Tokuda 2009). However, MsbA and LptABCDEFG do not share remarkable homologies with DevBCA. Although the NBDs are similar, MsbA shows a different overall structure when compared to DevC. MsbA

locates its NBD on the C-terminus of the peptide, and the transmembrane domain of MsbA has 6 transmembrane helices (Honorat *et al*. 2011) instead of 4 as found in DevC and homologous SBDs (2.3.2; Xu *et al*. 2009). The genome of *Anabaena* predicts several MsbA exporters including HetA/HepA and HetC. Both are involved in the formation of the polysaccharide layer enveloping the laminated layer (Holland and Wolk 1990, Khudyakov and Wolk 1997). Also, the transmembrane subunits of LptFGB do not share similarities to DevC in overall structure. Like MsbA, both LptF and LptG have 6 transmembrane helices. As any ABC-type NBD in general, LptB shows homologies to DevA. The periplasmic proteins LptC and LptA do not show any similarities to DevB, and the OM proteins LptE and LptD do not show similarities to TolC (despite the β-barrel of both LptD and TolC). The genome of *Anabaena* predicts *alr4067-alr4069* to encode homologues to LptA and LptFGB, while LptC, LptE, and LptD could not be identified. Taken together, DevBCA-TolC do not resemble the MsbA/Lpt-pathway.

In structure, DevA and DevC show high similarities to LolCDE, an ABC exporter involved in lipoprotein trafficking to the OM (Fig. 31 and Tokuda 2009). In contrast to DevAC, the LolCDE complex is formed by 2 asymmetric SBDs. Like DevC, LolC and LolE are classified as members of the MacB_PCD/FtsX superfamily, while DevA and LolD are members of the M0796 group (2.3.2.). The periplasmic chaperone of LolCDE, LolA is hardly comparable to the MFP DevB or to MFPs in general. This pathway is not known to involve an OM protein like TolC or LptD. So, despite a lot of similarities, DevBCA-TolC also does not seem to resemble the Lol pathway.

The destination of HGL export by DevBCA-TolC is beyond the OM. The MsbA/Lpt pathway as well as the Lol pathway do not traverse the OM in a way an EP is able to. Although the β-barrel protein LtpD is similar to the β-barrel domain of TolC, it is not likely that its function is similar. While TolC is utilized by an active motor from the CM, LptD does not seem to have an active driving force. It accepts incoming glycolipids from LptA and flips them to the outer leafleat of the OM by a yet unknown mechanism (Tokuda 2009). The periplasm is free of ATP, so an energy providing element can be excluded. Taken together, TolC-DevBCA can be considered as a uniquely adjusted system for the formation of an extracellular glycolipid layer in heterocysts. This EP/T1SS reflects a novel pathway for directed glycolipid transport (Fig. 31).

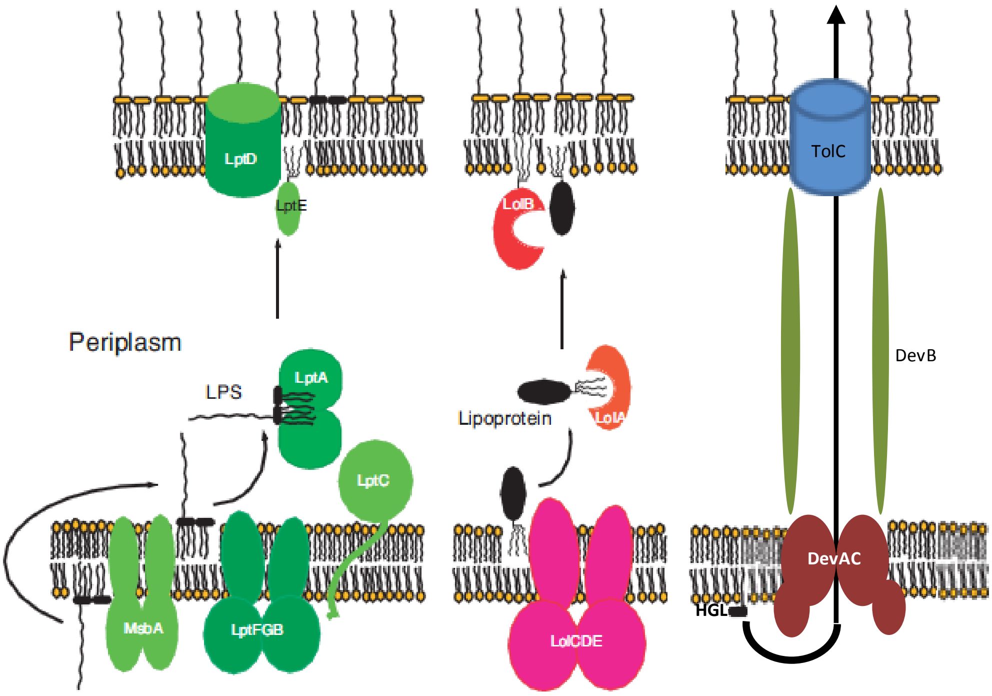

Figure 31. Glycolipid trafficking in Gram-negative bacteria

Scheme of the MsbA/Lpt pathway (on the left) and the Lol pathway (in the center; both taken from Tokuda (2009)). The DevBCA pathway (on the right) was added.

From the results obtained in this work, DevBCA-TolC did not seem to be involved in protein export, since the ATPase activity did not discriminate between proteinase K treated and untreated cell fractions (3. publication). DevBCA appeared to be monospecific toward the reduced HGL 1-(O-α-D-glucopyranosyl)-3,25-hexacosanediol because the ATPase activity was proportional to the percentage of this 3-enol tautomer (4.2.3). Nevertheless, in the context of other EPs -especially MacAB-TolC- it cannot be excluded that DevBCA-TolC has a broader substrate range. Exported proteins could also be involved in the formation of the laminated layer. Two major arguments support this thesis: (i) The T1SS MacAB-TolC exports proteins <u>and</u> non-proteinaceous metabolites. It is an example for T1SS not being monospecific. By this means, DevBCA could transport proteins or even other substrates in addition to glycolipids. (ii) The *tolC* knock-out mutant DR181 does not secrete at least 3 proteins into the medium (Moslavac *et al.* 2007). So, TolC actually participates in protein export. Of course, this must not involve DevBCA but various other exporters encoded by the genome of *Anabaena*.

A reason for not detecting proteins as substrates of DevBCA in fractions of *Anabaena* might be that in the used experimental setup DevBCA simply did not react toward proteins by changes in ATP hydrolysis. Since the mechanisms of substrate-translocation by ABC-type IMFs are not known yet (partially due to the lack a crystal structure showing the membrane integral part of the IMF) they could be different toward different substrates. Taken MacAB-TolC as example, the method of export of heat stable enterotoxin II and the macrolide erythromycin could differ due to the different nature and the different size of the substrates (~5,000 Da to ~730 Da). These export mechanisms may involve accessory (protein) factors that have not been identified yet, but they have been taken into consideration by Tikhonova *et al*. (2007). Maybe these factors are not necessary for HGL-export by DevBCA-TolC, but for the export of other substrates.

9.2 Topology of DevBCA-TolC

To traverse the periplasm, a "bridging model" was proposed for the ATP-driven EP MacAB-TolC. In this model, a MacA hexamer contacts TolC in a cogwheel-like manner by tip-to-tip interaction of the respective α-helical tips. This model was derived from *in silico* protein models based on crystals of MacA and TolC (Yum *et al.* 2009). It was confirmed by electron micrographs showing a funnel-like hexameric assembly of MacA and of MacA-TolC hybrids. These hybrids were based on MacA carrying the tip-regions of TolC instead of their native ones (1.3.4; Xu *et al.* 2010). Since the IMF MacB was demonstrated to form dimers (Lin *et al.* 2009) and TolC trimers (Koronakis *et al.* 2000), a MacB-to-MacA-to-TolC ratio of 2:6:3 could assemble the ATP-driven efflux pump. Our data on DevBCA-TolC support exactly this "bridging model" including the derived stoichiometry. Whenever the tip-to-tip interface between DevB and TolC had been modified, the interaction of the MFP with the OMF was nearly abolished. Furthermore, whenever the ability of DevB to form hexamers had been impaired, the interaction of the MFP with the OMF was remarkably decreased (5. manuscript I). As implied by the results of mutant in N^{333} to A (3. publication), this oligomeric state is pivotal for glycolipid export *in vivo*. In addition, no DevB variant used in this work -including the one with N^{333} mutated to A- was able to make DevAC responsive toward the glycolipid

substrate. So, a periplasmic DevB hexamer has a central role in the glycolipid efflux pump DevBCA-TolC.
The periplasmic domain of MacB shows common structural motifs to the TolC-docking domain of the RND-type IMF AcrB (Xu *et al*. 2009). For the RND-type EP AcrAB-TolC, a different model to MacAB-TolC assembly was proposed. *In vivo* cross-linking revealed contact sites in the α-helical domain of AcrA and in the α-helical barrel of TolC, and therefore it implied a 3:3:3 stoichiometry of AcrB:AcrA:TolC. It was proposed that the α-helical domain of AcrA docks into pockets provided by helices 7/8 and 3(/4) of TolC`s α-helical barrel. Thus, three molecules of AcrA would wrap around TolC (wrapping model; 1.3.4). In this model, AcrB was demonstrated to establish a stable interaction with the tip-regions of TolC via its TolC-docking domain. So, a substrate translocation channel is formed by the IMF and the OMF while the MFP is assumed to play a recruiting and stabilizing role only (Touzé *et al*. 2004; Tamura *et al*. 2005; Bavro *et al*. 2008; Symmons *et al*. 2009). It is not clear if the periplasmic domain of ABC-type IMFs directly contacts the OMF. In pull-down assays performed in 2005 (Lin *et al*.), a barely detectable interaction of MacB with TolC was observed, while more recent pull-down studies could not detect any interaction (Xu *et al*. 2009). In SPR, DevAC did not remarkably interact with TolC (and DevBCA-TolC did not resemble a wrapping model; 5. manuscript I). The interaction between the IMF and the OMF seems to be mediated by a funnel-like assembly of MFPs in ABC-type EPs/T1SSs.

As investigated by fluorescence quenching of W residues, the MF-type MFP EmrA directly binds to the substrates exported by EmrAB-TolC. EmrA only bound to substrates specific for its EP, and it did not bind foreign ones (Borges-Walmsley *et al.* 2003). In contrast to the RND-type IMF AcrB, MF-type IMFs are not supposed to directly contact TolC (Zgurskaya 2009), and ABC-type IMFs do not seem to do so. In the case of the MF-type EP EmrAB-TolC, drug molecules released from the IMF EmrB must reach TolC without escaping into the periplasm. EmrA appears to receive substrates from the IMF and to pass them to the OMF. This principle could be also true for ABC-type MFPs. The periplasmic domain of MacB bridges up to ~5 nm (Xu *et al.* 2009), and TolC protrudes up to ~10 nm into the periplasm via its α-helical domain (Koronakis *et al.* 2000). This is not sufficient for direct interaction of the IMF and the OMF, since the periplasm of *E. coli* was determined to have a diameter of ~22 nm (Matias *et al.* 2003). A central MacA hexamer would add ~7 nm to this complex solely by providing an α-helical

stem structure (Yum *et al.* 2009), and therefore it would nearly close the gap. In the proposed "bridging" model, it is likely that MacA interacts with the substrate of MacAB-TolC, since MacB and TolC would not be in direct contact. DevBCA and TolC even have to span up to 46 nm (Wilk *et al.* 2011). Because DevC`s periplasmic domain is predicted to be similar to that of MacB (2.3.2.), and TolC matches TolC from *E. coli* in structure (2.3.4.), both would bridge only ~15 nm of the periplasm (as mentioned above for MacB and TolC). It would be even hard for DevB to close the resulting gap: the α-helical domain of DevB is predicted to be up to ~17 nm in length (2.3.1). According to the bridging model proposed for MacAB-TolC (1.3.4) that is supported by the data risen in this work (3. publication, 5. manuscript I), DevBCA would span ~32 nm of *Anabaena*`s periplasm (and therefore invaginations of the CM and/or the OM would be necessary). So, it is even more likely that substrates interact with DevB, simply because they cannot directly proceed from DevAC to TolC due to their spatial distance in *Anabaena*`s large periplasm. However, this has still to be proven.
When the IMF would not or hardly be able to interact with the OMF directly, the mentioned funnel-like assembly of MacA -and of DevB- would be able to keep the export pathway sequestered from the surrounding periplasm. In this case, the respective MFPs would also have to provide a pathway of suitable milieu. When the IMF and the OMF would not be in direct contact (as proposed in the bridging model for MacAB-TolC interaction), an MFP trimer (as proposed in the "wrapping model" for AcrAB-TolC interaction mentioned above) would not be able to provide sequestration, since smaller substrates could escape to the periplasm. An MFP trimer would also not be able to provide a suitable milieu for e.g. hydrophobic substrates as HGLs.

Taken these considerations together, a bridging model including a tip-to-tip interface between the MFP and OMF is supported by the studies on DevBCA-TolC. A direct interaction between the IMF and the OMF would occupy the same binding sites of the OMF (as shown for AcrB-TolC), and does not seem to be relevant for ABC-type EPs/T1SS. The results and the interpretations of the *in vitro* and *in vivo* studies presented in this work are cumulated in the following model (Fig. 31):

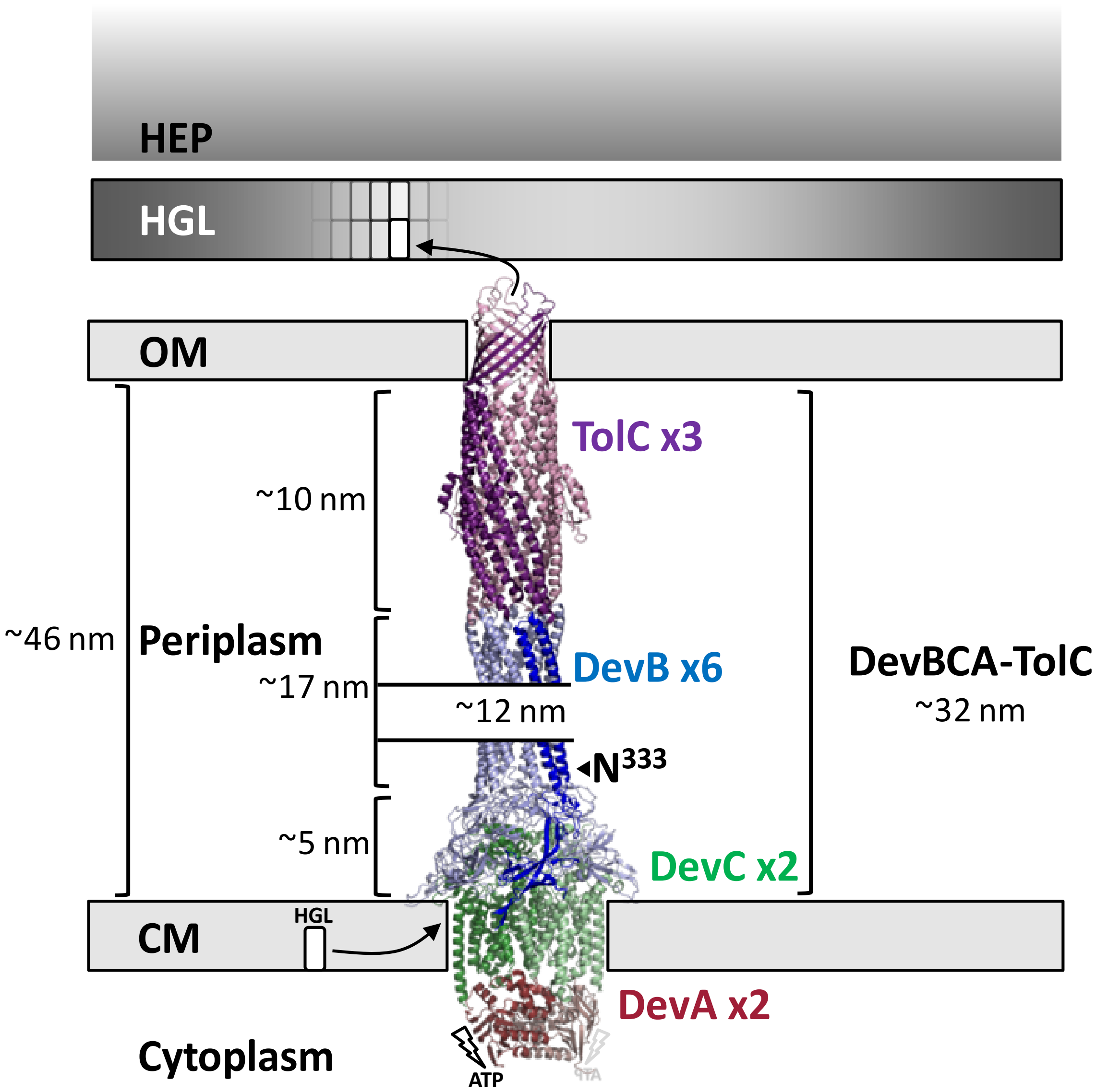

Figure 31. DevBCA-TolC in maturing *Anabaena* heterocysts

Theoretical model of DevBCA-TolC spanning the envelope of maturating heterocysts. HEP = heterocyst envelope polysaccharide, HGL = heterocyst glycolipid (layer). Since DevC or homologues of DevC are not completely crystallized yet, and an orientation of DevC-like IMFs in EPs is not known, DevC is replaced by a dummy.

9.3 Homologues of DevBCA

Like DevBCA-TolC, All0809/8/7-TolC assemble an ATP-driven efflux pump. The molar ratio of TolC to the MFP All0809 to the IMF All0808/7 was determined to be 3:6:2, it exactly resembles the molar ratio of TolC:DevB:DevAC (3. publication and 5. manuscript

I). So, similar to other described ATP-driven efflux pumps, a central MFP All0809 hexamer seems to play a key role in the physiological function of All0809/8/7-TolC. Consequently, a tip-to-tip cogwheel-like interaction of the MFP with the OMF in ATP-driven efflux pumps (as shown in Fig. 31) also is true for All0809 and TolC.

In contrast to DevB interaction with TolC, All0809 interaction with TolC has a higher pH optimum (6.5 to 6.2; 7. manuscript III). Since TolC is the only TolC-like OM protein predicted from the genome of *Anabaena*, several TolC-depending exporters have to compete with each other for the binding of the respective MFP to the OMF (e.g. DevB and All0809 compete for TolC). Different pH optima for the affinity of the MFP to TolC could determine the selection of the MFP needed for a specific purpose. This would add a further physiological manner of regulation besides differential expression and spatial seperation. The expression pattern of *all0809* (decreasing toward a minimum at 6-9 h and increasing to an almost initial level afterwards; 7. manuscript III) and the localization of All0807-GFP (localized in all cells of the filaments; 7. manuscript III) would confirm this assumption. DevB, exclusively formed in developing heterocysts in the middle of the maturation process, could more easily banish competing MFPs present in undifferentiated filaments by outperforming them in affinity to TolC at lower pH (e.g. All0809).
However, it remains to be demonstrated whether developing heterocysts locally and temporally change their periplasmic pH values (or the pH value of the continuous periplasm of the whole filament) to discriminate between heterocyst-specific and heterocyst-unspecific functions. An increase in respiration rate was described for heterocysts (Wolk 1994). It has not been shown so far whether respiration is also localized to the CM, where it could account for creation of a H^+-gradient across the CM. However, adjusting the pH value of the periplasm could prefer heterocyst- specific over heterocyst-unspecific functions. During heterocyst formation, the cell wall and the periplasm are subjected to remarkable changes, e.g. the protein composition (Moslavac *et al.* 2007, reviewed in Nicolaisen *et al*. 2009)) or rearrangements of the peptidoglycan (Lehner *et al*. 2011). To prove this suggestion, the pH optima of the interactions further homologues of DevB, other ABC-, RND-, and MF-type MFPs with TolC have to be elucidated. Some homologues of DevB also reacted toward diazotrophic conditions in the rate of their transcription (*all2652*, *alr3647*, and *all5347*/*hgdB;* 8.1.3), while others did not (*all4280* and *all4973*; 8.1.3). Responsive gene clusters may be involved in

heterocyst maturation (*all5347/hgdB* was even pivotal (Fan *et al*. 2005). In contrast, constitutive gene clusters do not appear to be involved in tasks related to diazotrophic growth. Members of both groups appear to be suitable to investigate the pH optima in binding to TolC to gain further insights into the proposed adjustment of the periplasmic pH. Also, heterocyst development-related and -unrelated functions different to EPs can be elucidated for this purpose.

All0809/8/7 did not react in ATP hydrolysis rate toward the presence of HGLs, and heterocysts of a mutant in *all0809* had a wild type-like laminated layer (7. manuscript II). So, specific contribution of All0809/8/7-TolC into export and/or formation of the laminated layer appears to be unlikely. Nevertheless, impairment in providing a microoxic environment for N_2-fixation can be deduced: when compared to the wild type, heterocysts of a mutant in *all0809* reduced INT to insoluble formazan crystals less frequently (7. manuscript II). Consequently, the wild type-like appearing laminated layer seems to be partially functional only, or the mutant is impaired in other mechanisms providing a microoxic environment.

The efflux pump All0809/8/7-TolC either seems to indirectly affect heterocyst maturation, or to adopt a heterocyst-specific function. An indirect effect of the mutation of *all0809* on heterocyst formation could be explained in the manner of the proposed function of the RND-type EP AcrEF-TolC in *E. coli*: during cell division, AcrEF-TolC are supposed to act as a cleaner for the periplasm from proteins and products of murein and membrane recycling. Overproduction of a periplasmic protein in an *acrEF* mutant resulted in filamentous *E. coli* (Lau and Zgurskaya 2005). Analogously, All0809/8/7-TolC could also play a role in maintaing the periplasm of *Anabaena*. A lack of this function could produce unforeseen -and maybe unseen- artefacts in the cell wall of developing heterocysts, and therefore somehow allow the entrance of O_2 into the heterocyst or prohibit supply of reductants to the mature heterocyst by periplasmic diffusion (Flores *et al*. 2006; Flores and Herrero 2010). On the other hand a heterocyst specific role of All0809/8/7-TolC could also be explained by this means: if All0809/8/7-TolC would function as a specific cleaner of the periplasm of developing heterocysts, its absence would impair the formation of a fully functional heterocyst cell wall. Then, proteins or other compounds could not be removed from the periplasm and would accumulate to concentrations inhibiting crucial heterocyst functions. Regarding a hypothetic cleaning of the periplasm from DevBCA, the opposed expression pattern of *all0809*(*/8/7*) would answer expectations: the amount of All0809/8/7-TolC decreases, when the amount of DevBCA-TolC increases, and *vice versa*. Since DevBCA are massively induced to export HGLs at a specific stage of developing heterocysts, and DevB has advantages to occupy the binding sites of TolC in the prolonged α-helical domain and the adjusted pH optimum discussed above, it would be necessary to remove DevBCA after they have fulfilled their stage-specific function in exporting HGLs. All0809/8/7-TolC could address this task, and therefore it could allow other exporters to form efflux pumps with TolC, since this OMF is the only one of its kind encoded by the genome of *Anabaena*.

Both suggestions could also explain the absent reaction of All0809/8/7 towards the exposed cell fractions. Since the ABC-exporter was not exposed towards enriched periplasm, potential substrates might have been too strongly diluted (in the soluble fraction used) to promote a detactable increase in ATPase activity. On the other hand, it is not clear, if the efflux pump would be able to recognize all periplasmic proteins/substrates, a disctinct part of them, or even only specifically modified ones. In addition, if some substrates of all0809/8/7-TolC were proteinaceous, additional factors for ATPase activity and export discussed for DevBCA-TolC and MacAB-TolC above might be absent in the experimental setup (at specific time points).

DevBCA-TolC is the first ABC-type EP/T1SS described for *Anabaena* and cyanobacteria in general, and (besides MacAB-TolC from *E. coli*) DevBCA-TolC is the second T1SS described not to be solely involved in protein secretion. DevBCA-TolC export HGLs necessary for the formation of the laminated layer of developing heterocysts, and therefore this EP is pivotal for diazotrophic growth. All0809/8/7-TolC is the second ABC-type EP/T1SS described for *Anabaena* necessary for heterocyst function. DevBCA, All0809/8/7-TolC, and MacAB-TolC assemble a central periplasmic MFP hexamer that interacts with the OMF by a cogwheel-like tip-to-tip interface. Therefore, the overall topology of ATP-driven EPs is different to that of RND-type EPs. Future studies on the other homologues of DevBCA-TolC and MacAB-TolC will underline the importance of this broadly distributed class of exporter systems in cyanobacteria and in Gram-negative bacteria in general.

10. Literature

Abramoff, M.D., Magelhaes, P.J., and Ram, S.J. (2004). Image processing with ImageJ. *Biophotonics International* **11**, 36-42.

Altschul, S.F., Madden, T.L., Schaffer, A.A., Zhang, J., Zhang, Z., Miller, W., and Lipman, D.J. (1997). Gapped BLAST and PSI-BLAST: a new generation of protein database search programs. *Nucleic Acids Res* **25**, 3389-3402.

Bavro, V.N., Pietras, Z., Furnham, N., Perez-Cano, L., Fernandez-Recio, J., Pei, X.Y., Misra, R., and Luisi, B. (2008). Assembly and channel opening in a bacterial drug efflux machine. *Mol Cell* **30**, 114-121.

Black, T.A., Cai, Y., and Wolk, C.P. (1993). Spatial expression and autoregulation of *hetR*, a gene involved in the control of heterocyst development in *Anabaena*. *Mol Microbiol* **9**, 77-84.

Borges-Walmsley, M.I., Beauchamp, J., Kelly, S.M., Jumel, K., Candlish, D., Harding, S.E., Price, N.C., and Walmsley, A.R. (2003). Identification of oligomerization and drug-binding domains of the membrane fusion protein EmrA. *J Biol Chem* **278**, 12903-12912.

Buikema, W.J., and Haselkorn, R. (1991). Characterization of a gene controlling heterocyst differentiation in the cyanobacterium *Anabaena* 7120. *Genes Dev* **5**, 321-330.

Gram, C. (1884). Über die isolirte Färbung der Schizomyceten in Schnitt- und Trockenpräparaten. *Fortschritte der Medicin* **2**, 185-189.

Cai, Y.P., and Wolk, C.P. (1990). Use of a conditionally lethal gene in *Anabaena* sp. strain PCC 7120 to select for double recombinants and to entrap insertion sequences. *J Bacteriol* **172**, 3138-3145.

Cao, B., Porollo, A., Adamczak, R., Jarrell, M., and Meller, J. (2006). Enhanced recognition of protein transmembrane domains with prediction-based structural profiles. *Bioinformatics* **22**, 303-309.

Chomczynski, P., and Sacchi, N. (2006). The single-step method of RNA isolation by acid guanidinium thiocyanate-phenol-chloroform extraction: twenty-something years on. *Nat Protoc* **1**, 581-585.

Cianciotto, N.P. (2005). Type II secretion: a protein secretion system for all seasons. *Trends Microbiol* **13**, 581-588.

Cole, C., Barber, J.D., and Barton, G.J. (2008). The Jpred 3 secondary structure prediction server. *Nucleic Acids Res* **36**, W197-201.

Delepelaire, P. (1994). PrtD, the integral membrane ATP-binding cassette component of the *Erwinia chrysanthemi* metalloprotease secretion system, exhibits a secretion signal-regulated ATPase activity. *J Biol Chem* **269**, 27952-27957.

Doerrler, W.T. (2006). Lipid trafficking to the outer membrane of Gram-negative bacteria. *Mol Microbiol* **60**, 542-552.

Ehira, S., Ohmori, M., and Sato, N. (2003). Genome-wide expression analysis of the responses to nitrogen deprivation in the heterocyst-forming cyanobacterium *Anabaena* sp. strain PCC 7120. *DNA Res* **10**, 97-113.

Elhai, J., and Wolk, C.P. (1988a). A versatile class of positive-selection vectors based on the nonviability of palindrome-containing plasmids that allows cloning into long polylinkers. *Gene* **68**, 119-138.

Elhai, J., and Wolk, C.P. (1988b). Conjugal transfer of DNA to cyanobacteria. *Methods Enzymol* **167**, 747-754.

Fan, Q., Huang, G., Lechno-Yossef, S., Wolk, C.P., Kaneko, T., and Tabata, S. (2005). Clustered genes required for synthesis and deposition of envelope glycolipids in *Anabaena* sp. strain PCC 7120. *Mol Microbiol* **58**, 227-243.

Fiedler, G., Arnold, M., Hannus, S., and Maldener, I. (1998). The DevBCA exporter is essential for envelope formation in heterocysts of the cyanobacterium *Anabaena* sp. strain PCC 7120. *Mol Microbiol* **27**, 1193-1202.

Fiedler, G., Muro-Pastor, A.M., Flores, E., and Maldener, I. (2001). NtcA-dependent expression of the *devBCA* operon, encoding a heterocyst-specific ATP-binding cassette transporter in *Anabaena* spp. *J Bacteriol* **183**, 3795-3799.

Flaherty, B.L., Van Nieuwerburgh, F., Head, S.R., and Golden, J.W. (2011). Directional RNA deep sequencing sheds new light on the transcriptional response of *Anabaena* sp. strain PCC 7120 to combined-nitrogen deprivation. *BMC Genomics* **12**, 332.

Flores, E., and Herrero, A. (2010). Compartmentalized function through cell differentiation in filamentous cyanobacteria. *Nat Rev Microbiol* **8**, 39-50.

Flores, E., Herrero, A., Wolk, C.P., and Maldener, I. (2006). Is the periplasm continuous in filamentous multicellular cyanobacteria? *Trends Microbiol* **14**, 439-443.

Frias, J.E., Flores, E., and Herrero, A. (1994). Requirement of the regulatory protein NtcA for the expression of nitrogen assimilation and heterocyst development genes in the cyanobacterium Anabaena sp. PCC 7120. *Mol Microbiol* **14**, 823-832.

Gantt, E. (1994). Supramolecular membrane organization. In*: The Molecular Biology of Cyanobacteria, Bryant, D.A. (ed)*, 119-138, Kluwer Academic Publishers, Dordrecht.

Geertsma, E.R., Nik Mahmood, N.A., Schuurman-Wolters, G.K., and Poolman, B. (2008). Membrane reconstitution of ABC transporters and assays of translocator function. *Nat Protoc* **3**, 256-266.

Gilson, L., Mahanty, H.K., and Kolter, R. (1990). Genetic analysis of an MDR-like export system: the secretion of colicin V. *EMBO J* **9**, 3875-3884.

Hanahan, D. (1985). Techniques for transformation of *Escherichia coli*. *DNA Cloning: A Practical Approach* **1**, 109-135.

Hanahan, D., Jessee, J., and Bloom, F. R. (1991). Plasmid transformation of *Escherichia coli* and other bacteria. *Methods Enzymol* **204**, 63-113.
Henderson, I.R., Navarro-Garcia, F., Desvaux, M., Fernandez, R.C., and Ala'Aldeen, D. (2004). Type V protein secretion pathway: the autotransporter story. *Microbiol Mol Biol Rev* **68**, 692-744.

Hoiczyk, E., and Hansel, A. (2000). Cyanobacterial cell walls: news from an unusual prokaryotic envelope. *J Bacteriol* **182**, 1191-1199.

Holland, D., and Wolk, C.P. (1990). Identification and characterization of *hetA*, a gene that acts early in the process of morphological differentiation of heterocysts. *J Bacteriol* **172**, 3131-3137.

Holland, I.B., Schmitt, L., and Young, J. (2005). Type 1 protein secretion in bacteria, the ABC-transporter dependent pathway. *Mol Membr Biol* **22**, 29-39.

Honorat, M., Falson, P., Terreux, R., Di Pietro, A., Dumontet, C., and Payen, L. (2011). Multidrug resistance ABC transporter structure predictions by homology modeling approaches. *Curr Drug Metab* **12**, 268-277.

Izoré, T., Job, V., and Dessen, A. (2011). Biogenesis, regulation, and targeting of the type III secretion system. *Structure* **19**, 603-612.

Nangana, T.K., Bavro, V.N., Zhang, L., Matak-Vinkovic, D., Barrera, N.P., Venien-Bryan, C., Robinson, C.V., Borges-Walmsley, M.I., and Walmsley, A.R. (2011). Evidence for the assembly of a bacterial tripartite multidrug pump with a stoichiometry of 3:6:3. *J Biol Chem* **286**, 26900-26912.

Kamio, Y., and Nikaido, H. (1976). Outer membrane of *Salmonella typhimurium*: accessibility of phospholipid head groups to phospholipase c and cyanogen bromide activated dextran in the external medium. *Biochemistry* **15**, 2561-2570.

Khudyakov, I., and Wolk, C.P. (1997). *hetC*, a gene coding for a protein similar to bacterial ABC protein exporters, is involved in early regulation of heterocyst differentiation in *Anabaena* sp. strain PCC 7120. *J Bacteriol* **179**, 6971-6978.

Kobayashi, N., Nishino, K., and Yamaguchi, A. (2001). Novel macrolide-specific ABC-type efflux transporter in *Escherichia coli*. *J Bacteriol* **183**, 5639-5644.

Koronakis, V., Eswaran, J., and Hughes, C. (2004). Structure and function of TolC: the bacterial exit duct for proteins and drugs. *Annu Rev Biochem* **73**, 467-489.

Koronakis, V., Sharff, A., Koronakis, E., Luisi, B., and Hughes, C. (2000). Crystal structure of the bacterial membrane protein TolC central to multidrug efflux and protein export. *Nature* **405**, 914-919.

Krogh, A., Larsson, B., von Heijne, G., and Sonnhammer, E.L. (2001). Predicting transmembrane protein topology with a hidden Markov model: application to complete genomes. *J Mol Biol* **305**, 567-580.

Kulp, A., and Kuehn, M.J. (2010). Biological functions and biogenesis of secreted bacterial outer membrane vesicles. *Annu Rev Microbiol* **64**, 163-184.

Laemmli, U.K. (1970). Cleavage of structural proteins during the assembly of the head of bacteriophage T4. *Nature* **227**, 680-685.

Lau, S.Y., and Zgurskaya, H.I. (2005). Cell division defects in *Escherichia coli* deficient in the multidrug efflux transporter AcrEF-TolC. *J Bacteriol* **187**, 7815-7825.

Lehner, J., Zhang, Y., Berendt, S., Rasse, T.M., Forchhammer, K., and Maldener, I. (2011). The morphogene AmiC2 is pivotal for multicellular development in the cyanobacterium *Nostoc punctiforme*. *Mol Microbiol* **79**, 1655-1669.

Lin, H.T., Bavro, V.N., Barrera, N.P., Frankish, H.M., Velamakanni, S., van Veen, H.W., Robinson, C.V., Borges-Walmsley, M.I., and Walmsley, A.R. (2009). MacB ABC transporter is a dimer whose ATPase activity and macrolide-binding capacity are regulated by the membrane fusion protein MacA. *J Biol Chem* **284**, 1145-1154.

Maldener, I., Fiedler, G., Ernst, A., Fernandez-Pinas, F., and Wolk, C.P. (1994). Characterization of *devA*, a gene required for the maturation of proheterocysts in the cyanobacterium *Anabaena* sp. strain PCC 7120. *J Bacteriol* **176**, 7543-7549.

Maldener, I., Hannus, S., and Kammerer, M. (2003). Description of five mutants of the cyanobacterium *Anabaena* sp strain PCC 7120 affected in heterocyst differentiation and identification of the transposon-tagged genes. *FEMS Microbiol Lett* **224**, 205-213.

Maldener, I. and Muro-Pastor, A. M. (2010). Cyanobacterial Heterocysts. *Encyclopedia of Life Sciences*, John Wiley & Sons, Ltd.

Marchler-Bauer, A., Lu, S., Anderson, J.B., Chitsaz, F., Derbyshire, M.K., DeWeese-Scott, C., Fong, J.H., Geer, L.Y., Geer, R.C., Gonzales, N.R., *et al.* (2011). CDD: a Conserved Domain Database for the functional annotation of proteins. *Nucleic Acids Res* **39**, D225-229.

Mariscal, V., Herrero, A., and Flores, E. (2007). Continuous periplasm in a filamentous, heterocyst-forming cyanobacterium. *Mol Microbiol* **65**, 1139-1145.

Matias, V.R., Al-Amoudi, A., Dubochet, J., and Beveridge, T.J. (2003). Cryo-transmission electron microscopy of frozen-hydrated sections of *Escherichia coli* and *Pseudomonas aeruginosa*. *J Bacteriol* **185**, 6112-6118.

Modali, S.D., and Zgurskaya, H.I. (2011). The periplasmic membrane proximal domain of MacA acts as a switch in stimulation of ATP hydrolysis by MacB transporter. *Mol Microbiol* **81**, 937-951.

Moslavac, S., Nicolaisen, K., Mirus, O., Al Dehni, F., Pernil, R., Flores, E., Maldener, I., and Schleiff, E. (2007). A TolC-like protein is required for heterocyst development in *Anabaena* sp. strain PCC 7120. *J Bacteriol* **189**, 7887-7895.

Mullineaux, C.W., Nenninger, A., Ray, N., and Robinson, C. (2006). Diffusion of green fluorescent protein in three cell environments in *Escherichia coli*. *J Bacteriol* **188**, 3442-3448.

Murakami, S., Nakashima, R., Yamashita, E., and Yamaguchi, A. (2002). Crystal structure of bacterial multidrug efflux transporter AcrB. *Nature* **419**, 587-593.

Narita, S. (2011). ABC transporters involved in the biogenesis of the outer membrane in gram-negative bacteria. *Biosci Biotechnol Biochem* **75**, 1044-1054.

Nicolaisen, K., Hahn, A., and Schleiff, E. (2009). The cell wall in heterocyst formation by *Anabaena* sp. PCC 7120. *J Basic Microbiol* **49**, 5-24.

Olmedo-Verd, E., Flores, E., Herrero, A., and Muro-Pastor, A.M. (2005). HetR-dependent and -independent expression of heterocyst-related genes in an *Anabaena* strain overproducing the NtcA transcription factor. *J Bacteriol* **187**, 1985-1991.

Rippka, R. (1988). Isolation and purification of cyanobacteria. *Methods Enzymol* **167**, 3-27.

Saier, M.H., Jr., Beatty, J.T., Goffeau, A., Harley, K.T., Heijne, W.H., Huang, S.C., Jack, D.L., Jahn, P.S., Lew, K., Liu, J., *et al.* (1999). The major facilitator superfamily. *J Mol Microbiol Biotechnol* **1**, 257-279.

Sievers, F., Wilm, A., Dineen, D., Gibson, T.J., Karplus, K., Li, W., Lopez, R., McWilliam, H., Remmert, M., Soding, J., *et al.* (2011). Fast, scalable generation of high-quality protein multiple sequence alignments using Clustal Omega. *Mol Syst Biol* **7**, 539.

Sigal, N., Lewinson, O., Wolf, S.G., and Bibi, E. (2007). *E. coli* multidrug transporter MdfA is a monomer. *Biochemistry* **46**, 5200-5208.

Silhavy, T.J., Kahne, D., and Walker, S. (2010). The bacterial cell envelope. *Cold Spring Harb Perspect Biol* **2**, a000414.

Staron, P., Forchhammer, K., and Maldener, I. (2011). Novel ATP-driven pathway of glycolipid export involving TolC protein. *J Biol Chem* **286**, 38202-38210.

Su, Z., Olman, V., Mao, F., and Xu, Y. (2005). Comparative genomics analysis of NtcA regulons in cyanobacteria: regulation of nitrogen assimilation and its coupling to photosynthesis. *Nucleic Acids Res* **33**, 5156-5171.

Symmons, M.F., Bokma, E., Koronakis, E., Hughes, C., and Koronakis, V. (2009). The assembled structure of a complete tripartite bacterial multidrug efflux pump. *Proc Natl Acad Sci U S A* **106**, 7173-7178.

Tamura, N., Murakami, S., Oyama, Y., Ishiguro, M., and Yamaguchi, A. (2005). Direct interaction of multidrug efflux transporter AcrB and outer membrane channel TolC detected via site-directed disulfide cross-linking. *Biochemistry* **44**, 11115-11121.

Tanabe, M., Szakonyi, G., Brown, K.A., Henderson, P.J., Nield, J., and Byrne, B. (2009). The multidrug resistance efflux complex, EmrAB from *Escherichia coli* forms a dimer *in vitro*. *Biochem Biophys Res Commun* **380**, 338-342.

Tikhonova, E.B., Dastidar, V., Rybenkov, V.V., and Zgurskaya, H.I. (2009). Kinetic control of TolC recruitment by multidrug efflux complexes. *Proc Natl Acad Sci U S A* **106**, 16416-16421.

Tikhonova, E.B., Devroy, V.K., Lau, S.Y., and Zgurskaya, H.I. (2007). Reconstitution of the *Escherichia coli* macrolide transporter: the periplasmic membrane fusion protein MacA stimulates the ATPase activity of MacB. *Mol Microbiol* **63**, 895-910.

Tikhonova, E.B., Yamada, Y., and Zgurskaya, H.I. (2011). Sequential mechanism of assembly of multidrug efflux pump AcrAB-TolC. *Chem Biol* **18**, 454-463.

Tikhonova, E.B., and Zgurskaya, H.I. (2004). AcrA, AcrB, and TolC of *Escherichia coli* form a stable intermembrane multidrug efflux complex. *J Biol Chem* **279**, 32116-32124.

Tokuda, H. (2009). Biogenesis of outer membranes in Gram-negative bacteria. *Biosci Biotechnol Biochem* **73**, 465-473.

Touzé, T., Eswaran, J., Bokma, E., Koronakis, E., Hughes, C., and Koronakis, V. (2004). Interactions underlying assembly of the *Escherichia coli* AcrAB-TolC multidrug efflux system. *Mol Microbiol* **53**, 697-706.

Towbin, H., Staehelin, T., and Gordon, J. (1979). Electrophoretic transfer of proteins from polyacrylamide gels to nitrocellulose sheets: procedure and some applications. *Proc Natl Acad Sci U S A* **76**, 4350-4354.

Tseng, T.T., Gratwick, K.S., Kollman, J., Park, D., Nies, D.H., Goffeau, A., and Saier, M.H., Jr. (1999). The RND permease superfamily: an ancient, ubiquitous and diverse family that includes human disease and development proteins. *J Mol Microbiol Biotechnol* **1**, 107-125.

Veesler, D., and Cambillau, C. (2011). A common evolutionary origin for tailed-bacteriophage functional modules and bacterial machineries. *Microbiol Mol Biol Rev* **75**, 423-433.

Wilk, L., Strauss, M., Rudolf, M., Nicolaisen, K., Flores, E., Kuhlbrandt, W., and Schleiff, E. (2011). Outer membrane continuity and septosome formation between vegetative cells in the filaments of *Anabaena* sp. PCC 7120. *Cell Microbiol* **13**, 1744-1754.

Winkenbach, F., Wolk, C. P., and Jost, M. (1972). Lipids of membranes and of the cell envelope in heterocysts of a blue-green alga. *Planta* **107**, 69-80.

Wolk, C.P., Ernst, A., and Elhai, J. (1994). Heterocyst metabolism and development. In: *The Molecular Biology of Cyanobacteria, Bryant, D.A. (ed),* 769-823, Kluwer Academic Publishers, Dordrecht

Wolk, C.P., Vonshak, A., Kehoe, P., and Elhai, J. (1984). Construction of shuttle vectors capable of conjugative transfer from *Escherichia coli* to nitrogen-fixing filamentous cyanobacteria. *Proc Natl Acad Sci U S A* **81**, 1561-1565.

Xu, Y., Lee, M., Moeller, A., Song, S., Yoon, B.Y., Kim, H.M., Jun, S.Y., Lee, K., and Ha, N.C. (2011). Funnel-like hexameric assembly of the periplasmic adapter protein in the tripartite multidrug efflux pump in gram-negative bacteria. *J Biol Chem* **286**, 17910-17920.

Xu, Y., Sim, S.H., Nam, K.H., Jin, X.L., Kim, H.M., Hwang, K.Y., Lee, K., and Ha, N.C. (2009). Crystal structure of the periplasmic region of MacB, a noncanonic ABC transporter. *Biochemistry* **48**, 5218-5225.

Xu, Y., Sim, S.H., Song, S., Piao, S., Kim, H.M., Jin, X.L., Lee, K., and Ha, N.C. (2010). The tip region of the MacA alpha-hairpin is important for the binding to TolC to the *Escherichia coli* MacAB-TolC pump. *Biochem Biophys Res Commun* **394**, 962-965.

Yamanaka, H., Kobayashi, H., Takahashi, E., and Okamoto, K. (2008). MacAB is involved in the secretion of *Escherichia coli* heat-stable enterotoxin II. *J Bacteriol* **190**, 7693-7698.

Yang, D.C., Peters, N.T., Parzych, K.R., Uehara, T., Markovski, M., and Bernhardt, T.G. (2011). An ATP-binding cassette transporter-like complex governs cell-wall hydrolysis at the bacterial cytokinetic ring. *Proc Natl Acad Sci U S A* **108**, E1052-1060.

Yeo, H.J., and Waksman, G. (2004). Unveiling molecular scaffolds of the type IV secretion system. *J Bacteriol* **186**, 1919-1926.

Yin, Y., He, X., Szewczyk, P., Nguyen, T., and Chang, G. (2006). Structure of the multidrug transporter EmrD from *Escherichia coli*. *Science* **312**, 741-744.

Yum, S., Xu, Y., Piao, S., Sim, S.H., Kim, H.M., Jo, W.S., Kim, K.J., Kweon, H.S., Jeong, M.H., Jeon, H., *et al.* (2009). Crystal structure of the periplasmic component of a tripartite macrolide-specific efflux pump. *J Mol Biol* **387**, 1286-1297.

Zgurskaya, H.I. (2009). Multicomponent drug efflux complexes: architecture and mechanism of assembly. *Future Microbiol* **4**, 919-932.

Zgurskaya, H.I., Krishnamoorthy, G., Ntreh, A., and Lu, S. (2011). Mechanism and function of the outer membrane channel TolC in multidrug resistance and physiology of *enterobacteria*. *Front Microbiol* **2**, 189.

Zgurskaya, H.I., Yamada, Y., Tikhonova, E.B., Ge, Q., and Krishnamoorthy, G. (2009). Structural and functional diversity of bacterial membrane fusion proteins. *Biochim Biophys Acta* **1794**, 794-807.

Zhang, C.C., Laurent, S., Sakr, S., Peng, L., and Bedu, S. (2006). Heterocyst differentiation and pattern formation in cyanobacteria: a chorus of signals. *Mol Microbiol* **59**, 367-375.

11. Appendix

11.1 Secondary structure predictions

The following figures show secondary structure predictions of important proteins mentioned in this work. These predictions were performed by using MINNOU as described (2.2). Red cylinders indicate α-helices and green arrows indicate β-sheets. Yellow sequence highlights indicate transmembrane helices.

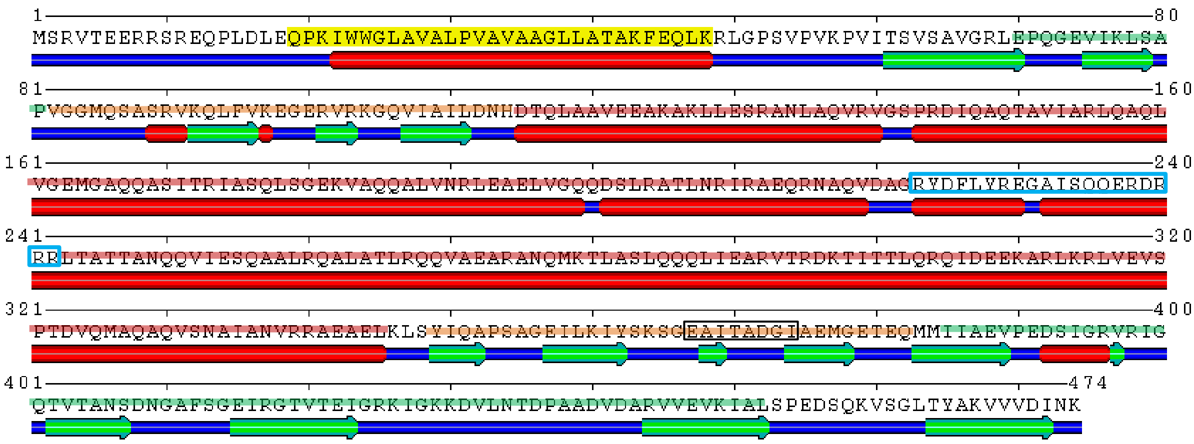

Figure 32. Secondary structure prediction of DevB

Highlighted in green = β-barrel domain; in brown = lipoyl domain; in red = α-helical domain; blue box = tip region; black box = (supposed) barrier forming loop (6.1.3).

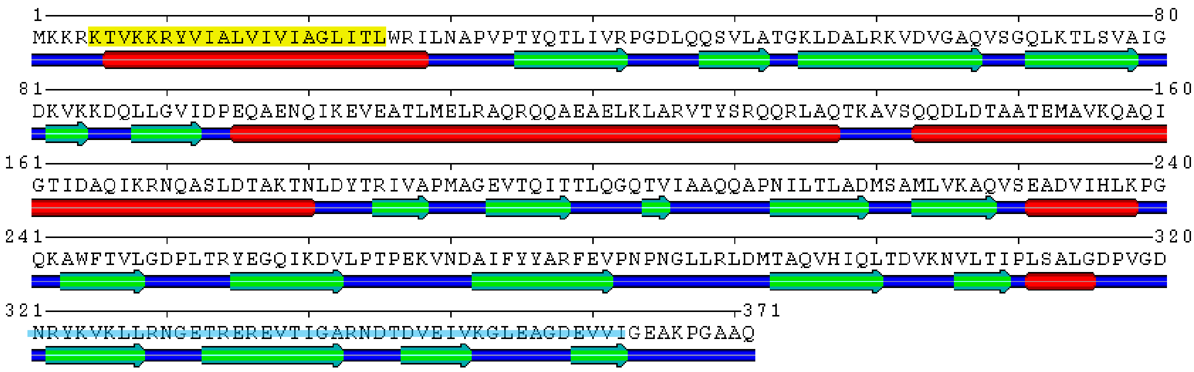

Figure 33. Secondary structure prediction of MacA from *E. coli*

Highlighted in blue = putative β-roll (not encoded by *devB*).

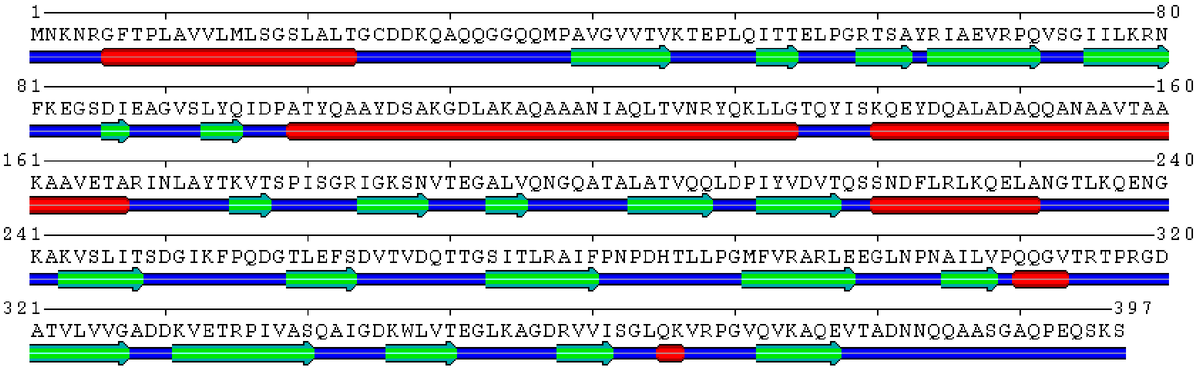

Figure 34. Secondary structure prediction of AcrA from *E. coli*

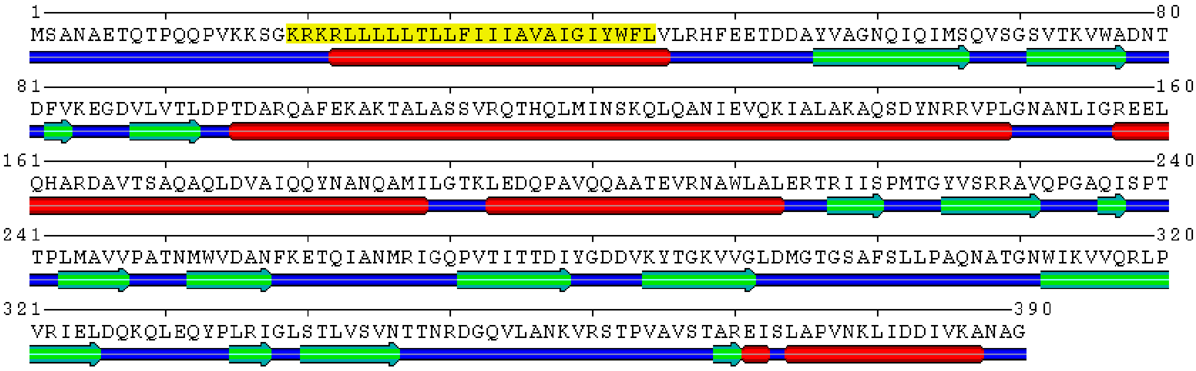

Figure 35. Secondary structure prediction of EmrA from *E. coli*

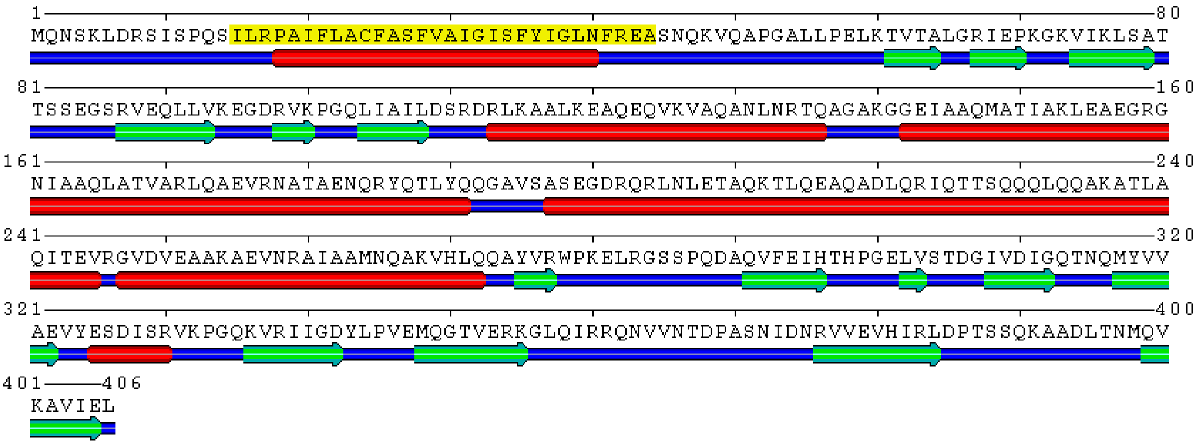

Figure 36. Secondary structure prediction of All0809

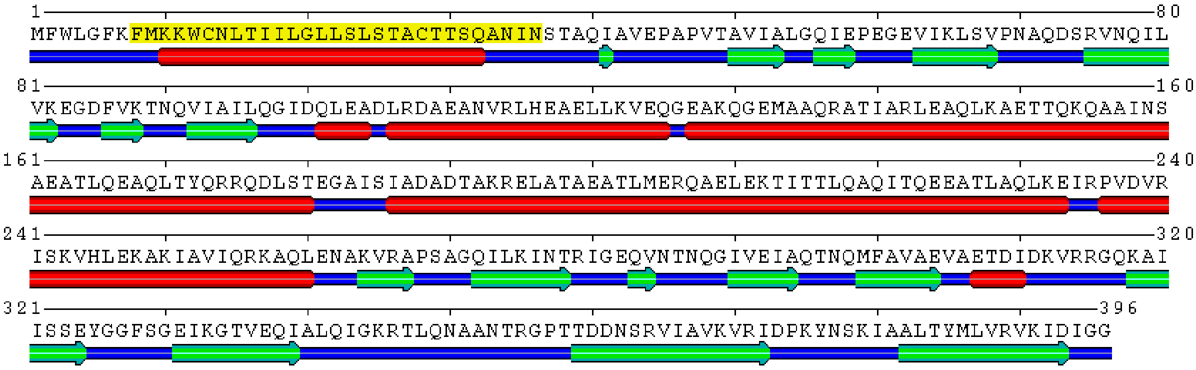

Figure 37. Secondary structure prediction of All2652

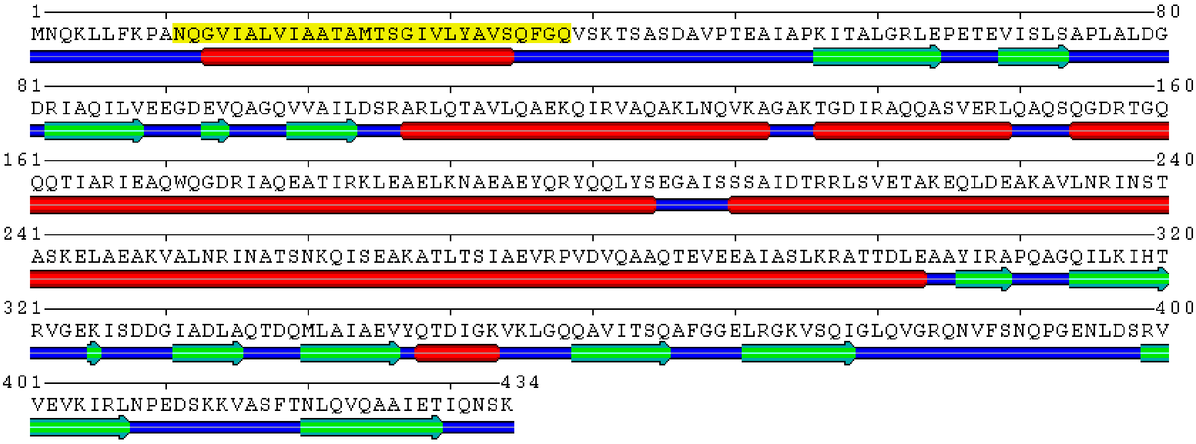

Figure 38. Secondary structure prediction of Alr3647

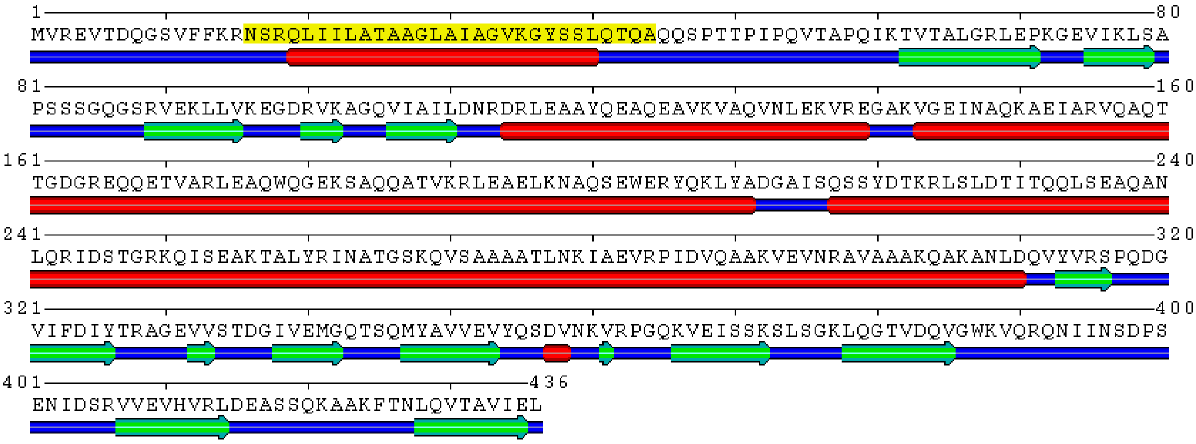

Figure 39. Secondary structure prediction of Alr4280

Apendix

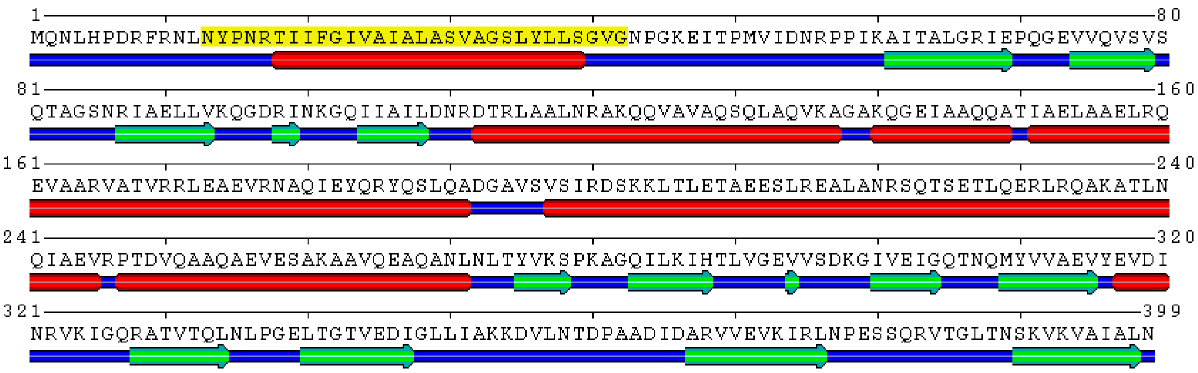

Figure 40. Secondary structure prediction of Alr4973

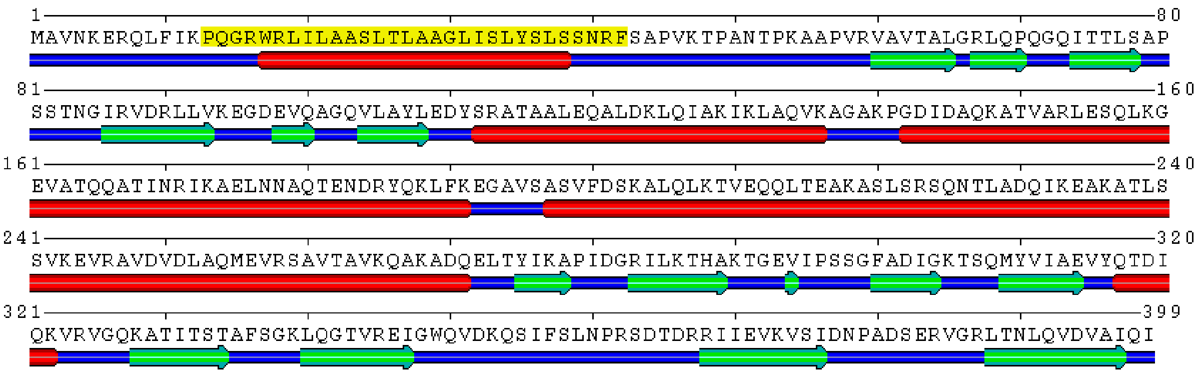

Figure 41. Secondary structure prediction of All5347

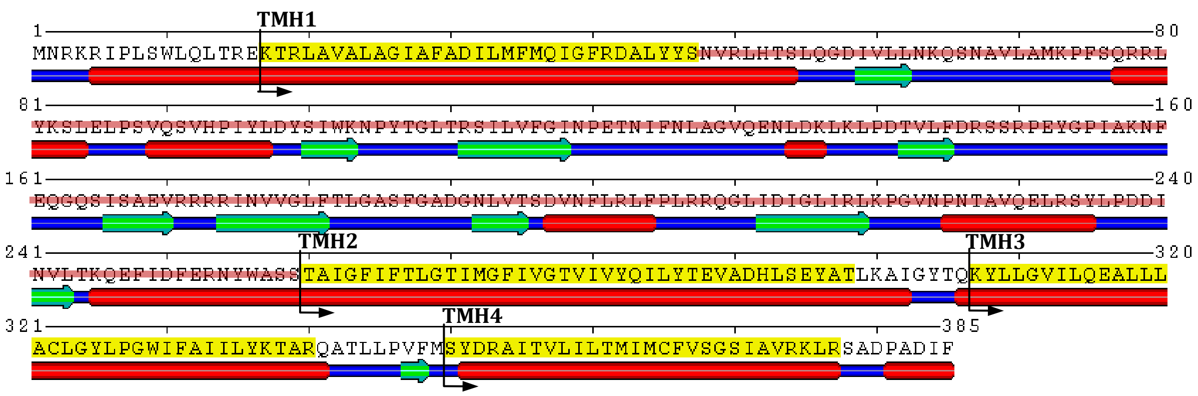

Figure 42. Secondary structure prediction of DevC

TMH = transmembrane helix; highlighted (in red) = periplasmic core domain (MacB_PCD; 2.3.2).

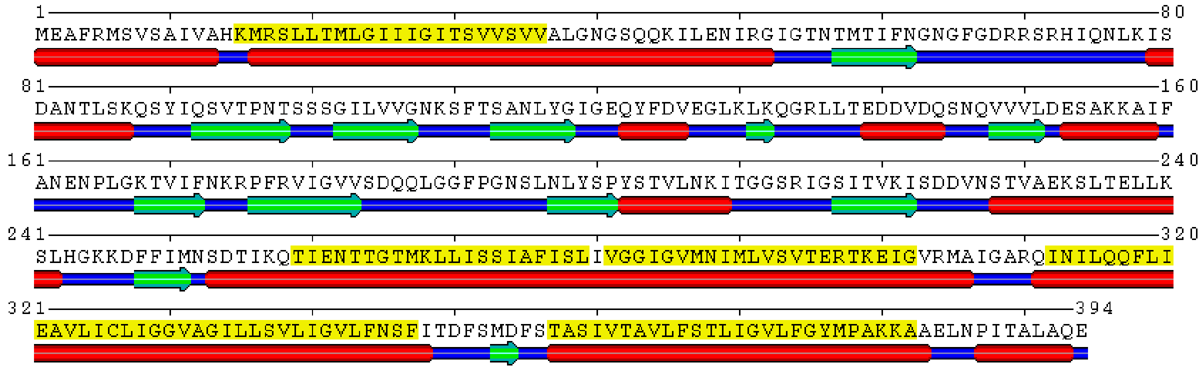

Figure 43. Secondary structure prediction of MacB from *E. coli*

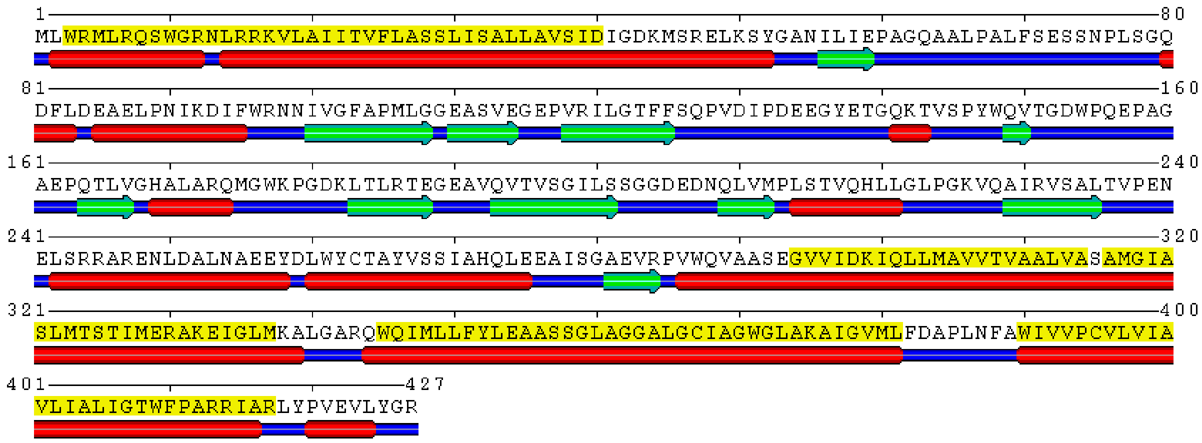

Figure 44. Secondary structure prediction of FtsX from *E. coli*

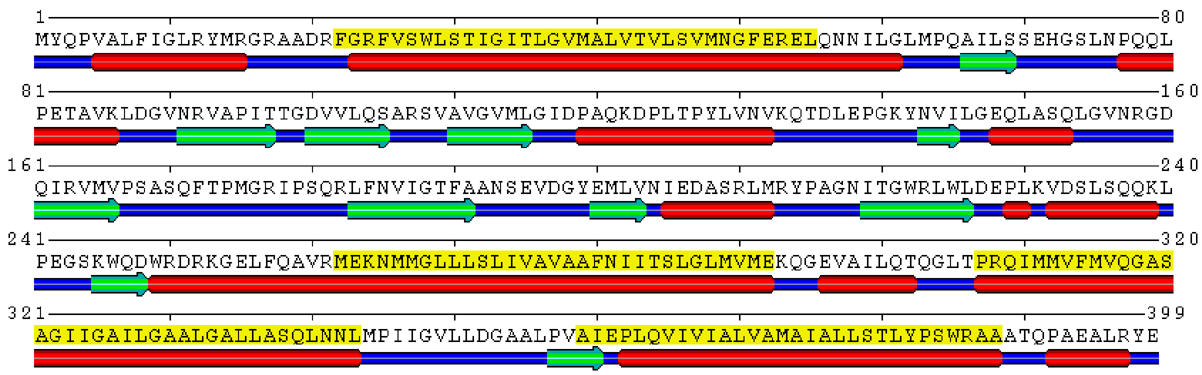

Figure 45. Secondary structure prediction of LolE from *E. coli*

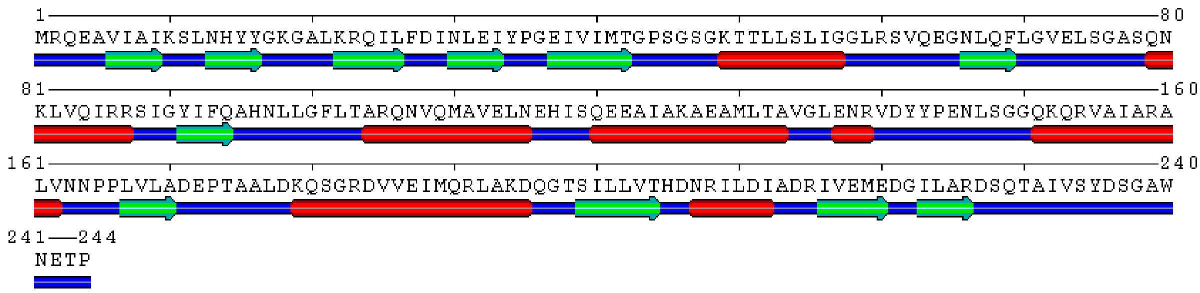

Figure 46. Secondary structure prediction of DevA

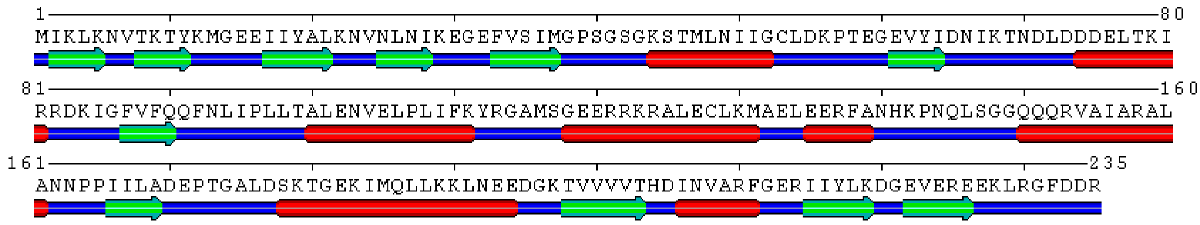

Figure 47. Secondary structure prediction of MJ0796 from *M. jannaschii*

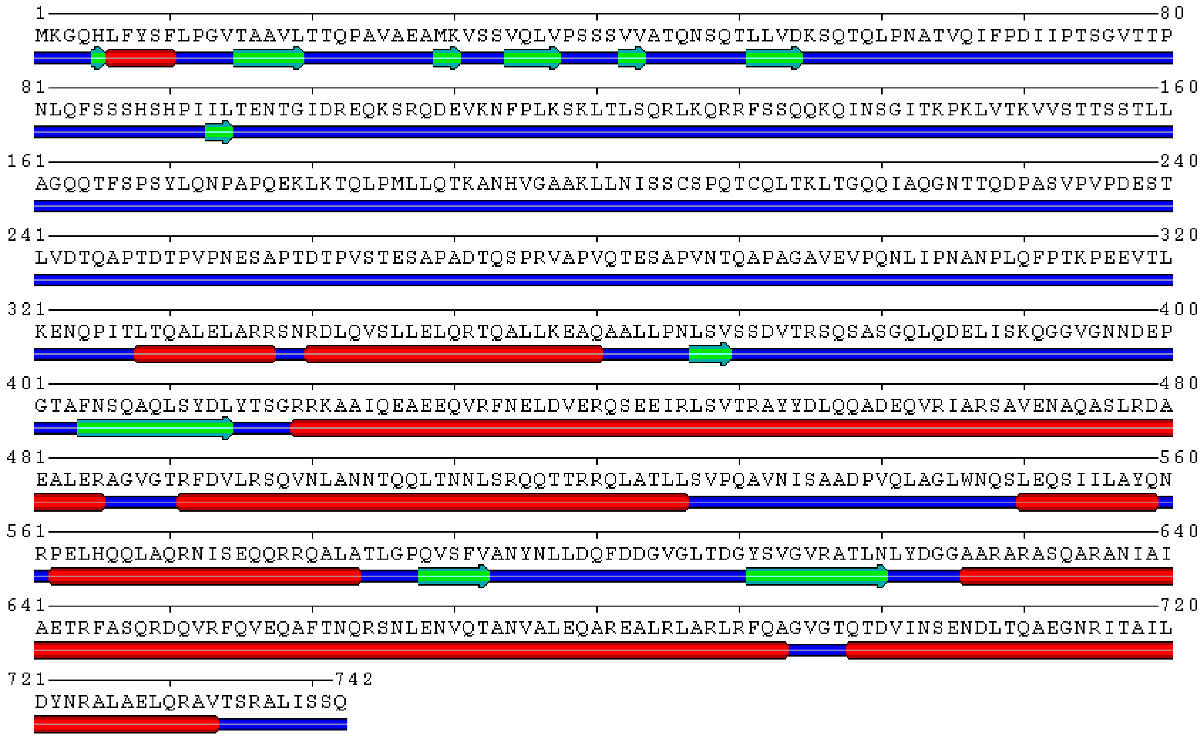

Figure 48. Secondary structure prediction of TolC from *Anabaena*

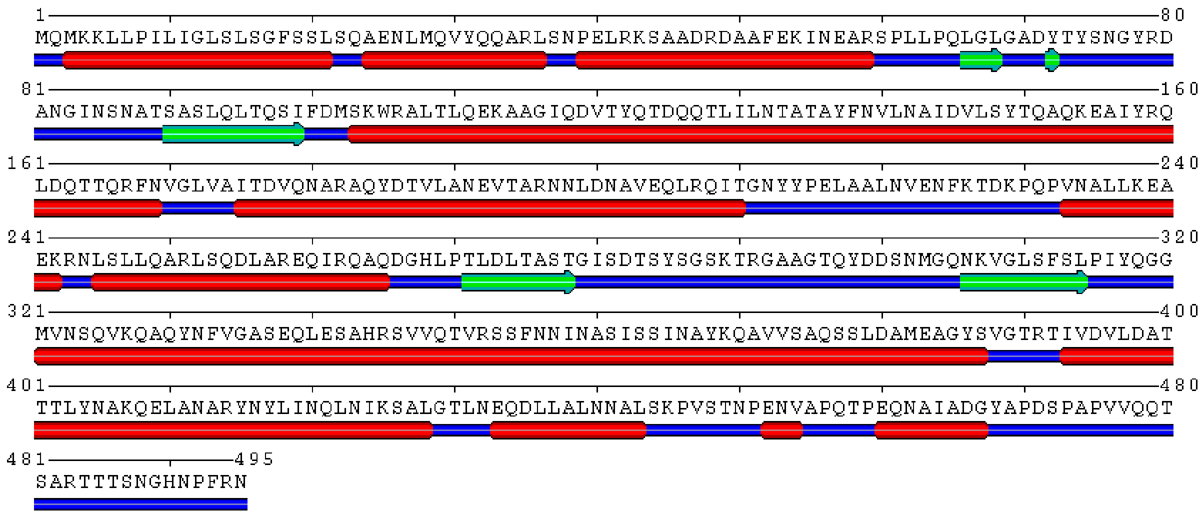

Figure 49. Secondary structure prediction of TolC from *E. coli*

11.2 Used strains

Tab. 1. Used *Anabaena* strains

Strain	Genotype	Resistances	Source
PCC 7120	Wild type	-	C. P. Wolk
CSE2	*ntcA::C.S3*	Sm^r	Frías *et al*. 1994
216	*hetR*_S179N	-	Buikema and Haselkorn 1991
DR181	*alr2887::C.K3*	Nm^r	Moslavac *et al.* 2007
$DR181^{TolC\_c6H}$	*alr2887::C.K3, alr2887'::alr2887*^{c6H}	Nm^r, Cm^r, Em^r	This study
M7	*alr3712::Tn5*	Nm^r, Sm^r,	Maldener *et al.* 1994
$M7^{DevA\_c6H}$	*alr3712::Tn5 + alr3712'::alr3712*^{c6H}	Nm^r, Sm^r, Cm^r, Em^r	This study
DR74	*alr3710::C.K3*	Nm^r	Fiedler *et al.* 1998
$DR74^{DevB}$	*alr3710::C.K3 + nucA::alr3710-12*	Nm^r, Sm^r, Sp^r	This study
$DR74^{DevB\_N333A}$	*alr3710::C.K3 + nucA::alr3710*^{N333A}*-12*	Nm^r, Sm^r, Sp^r	This study
M0809 F	*all0809::C.K3F*	Nm^r	This study
M0809 R	*all0809::C.K3R*	Nm^r	This study
C0809	*all0809::C.K3 + nucA::all0809*	Nm^r, Sm^r, Sp^r	This study
All0807-GFP	*nucA::all0807:eGFP*	Nm^r, Sm^r, Sp^r	This study
All2652 F	*all2652::C.K3F*	Nm^r	This study
Alr3647 F	*alr3647::C.K3F*	Nm^r	This study
Alr3647 R	*alr3647::C.K3R*	Nm^r	This study
Alr4280 F	*alr4280::C.K3F*	Nm^r	This study
Alr4280 R	*alr4280::C.K3R*	Nm^r	This study
Alr4973 R	*alr4280::C.K3R*	Nm^r	This study
All5347 F	*alr4280::C.K3F*	Nm^r	This study
All5347 R	*alr4280::C.K3R*	Nm^r	This study

alr2887= tolC/hgdD, alr3710 = devB, alr3711 = devC, alr3712 = devA

Tab. 2. Used *E. coli* strains

Strain	Genotype	Purpose	Source
DH5α	F-, φ80*lac*ZΔM15, Δ(*lac*ZYA-*arg*F), U169, *rec*A1, *end*A1, *hsd*R17 (rk-, mk+), *gal*-*pho*A, *sup*E44 λ-*thi*-1, *gyr*A96, *rel*A1	Cloning	Hanahan 1985
DH10B	F-, *mcr*A, Δ(*mrr-hsd*RMS-*mcr*BC), φ80*lac*ZΔM15, Δ*lac*X74, *rec*A1, *end*A1, *ara*D139, Δ(*ara, leu*)7697, *gal*U, *gal*K, λ-*rps*L, *nup*G	Cloning	Hanahan *et al.* 1991
Rosetta-gami	Δ(ara-leu)7697 ΔlacX74 ΔphoA PvuII phoR araD139 ahpC galE galK rpsL (DE3) F'[lac$^+$ lacI^q pro] gor522::Tn10 trxB pLysSRARE (Cam^R, Str^R, Tet^R)	Protein expression	Merck
HB101 (pRL528)	*F–, thi-1, hsdS20 (rB–, mB–), supE44, recA13, ara-14, leuB6, proA2, lacY1, galK2, rpsL20 (strr), xyl-5, mtl-1*	Conjugation	Elhai and Wolk 1988b
J53 (RP-4)	*R+, met, pro (RP-4:Ap,Tc, Km, Tra+, IncP)*	Conjugation	Wolk *et al.* 1984

11.3 Generated constructs

Tab. 3. Generated constructs

Insert	Construct	Vector/Resistance	Purpose
TolC_c6H	pIM318	pRL271/Cm^r, Em^r	*in vivo* crosslink bait
DevA_c6H	pIM322	pRL271/Cm^r, Em^r	*in vivo* crosslink bait
DevBCA	pIM442	pCSEL24/Sm^r, Sp^r	complementation
DevB^{N333A}CA	pIM444	pCSEL24/Sm^r, Sp^r	complementation
TolC^{sol}_iGS	pIM378	pET42a/Km^r	SPR/ITC
TolC^{sol}_i8H	pIM380	pET42a/Km^r	SPR
DevB^{sol}	pIM381	pET42a/Km^r	SPR/ITC/SEC/ATP
DevB^{sol}_c8H	pIM383	pET42a/Km^r	SPR
DevB^{sol}_i8H	pIM384	pET42a/Km^r	SPR
DevB^{sol}_V469C	pIM397	pET42a/Km^r	SPR
DevB^{sol}_N333A	pIM416	pET42a/Km^r	SPR/SEC
DevAC_iGS	pIM409	pET42a/Km^r	SPR/ATP
DevAC_i8H	pIM410	pET42a/Km^r	SPR
B* (DevB*)	pIM411	pET42a/Km^r	SPR
B-αHD	pIM420	pET42a/Km^r	SPR/SEC/ATP
B-DαHD	pIM421	pET42a/Km^r	SPR/SEC/ATP
B-DαHD*	p M445	pET42a/Km^r	SPR
B-PαHD	pIM422	pET42a/Km^r	SPR/SEC/ATP
B-PαHD*	p M446	pET42a/Km^r	SPR
B$_x$LipD	pIM423	pET42a/Km^r	SPR/SEC/ATP
B$_x$LipD*	pIM447	pET42a/Km^r	SPR
B-βBD	pIM424	pET42a/Km^r	SPR/SEC/ATP
B-βBD*	pIM448	pET42a/Km^r	SPR
(TolC/) D*	pIM412	pET42a/Km^r	SPR
D$_x$αHD3/4	pIM413	pET42a/Km^r	SPR
D$_x$αHD3/ *	pIM449	pET42a/Km^r	SPR
D$_x$αHD7/8	pIM414	pET42a/Km^r	SPR
D$_x$αHD7/8*	pIM450	pET42a/Km^r	SPR
B-StrepII	pIM408	pET42a/Km^r	Reconstitution/ATP
TolC	pIM407	pET42a/Km^r	Reconstitution
B$_{4GS}$Loop	pIM533	pET42a/Km^r	SPR/ATP
B$_{0809}$Loop	pIM534	pET42a/Km^r	SPR/ATP
All0809	pIM530	pET42a/Km^r	SPR/ TP
All0808/7	pIM531	pET42a/Km^r	SPR/ATP
all0809::C.K3F	pIM391	pRL277/Sm^r, Sp^r	Knock-out
all0809::C.K3R	pIM392	pRL277/Sm^r, Sp^r	Knock-out
all0809	pIM450	pCSEL24/Sm^r, Sp^r	Complementation
all0807:eGFP	pIM521	pCSEL24/Sm^r, Sp^r	Localization
alr3712:eGFP	pIM522	pCSEL24/Sm^r, Sp^r	Localization
all2652::C.K3F	pIM356	pRL277/Sm^r, Sp^r	Knock-out
all3647::C.K3F	pIM357	pRL277/Sm^r, Sp^r	Knock-out
all3647::C.K3R	pIM358	pRL277/Sm^r, Sp^r	Knock-out
all4280::C.K3F	pIM359	pRL277/Sm^r, Sp^r	Knock-out
all4280::C.K3R	pIM360	pRL277/Sm^r, Sp^r	Knock-out
all4973::C.K3R	pIM361	pRL277/Sm^r, Sp^r	Knock-out
all5347::C.K3F	pIM362	pRL277/Sm^r, Sp^r	Knock-out
all5347::C.K3R	pIM363	pRL277/Sm^r, Sp^r	Knock-out

SPR = surface plasmon resonance, ITC = isothermal titration calorimetry, SEC = size exclusion chromatography, ATP = ATPase assay, B = DevB, D = TolC. pRL271 and 277 were described in Black *et al*. (1993), pCSEL24 was described in Olmedo-Verd *et al*. (2005). pET42a was derived from Merck.

11.4 Used Oligonucleotides

Tab. 4. Used Oligonucleotides

Oligonucleotides	**Sequence**
271_TolC_c6H	5´: CTCGAGATGGAAGTAAGTAGTGTACAACTTG
	3´: CTCGAGCAATAAAAAACGCCCGGCGGCA
271_DevA_c6H	5´: CTCGAGATGGTGAGACAAGAAGCTGTAATTG
	3´: CTCGAGCAATAAAAAACGCCCGGCGGCA
60_TolC_c6H	5´: CCATGGAAGTAAGTAGTGTACAACTTG
	3´: GGATCCAGTGACAGCACGTTGTAG
60_DevA_c6H	5´: CCATGGTGAGACAAGAAGCTGTAATTG
	3´: GGATCCATCATAACTAACAATCGCTG
24_BCA	5´: GAATTCGTACAGTCTGTTACCTTTACC
	3´: CTGCAGTTGATACTCAATTTAAAAAATG
DevB_N333A	5´: CAAGTTAGTGCTGCGATCGCCAACGTCAGAAGAGCCGAG
	3´: GGCGATCGCAGCACTAACTTGAGCTTGAGCCATCTGCACATC
42_TolC	5´: GGATCCAATACTCAAGCACCTGCG
	3´: CTCGAGCTACTGACTACTAATTAATGCTCTAG
TolC_iGS1	5´: AGTGGTTCCGGAAGTGGTTCCGGAGGGAGAAGGAAAGCTGCTATTC
	3´: TCCGGAACCACTTCCGGAACCACTTAATAAAGCGGCCTGTGC
TolC_iGS2	5´: TCCGGTAGTGGATCCGGTAGTGGAGGAGCCGCTAGAGCCAG
	3´: TCCACTACCGGATCCACTACCGGACCCCAAGGTTGCTAATGC
TolC_i8H1	5´: CACCACCATCACCACCATCACCACGGGAGAAGGAAAGCTGCTATTC
	3´: GTGGTGATGGTGGTGATGGTGGTGTAATAAAGCGGCCTGTGC
TolC_i8H2	5´: CATCATCACCATCATCACCATCATGGAGCCGCTAGAGCCAG
	3´: ATGATGGTGATGATGGTGATGATGCCCCAAGGTTGCTAATGC
42_DevB	5´: GGATCCTCAAGGGTGACGGAAGAG
	3´: CTCGAG(TTA)TTTATTAATGTCAACCACTACC
DevB_i8H	5´: CACCACCATCACCACCATCACCACTCCCAGCAGGAGCGAGACAG
	3´: GTGGTGATGGTGGTGATGGTGGTGATAGCGTCCCGCATCTACTTG
DevB_MA	5´: GGTTCCGGAAGTGGTTCCGGTTCAGGATCTGGTTCAACAGCTAAATTTGAGC
	3´: GGAACCACTTCCGGAACCTGAACCTCCCAGGAACCCCACTAGGACTGCTG
DevB_V469C	3´: TTATTTATTAATGTCAACGCATACCTTGGCGTAG
42_DevAC	5´: GGATCCAGACAAGAAGCTGTAATTGCCA
	3´: CTCGAGTTAGAAAATATCGGCTGGGTCAGC
DevAC_iGS	5´: AGTGGTTCCGGAAGTGGTTCCGGAAATCGTAAAAGAATCCCTCTATC
	3´: TCCGGAACCACTTCCGGAACCACTAGGGGTTTCGTTCCAAGCGCC
DevAC_i8H	5´: CACCACCATCACCACCATCACCACAATCGTAAAAGAATCCCTCTATC
	3´: GTGGTGATGGTGGTGATGGTGGTGAGGGGTTTCGTTCCAAGCGCC
RT_*tolC*	5´: TTCCCAATGCCAATCCTCTG
	3´: GGTAATAAAGCGGCCTGTGC
RT_*devB*	5´: TGTGATTGCCCGCTTACAGG
	3´: TACGCTGCTCGGCTCTAATG
RT_*rnpB*	5´: GTTAGCTTAACTGATTTGAG
	3´: CCCTAGTCCCCAGTCCCCAATCTTG
B*	5´: GGTGGATCTGGGGGCAGTGGAGGTCTGACTGCGACTACTGCT
	3´: ACCTCCACTGCCCCCAGATCCACCTCCCGCATCTACTTGAGC
B-αHD	5´: CTGACTGCGACTACTGCTAAATTAAGCTACATTCAAGC
	3´: TCCCGCATCTACTTGAGCGTGGTTATCCAAAATTGC
	5´: GCTCAAGTAGATGCGGGACGCTATGATTTTCTCTAC
	3´: AGCAGTAGTCGCAGTCAGTCGCCTTCTGTCTCGCTC
B-DαHD	5´: CTGACTGCGACTACTGCTATTGACGAAGAAAAAGCC
	3´: TCCCGCATCTACTTGAGCCGCCTGTAAGCGGGCAAT
B-PαHD	5´: CAGTTAGTTGGTGAAATG
	3´: CATTTCACCAACTAACTGGTGGTTATCCAAAATTGC
	5´: ATAACTACATTACAAAGACAAAAATTAAGCTACATTCAAG
	3´: TTGTCTTTGTAATGTAGTTATG
B_xLipD	5´: TCTTCAGGTGGATCTTCAAAGATTGGTTCAGGATC
	3´: ACCACCGCTACTTCCGCCAGCTGTTGAACCAGATC
	5´: GGCGGAAGTAGCGGTGGTGATAACCACGATACCCAAC
	3´: TGAAGATCCACCTGAAGAAGCCGAAAGTTTAATCAC
B-ßBD	3´: TGATGATTATTGCTGAAGTAACTCGAG
B-N	5´: GAGAAGGAAAGCTGCTATTC
D*	5´: GGTGGATCTGGGGGCAGTGGAGGTAACTTAGCTAATAACACC

	3´: ACCTCCACTGCCCCCAGATCCACCCAAGCTAGCTTGGGCATTTTC
	5´: AGTTCTGGGTCGAGCGGTTCTTCAAACTCAGAAAATGACTTAAC
	3´: TGAAGAACCGCTCGACCCAGAACTCGCTAGACGCAGTGCTTC
D$_x$αHD3/4	5´: GCACTTGCACTAGCGCTGGCACTAAATGCCCAAGCTAGCTTG
	3´: TAGTGCCAGCGCTAGTGCAAGTGCGACTTGTTCATCTGCCTG
	5´: CTTGCGCTCGCACTAGCCCTGGCTCGGCAACAAACGACTCGTC
	3´: AGCCAGGGCTAGTGCGAGCGCAAGGGTGTTATTAGCTAAGTT
D$_x$αHD7/8	5´: GCACTTGCACTAGCGCTGGCACTAGAAGCACTGCGTCTAGCG
	3´: TAGTGCCAGCGCTAGTGCAAGTGCGGCAGTTTGCACGTTTTC
	5´: CTTGCGCTCGCACTAGCCCTGGCTACGGCAATTCTCGATTAC
	3´: AGCCAGGGCTAGTGCGAGCGCAAGTAAGTCATTTTCTGAGTT
B-StrepII	3´: TTATTTTTCGAACTGCGGGTGGCTCCATTTATTAATGTCAACCACTACC
B$_{4GS}$Loop	5´: AGTGGTTCCGGAAGTGGTTCCGGAGCCGAAATGGGAGAAACC
	3´: TCCGGAACCACTTCCGGAACCACTTCCTGACTTGCTATAAATTTTTAAG
B$_{0809}$Loop	5´: TTAGTCTCTACTGATGGCATTGCCGAAATGGGAGAAACC
	3´: GCCATCAGTAGAGACTAATTCTCCTGACTTGCTATAAATTTTTAAG
All0809 (OEX)	5´: GGATCCCAGAATTCAAAGCTCGAC
	3´: GAACCACTTCCGGAACCTGAACCAGATCCTGAACCATAGGGTTAAATTTTCGGGAAG
	5´: GGTTCCGGAAGTGGTTCCGGTTCAGGATCTGGTTCAAATCGCTGGACGTAAAATC
	3´: CTCGAGTCACAGTTCAATAACTGCTTTAAC
All0808/7 (OEX)	5´: GGATCCCTGAAAGTCATTTCCGTTC
	3´: GTGGTGATGGTGGTGATGGTGGTGGCTAATTACGGCAGGAGTG
	5´: CACCACCATCACCACCATCACCACTTTCAACAATTGCGGCGACG
	3´: CTCGAGTTAAAACATTTCGGCTGGATC
KO *all0809*	5´: CTCGAGATATAGGGTTAAATTTTCGGG
	3´: CTCGAGTCAATATTGCTTGCAGGGTCG
CP *all0809*	5´: GAATTCAAGTGACTATATACTGTTGCTTTG
	3´: GTCGAGCTTTGAGTTCTGCACAATCCCATACCTTTGTAGC
	5´: GTGCAGAACTCAAAGCTCGACCGTTCAATTTCTCCTCAATC
	3´: CTGCAGTCACAGTTCAATAACTGCTTTAAC
GFP *all0807*	5´: CTCGAGATGCTGAAAGTCATTTCCG
	3´: CGAACCGGATCCAGAACCGCTAATTACGGCAGGAGT
GFP *devA*	5´: CTCGAGATGAGACAAGAAGCTGTAATTG
	3´: CGAACCGGATCCAGAACCAGGGGTTTCGTTCCAAGC
KO *all2652*	5´: CTCGAGGAAAATCTGGCTAAGGGTATG
	3´: CTCGAGTTTAGCTTTCTCTAAATGCAC
KO *alr3647*	5´: CTCGAGAAGATGTAGAAGAAGTAC
	3´: CTCGAGAACTTTGGCTTCTGCTAGTTC
KO *alr4280*	5´: CTCGAGACAAGAAACAGTAGCTAG
	3´: CTCGAGGCTTTGAGGACTGATTAAAAC
KO *alr4973*	5´: CTCGAGATGCAAAACCTCCATCCAG
	3´: CTCGAGTCAATTTAAGGCGATCGCTAC
KO *all5347*	5´: CTCGAGATGGCAGTAAATAAAGAAC
	3´: CTCGAGTTAAATTTGAATCGCTAC
RT *all0809*	5´: TAGCCCAAGCCAACCTCAAC
	3´: ACCTCTACCTTCCGCCTCTAAC
RT *all2652*	5´: GGCTAATGTACGCTTGCATGAG
	3´: GCTTCTTGTAGGGTTGCTTCTG
RT *alr3647*	5´: CAGACGCTTGAGTGTGGAAAC
	3´: CTTCGGCAATACTGGTGAGTG
RT *alr4280*	5´: TGCGGAAGTGCGTCCTATTG
	3´: TGGCTGGTTTGACCCATCTC
RT *alr4973*	5´: GTCGCCTAAAGCTGGTCAAATC
	3´: AGTTACAGTTGCGCGTTGTC
RT *all5347*	5´: GAAGGTGCTGTTTCTGCATCTG
	3´: AGCCCGTACTTCTTTGACACTG

11.5 Segregation status of mutants in *devB* homologues

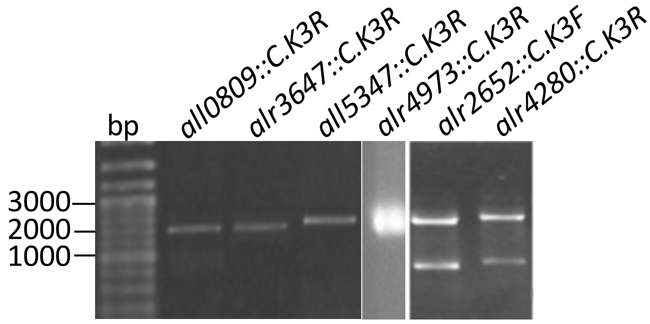

Figure 47. Segregation status of mutants in *devB* homologues

Agarose gels of PCRs checking the segregation status of mutants in homologues of *devB*. bp = DNA standard (length in bp is indicated on the left). Bands at ~1000 bp = gene copies not disrupted by a C.K3 cassette; bands at ~2000 bp = gene copies disrupted by a C.K3 cassette (of ~1000 bp in length).

11.6 Purification of GST-tagged recombinant proteins

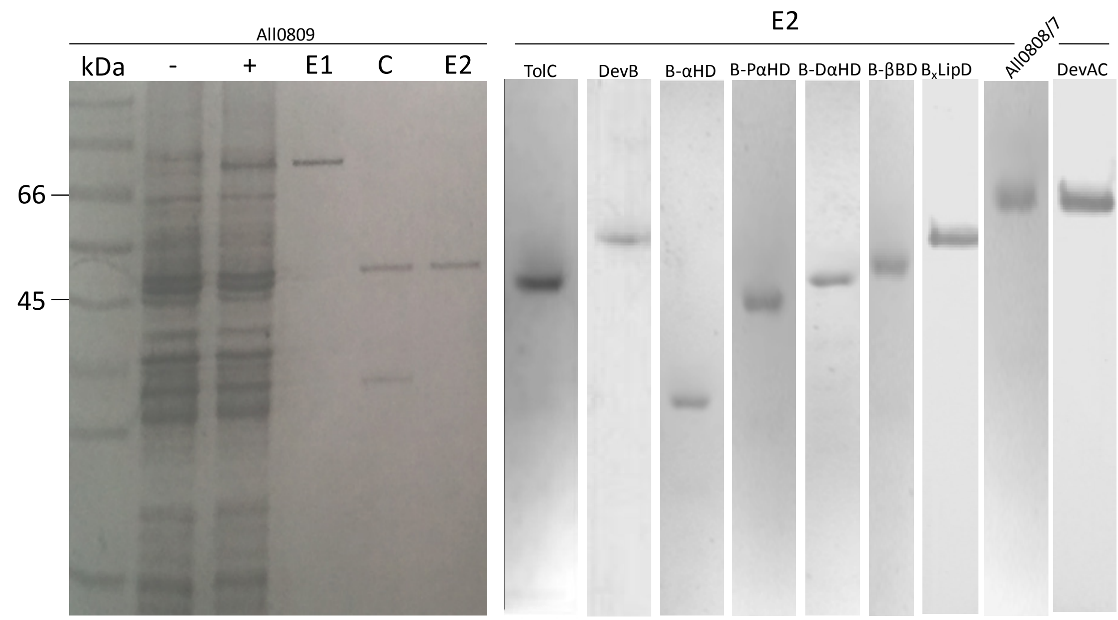

Figure 48. Exemplary purification of often used constructs

SDS-gels showing the principle purifications of GST-tagged proteins (here: All0809)/elutions of GST-cleaved proteins often used constructs in this work. kDa = protein standard (MW is indicated on the left); - = before induction; + = after induction with IPTG; E1 = eluate from Ni-NTA purification, C = cleavage of protein and GST tag with Factor Xa, E2 = eluate after GST purification and/or application of removal resin (Qiagen).

12. Abbrevations

°C	degree Celsius
Aa	amino acid
ABC	ATP-binding cassette
ATP	adenosine triphosphate
bp	base pairs
Fig.	figure
CM	cytoplasmic membrane
Cm	chloramphenicol
CMC	critical micelle concentration
EDTA	ethylenediaminetetraacetic acid
EP	efflux pump
et al.	and others
FC1	flow cell 1
FC2	flow cell 2
GOGAT	glutamine-2-oxoglutarate-amido transferase
GS	glutamine synthetase
GST	glutathione S-tranferase
h	hour
HEP	heterocyst-specific polysaccharides
HGL	heterocyst-specific glycolipids
IMF	inner membrane factor
ITC	isothermal titration calorimetry
Km	Kanamycin
IPTG	isopropyl β-D-1-thiogalactopyranoside
kDa	kilo-Dalton
M	molar
MES	2-Morpholino-ethansulfonsäure
MF	Major facilitator
MFP	membrane fusion protein
NADH	nicotinamide adenine dinucleotide

NBD	nucleotide binding domain
nm	nanometer
Nm	neomycin
no.	number
NTA	nitrilotriacetic acid
OD	optical density
OM	outer membrane
OMF	outer membrane factor
PCC	Pasteur Culture Collection
PEP	phosphoenolpyruvate
PMSF	phenylmethansulfonyl fluoride
PVDF	polyvinyliden fluoride
RNA	ribonucleic acid
RND	Resistance-nodulation-division
rpm	rounds per minute
RU	resonance units
SBD	substrate binding domain
SDS-PAGE	sodium dodecyl sulfate polyacrylamide gel electrophoresis
SEC	size exclusion chromatography
Sm	streptomycin
Sp	spectinomycin
SPR	surface plasmon resonance
T1SS-T7SS	type 1-7 secretion system
Tab.	table
wt/vol	weight/volume
wt/wt	weight/weight

Acknowledgement

Thank you to everyone who supported me during this work.

Especially I would like to thank PD Dr. Iris Maldener for this giving me the opportunity to work on this interesting topic, for her guidance, for her assistance, for her scientific ideas, and for sharing her experience.

I also would like to thank Prof. Dr. Karl Forchhammer for his guidance, for his assistance, for his scientific ideas, and for sharing his experience.

I want to thank Frank, Josef, Max, Sascha, Su, and Susanne for the friendly and funny working atmosphere, for their help and for their advices. In addition, I want to thank Frank, Susanne and Sascha for prolonged scientific and non-scientific discussions, Max and Josef for the beer, and Su for a lot of funny and cynical comments.

Thank you Javi for helping me out a lot in my work, and for teaching me a lot of bad words in Spanish!

Thank you Christina for the cigarette breaks we took together.

Thank you to everyone else at the institute.

I also want to thank my wife Silke and my parents for supporting me.